UNCLASSIFIED

SECURITY CLASSIFICATION OF THIS PAGE (When Data Entered)

DTIC FILE COPY

(1)

AD-A196 384

REPORT DOCUMENTATION PAGE

READ INSTRUCTIONS BEFORE COMPLETING FORM

1. REPORT NUMBER: AFIT/CI/NR 88-160	2. GOVT ACCESSION NO.
3. RECIPIENT'S CATALOG NUMBER	
4. TITLE (and Subtitle): BIT-TO-BIT ERROR DEPENDENCE IN DIRECT-SEQUENCE SPREAD-SPECTRUM MULTIPLE-ACCESS PACKET RADIO SYSTEMS	5. TYPE OF REPORT & PERIOD COVERED: PHD ~~MS~~ THESIS
	6. PERFORMING ORG. REPORT NUMBER
7. AUTHOR(s): ROBERT KENDALL MORROW, JR	8. CONTRACT OR GRANT NUMBER(s)
9. PERFORMING ORGANIZATION NAME AND ADDRESS: AFIT STUDENT AT: PURDUE UNIVERSITY	10. PROGRAM ELEMENT, PROJECT, TASK AREA & WORK UNIT NUMBERS
11. CONTROLLING OFFICE NAME AND ADDRESS	12. REPORT DATE: 1988
	13. NUMBER OF PAGES: 109
14. MONITORING AGENCY NAME & ADDRESS (if different from Controlling Office): AFIT/NR, Wright-Patterson AFB OH 45433-6583	15. SECURITY CLASS. (of this report): UNCLASSIFIED
	15a. DECLASSIFICATION/DOWNGRADING SCHEDULE

16. DISTRIBUTION STATEMENT (of this Report)

DISTRIBUTED UNLIMITED: APPROVED FOR PUBLIC RELEASE

DTIC ELECTE S AUG 0 2 1988 D

17. DISTRIBUTION STATEMENT (of the abstract entered in Block 20, if different from Report)

SAME AS REPORT

18. SUPPLEMENTARY NOTES

Approved for Public Release: IAW AFR 190-1
LYNN E. WOLAVER 21 July 88
Dean for Research and Professional Development
Air Force Institute of Technology
Wright-Patterson AFB OH 45433-6583

19. KEY WORDS (Continue on reverse side if necessary and identify by block number)

20. ABSTRACT (Continue on reverse side if necessary and identify by block number)

ATTACHED

DD FORM 1 JAN 73 1473 EDITION OF 1 NOV 65 IS OBSOLETE

UNCLASSIFIED

SECURITY CLASSIFICATION OF THIS PAGE (When Data Entered)

ABSTRACT

Morrow, Robert Kendall, Jr., Ph.D., Purdue University, May 1988. Bit-to-Bit Error Dependence in Direct-Sequence Spread-Spectrum Multiple-Access Packet Radio Systems. Major Professor: James S. Lehnert.

Slotted direct-sequence spread-spectrum multiple-access (DS/SSMA) packet broadcasting systems with random signature sequences are analyzed within the framework of the lower three layers of the International Standards Organization Reference Model of Open Systems Interconnection. At the physical layer, we show that a widely-used Gaussian approximation (which we call the Standard Gaussian Approximation) for the probability of data bit error in a chip and phase asynchronous system is accurate only when there are a large number of simultaneous users on the channel; otherwise, this approximation can be optimistic by several orders of magnitude. For interfering signals with fixed delays and phases relative to the desired signal, however, the Standard Gaussian Approximation is quite accurate for any number of simultaneous users. To obtain a closer approximation to the probability of data bit error for an asynchronous system, we introduce the Improved Gaussian Approximation, which involves finding the distribution of the multiple-access interference variance over all possible delay and phase values and then taking a Gaussian approximation over the support of the distribution and averaging the results.

To accurately analyze packet performance at the data link layer, we first use the theory of moment spaces to gain insight on the effect of bit-to-bit error dependence caused by the constant relative delays and (possibly) phases of the

interfering signals over the duration of a desired packet. If no error control is used, we find that this error dependence increases the average probability of packet success. When error control is employed and the channel is lightly loaded, then packet performance diminishes when bit error dependencies exist, but performance improves when the channel is heavily loaded and the multiple-access interference is high. Numerical results for the probability of packet success are obtained through the Improved Gaussian Approximation.

At the network layer, provided packet losses occur only from data bit errors due to multiple-access interference, we show that a DS/SSMA packet radio system using the slotted ALOHA protocol possesses a significant throughput advantage over that of an equivalent narrow-band slotted ALOHA system. Furthermore, if error control is used to correct some of the data bit errors in the packet, then the maximum throughput per unit bandwidth of the DS/SSMA system is also higher.

CHAPTER 1
INTRODUCTION

Finding efficient methods of transmitting digital data between two or more nodes in a communication network is a topic of great interest: as the need for reliable communication increases, higher and higher demands are placed upon the limited radio spectrum to provide channels to carry this data. Packet broadcasting systems have been widely used to allocate radio communication channels in such a way that users with bursty traffic can share a common frequency without significant degradation to a single user's throughput or average packet delay. Because of the multiple-access nature of the packet system, total channel throughput is increased dramatically. Spread-spectrum radio systems also allow multiple-access to the channel by wide-band averaging (direct sequence) or avoidance (frequency hopping), making it possible for multiple users to send data on the channel simultaneously. Additional advantages of the spread-spectrum signaling technique include communication security and reduced intersymbol interference from multipath.

If two or more packets are transmitted simultaneously over a narrow-band communication channel, a "collision" occurs, resulting in the destruction of all packets involved. Since multiple users can coexist on a spread-spectrum channel, the concept of a packet collision is no longer applicable in the strict sense; instead, the probability of a successful packet gradually reduces as channel traffic increases. Because of this special multiple-access capability, spread-spectrum packet communication is well-suited to the ALOHA transmission technique, whereby a message is transmitted as soon as it arrives if the system is unslotted, or at the beginning of the next time slot otherwise.

One of the major analytical difficulties in modeling a direct-sequence spread-spectrum multiple-access (DS/SSMA) communication system is the bit-

to-bit error dependence present in the multiple-access interference statistic, corresponding to a communication channel with memory. Although we can calculate arbitrarily tight upper and lower bounds on the probability of a single bit error due to multiple-access interference, determining the probability of *packet* error is no longer straightforward.

1.1. Previous Research

The International Standards Organization (ISO) has developed a Reference Model of Open Systems Interconnection (OSI) [1] composed of seven layers, of which the lower three are most applicable to the special nature of spread-spectrum communications. The lowest is the *physical layer,* which is concerned with transmitting raw data bits over a communication channel. The second level is the *data link layer,* which determines the packet structure, error control capability, and transmitter-receiver bit and word synchronization methods. Finally, the *network layer* controls message routing on the shared channel and regulates the flow of packets.

The majority of direct-sequence spread-spectrum research has been done at the physical layer in the area of modeling the nature of the multiple-access interference and attempting to obtain bounds or approximations to the probability of bit error. Lehnert has developed a technique to obtain upper and lower bounds on the probability of data bit error by constructing the actual density function for the multiple-access interference, given random signature sequences for all users [2]. This method can be applied in a straightforward manner to derive a similar density for deterministic sequences as well. Prior work in this area involved the theory of moment spaces [3] to bound the effect of multiple-access interference on a single data bit, and the use of a Gaussian density approximation [4] after determining the mean and variance of the multiple-access interference statistic. In [5], bounds on the bit error probability for deterministic sequences were developed from the convexity properties of the error probability function, and the characteristic function of the multiple-access interference component is integrated in [6] to find an approximation to the data bit error.

Research applicable to the data link layer in direct-sequence spread-spectrum communications is relatively sparse. An attempt has been made in [7] to bound the packet error probability in a system employing convolutional coding and Viterbi decoding for error control. The authors assume a certain worst-case conditioning to force independent channel error events; because of this, the derived lower bound on system performance is probably loose.

The networking aspect of spread spectrum packet radio has been addressed to a greater degree than that of the data link layer, but the area is by no means thoroughly researched, in part due to the complex nature of the multiple-access interference present at the physical layer. Most work in the networking area suffers from an oversimplification of the lower two levels of the ISO standard to allow a reasonably complex network model to be solved with moderate effort. For example, a common simplification at the physical layer is to assume that once the receiver acquires a packet through successful decoding of the synchronization preamble or header, then the remainder of the packet will always be received correctly [8]-[11]. Various assumptions are made to insure that the receiver cannot always synchronize or decode the header properly, such as in [8], which analyzes a slotted ALOHA packet radio network by basing performance solely on whether capture is attained, which is in turn deemed successful if and only if no other transmissions occur within a certain "vulnerability period" after the beginning of a desired transmission. The communication channel is considered noiseless for the duration of the packet, so successful capture is equivalent to a successful packet transmission.†

Raychaudhuri [13] derives a networking model in a manner somewhat similar to that used in this paper, but uses a form of idealized spread-spectrum coding which essentially provides a noiseless channel until the number of simultaneous users exceeds a certain threshold, after which the channel rapidly becomes useless. This approach is also taken in [14], only the channel is considered noiseless when λ or fewer users transmit simultaneously,

† This idealistic channel assumption is not without historical precedent. In his paper on narrow-band ALOHA networks, Abramson [12] assumes that a communication channel is useless if two or more transmissions overlap; otherwise the channel is considered noiseless.

and useless otherwise. Signature sequences used in practice result in a more gradual channel deterioration as the number of interfering users increases. Polydoros and Sylvester [15] discuss the necessity of incorporating a more realistic approach to packet error probabilities.

Brazio [16], [17] performs a detailed analysis of multihop packet networks incorporating various spread-spectrum signaling schemes. For his numerical results, tractability is maintained once again by assuming an idealized capture model, approximations to the probability of bit error, independent bit error events, and no error correction capability.

None of the networking papers researched incorporates bounds on or an accurate approximation to the probability of bit error in the multiple-access environment (the most detailed work uses only a simple Gaussian approximation), nor have they accounted for the bit-to-bit error dependency present on the communication channel.

1.2. Thesis Overview

All of the previous work in analyzing the networking aspect of spread-spectrum packet radio systems have made simplifications at the physical and data link layers to allow tractability of analysis at the network layer. Due to the complex nature of the DS/SSMA signaling environment, this thesis takes a different approach: that of performing an accurate analysis of the physical and data link layers, and comparing these results to various less-accurate but widely-used approximations when analyzing the throughput and network capacity for a simple slotted ALOHA networking protocol. This protocol allows us to use fixed packet lengths and provides full overlap of all packets within a slot. In addition, all links in the network are assumed to be single hop, with no hidden terminals. This situation is likely to be encountered in a large single-room factory assembly facility, for example, where fixed and mobile machinery are controlled by a central computer via spread-spectrum packet communication. The slotted ALOHA model provides the framework to incorporate a more accurate picture of packet behavior at the lower two ISO layers while still producing useful results at the network level.

In this thesis, a method is presented in Chapter 2 which calculates the probability of data bit error at a computational complexity equivalent to that needed for the bounds technique, but with an accuracy that is much greater than that offered by a widely-used Gaussian approximation. These results provide the groundwork for calculating in Chapter 3 the probability of packet success while accounting for the dependence of data bit error events due to the multiple-access interference (MAI). The results are valid whether or not the packet has block error correction capability. Next, equations modeling the throughput versus offered channel traffic are derived in Chapter 4 for a slotted direct-sequence spread-spectrum multiple-access packet network, and throughput vs offered rate plots are generated while using different approximations for the probability of packet success. The effect on throughput is studied when a block error correcting code is implemented within each packet. Finally, network capacity for various packet and signature sequence lengths is determined, and the throughput per unit bandwidth at capacity of the DS/SSMA method is compared with that of a narrow-band channel. In Chapter 5, we offer some conclusions and suggestions for further research.

CHAPTER 2
THE PHYSICAL LAYER:
PROBABILITY OF DATA BIT ERROR

2.1. Introduction

At the *physical layer,* we are concerned with the transmission of raw data bits over the communication channel [1], so our analysis is directed toward finding the probability of data-bit error P_e for a given signaling technique. An appropriate DS/SSMA system model is used to derive an expression for the transmitted signal, which is then passed through a correlation receiver; the signal present at the receiver's decision block has the necessary form to perform a statistical analysis from which P_e may be determined.

In this chapter, we present three general methods by which the probability of bit error may be determined when interfering transmitters employ random signature sequences. The first technique, developed in [2], is somewhat involved but produces arbitrarily tight bounds on P_e. We specialize this procedure to rectangular chip pulses, calculate the computational complexity, and use these bounds to check the accuracy of the other two techniques. The second technique we use for calculating P_e is the *Standard Gaussian Approximation,* which is based upon the assumption that the MAI is a Gaussian random variable. This approximation derives much of its appeal from the fact that it is very easy to compute, with computational complexity of order 1 regardless of the size of N (the number of chips per data-bit), or K (the number of simultaneous users). We show, however, that when the interfering signals are averaged over their relative delays and phases, the Standard Gaussian Approximation is accurate only when K is large, leading to the unfortunate consequence that the approximation is good when the bit error rate is high and the system is performing poorly. Furthermore, when K

is small, the Standard Gaussian Approximation is optimistic compared to the actual P_e, so systems designed around this approximation may perform worse than expected. These shortcomings may be overcome through a new technique called the *Improved Gaussian Approximation,* which is based upon the premise that, given a specific desired signature sequence, if the phase and delay of each interfering signal are *fixed,* then the MAI is closely approximated by a Gaussian random variable. After finding the distribution of the variance of this random variable for all possible combinations of delay and phase values, and for all desired signature sequences, we can determine P_e with much greater accuracy than with the Standard Gaussian Approximation, but at an equivalent computational complexity to that offered by the method of bounds.

2.2. System Model

2.2.1. Transmitted Signal

The spread-spectrum system model examined in this thesis is similar to that used in [2] and [4], shown in Figure 2.1 for K users. The k-th user's data signal $b_k(t)$ consists of a sequence of unit amplitude, positive and negative, rectangular pulses of duration T. If we define a rectangular pulse as

$$p_T(t) = \begin{cases} 1, & 0 \le t \le T \\ 0, & \text{elsewhere} \end{cases} \tag{2.1}$$

then the k-th data signal becomes

$$b_k(t) = \sum_{j=-\infty}^{\infty} b_j^{(k)} p_T(t - jT), \tag{2.2}$$

where the b_j are taken from a random binary data stream having values of $+1$ or -1 with equal probability. The k-th user is assigned a spreading waveform $a_k(t)$, also consisting of unit amplitude, positive and negative, rectangular pulses of duration T_c. Hence,

$$a_k(t) = \sum_{j=-\infty}^{\infty} a_j^{(k)} p_{T_c}(t - jT_c), \tag{2.3}$$

with the a_j being produced by another binary stream of $+1$ and -1 values independent of b_j. The k-th user's spreading sequence (or *signature sequence*)

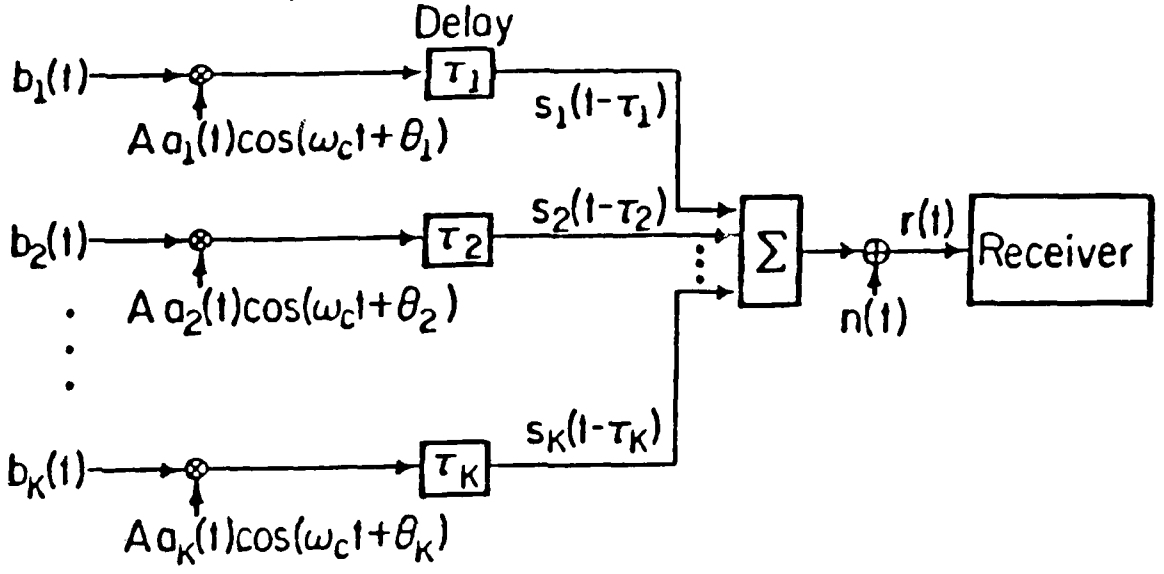

Figure 2.1. DS/SSMA system model.

has N elements per data symbol. If we define a single spreading pulse as a *chip*, then we have N chips per data bit, and $T = NT_c$.

Phase modulation in this system is performed by combining a total of three signals: carrier, signature sequence, and data sequence. The k-th user's carrier is given by

$$c_k(t) = \sqrt{2P}\sin(\omega_c t + \theta_k), \tag{2.4}$$

where P is the signal power, ω_c is the carrier frequency in radians per second, and θ_k is the phase parameter of the k-th carrier with respect to $c_1(t)$. Phase modulation by $a_k(t)$ and $b_k(t)$ produces the transmitted signal

$$\begin{aligned} s_k(t) &= \sqrt{2P}\sin(\omega_c t + \theta_k + (\pi/2)a_k(t)b_k(t)) \\ &= \sqrt{2P}a_k(t)b_k(t)\cos(\omega_c t + \theta_k). \end{aligned} \tag{2.5}$$

To account for the lack of time synchronism between transmitted signals, we incorporate a delay parameter τ_k into (2.5), giving

$$s_k(t-\tau_k) = \sqrt{2P}a_k(t-\tau_k)b_k(t-\tau_k)\cos(\omega_c t + \phi_k), \tag{2.6}$$

where $\phi_k = \theta_k - \omega_c \tau_k$. Since the delays and phases are all referenced to signal 1, which we call the *desired signal,* it follows that $\tau_1 = \phi_1 = 0$. Furthermore, we take relative delays modulo T and relative phases modulo 2π.

2.2.2. Demodulated Signal

If K users each transmit a signal of the form (2.6) onto a noiseless, attenuation-free communication channel, then $n(t) = 0$ in Figure 2.1 and

$$r(t) = \sum_{k=1}^{K} s_k(t-\tau_k). \tag{2.7}$$

At receiver 1 (the *desired receiver*), $r(t)$ is multiplied by a signal from a local oscillator which is both phase-synchronized to the carrier frequency and phase modulated by a time-synchronized copy of the desired signature sequence, and the result is then integrated over the period of a data bit, producing the output

$$Z_1 = \int_0^T r(t)a_1(t)\cos\omega_c t\, dt\ . \tag{2.8}$$

By assuming that $\omega_c \gg 1/T$ and that the double frequency component of $r(t)\cos\omega_c t$ is completely eliminated by the post-detection filter, we have

$$Z_1 = T\sqrt{P/2}\left[b_0^{(1)} + \sum_{k=2}^{K} I_{k,1}(\underline{b}_k,\tau_k,\phi_k)\right] \tag{2.9}$$

where $I_{k,1}$ is the interference at the desired receiver from the k-th user, given by

$$I_{k,1}(\underline{b}_k,\tau,\phi) = T^{-1}[B_{k,1}(\underline{b}_k,\tau)]\cos\phi \tag{2.10}$$

with

$$B_{k,1}(\underline{b}_k,\tau) = b_{-1}^{(k)}R_{k,1}(\tau) + b_0^{(k)}\hat{R}_{k,1}(\tau)\ . \tag{2.11}$$

The vector $\underline{b}_k=(b_{-1}^{(k)},b_0^{(k)})$ represents a pair of consecutive data bits from the k-th signal, each of which partially overlaps the desired signal. The continuous-time partial cross-correlation functions are defined [4] as

$$R_{k,i}(\tau) = \int_0^{\tau} a_k(t-\tau)a_i(t)dt\ , \qquad 0 \le \tau \le T\ ; \tag{2.12}$$

$$\hat{R}_{k,i}(\tau) = \int_{\tau}^{T} a_k(t-\tau)a_i(t)dt\ , \qquad 0 \le \tau \le T\ . \tag{2.13}$$

Under our random signature sequence assumption, the probability is high that interfering data will have signature sequences with low cross-correlation values with the desired signature sequence, so when the two sequences are multiplied together at the receiver, the resulting interference from the k-th transmitter will integrate to a value $I_{k,1}(\underline{b}_k,\tau_k,\phi_k)$ close to zero for $k \in \{2, \ldots, K\}$. In actual systems, sequences are carefully chosen so that cross-correlation values are kept small.

2.3. Motivation for the Random Signature Sequence Approach

Although specific signature sequences are chosen for each user in actual DS/SSMA systems, analysis is sometimes facilitated by assuming that all users employ signature sequences that are completely random. Indeed, there are many situations where deterministic sequence analysis becomes either *impractical or impossible*, such as: 1) the sequences of the interfering users are unknown; 2) there are many users in the network; or 3) users may employ different sequences for each of a number of consecutive data bits. In case 1, that of unknown interfering sequences, using deterministic sequences in the analysis is impossible, while in the other two situations deterministic analysis produces prohibitive computational complexity. The random sequence approach also offers simplified delay analysis, since receiver performance may be determined completely by examining interfering signal delays over a single chip, not over one or more data bits as required by deterministic sequences. If signature sequences are truly random, however, it follows that certain "bad" combinations of sequences could occur (albeit with low probability) between simultaneous transmissions which can render the communication channel essentially useless for two or more users over a period of time. Since this situation is (hopefully) avoided in actual systems, one can argue that random sequence *analysis produces a lower bound on actual system performance* [17].

The results in this thesis are obtained by assuming that all *interfering* users have random signature sequences, and that a different sequence is used for each data bit. However, most of the computations are performed by first conditioning on a *specific* desired signature sequence (actually, a specific autocorrelation value for a given sequence). The probability of data bit error is then calculated for each of these particular autocorrelation values, and the results are averaged to obtain the probability of data bit error for a desired sequence that is also randomly generated. If the desired signature sequence is known, then there may be no need to average over all possible desired sequences, since accuracy will be reduced and computational complexity increased by doing so.

2.4. Bounds on the Probability of Data Bit Error

To obtain arbitrarily tight bounds on the probability of bit error in a direct-sequence spread-spectrum signal, we can follow the procedure developed in [2] with some simplifications and improvements in accuracy. The procedure derives its utility by constructing the actual multiple-access interference density function from all possible cross-correlation values of random signature sequences, but with computational complexity that is only polynomial in N and K. In this thesis, we assume that no additive white Gaussian noise (AWGN) is present, so that all data bit errors are produced by multiple-access interference alone, and we specialize this technique to rectangular chip pulses. In all cases, conditioning on the number of simultaneous users K is implicit.

2.4.1. The Correlation Receiver Output Statistic

We begin our calculation of the output statistic of correlation receiver 1 by manipulating (2.12) and (2.13) as follows. Since there are N chips per data bit, we can define the discrete aperiodic cross correlation function as

$$C_{k,i}(n) = \begin{cases} \sum_{j=0}^{N-1-n} a_j^{(k)} a_{j+n}^{(i)}, & 0 \le n \le N-1 \\ \sum_{j=0}^{N-1+n} a_{j-n}^{(k)} a_j^{(i)}, & 1-N \le n < 0 \\ 0, & |n| \ge N \end{cases} \tag{2.14}$$

allowing us to rewrite (2.12) and (2.13) as

$$R_{k,i}(\tau) = T_c [C_{k,i}(l-N)] + (\tau - lT_c)[C_{k,i}(l+1-N) - C_{k,i}(l-N)], \tag{2.15}$$

and

$$\hat{R}_{k,i}(\tau) = T_c [C_{k,i}(l)] + (\tau - lT_c)[C_{k,i}(l+1) - C_{k,i}(l)], \tag{2.16}$$

where $0 \le lT_c \le \tau \le (l+1)T_c \le T$. For $i=1$, the parameter l represents the number of complete chips in the time offset between the k-th and desired signals; i.e.,

$$l = \left\lfloor \frac{\tau_k}{T_c} \right\rfloor . \tag{2.17}$$

Suppose each interfering signal uses randomly-generated signature sequences with a new sequence being selected for each consecutive data bit. In this case, we need only examine delays over a single chip, since the average effect of interfering signals on the desired signal is the same regardless of the number of chips that an interfering data bit is displaced relative to the desired signal. Put another way, the k-th interfering signal is an infinite sequence of pulses of duration T_c with amplitudes uniform on $\{-1,1\}$, and having a random time displacement S_k to the desired signal, where $0 \leq S_k < T_c$. We can now let $l = N-1$, for example, which simplifies (2.15) and (2.16) to

$$\begin{aligned} R_{k,1}(S_k) &= T_c\,[C_{k,1}(-1)] + S_k[C_{k,1}(0) - C_{k,1}(-1)] \\ &= (T_c - S_k) \sum_{j=0}^{N-2} a_{j+1}^{(k)} a_j^{(1)} + S_k \sum_{j=0}^{N-1} a_j^{(k)} a_j^{(1)}, \end{aligned} \tag{2.18}$$

and

$$\hat{R}_{k,1}(S_k) = (T_c - S_k) a_N^{(k)} a_{N-1}^{(1)} , \tag{2.19}$$

where $a_N^{(k)}$ represents the first chip in data bit $b_0^{(k)}$; this chip is independent of $a_0^{(k)}$, the first chip in data bit $b_{-1}^{(k)}$. Substituting (2.18) and (2.19) into (2.11) gives

$$\begin{aligned} B_{k,1}(S_k) = (T_c - S_k) &\left[\sum_{j=0}^{N-2} a_{j+1}^{(k)} a_j^{(1)} + a_N^{(k)} a_{N-1}^{(1)} \right] \\ &+ S_k \sum_{j=0}^{N-1} a_j^{(k)} a_j^{(1)} . \end{aligned} \tag{2.20}$$

Note that since the signature sequence of the k-th interfering signal is random, $B_{k,1}(S_k)$ no longer depends upon the interfering data bits $b_{-1}^{(k)}$ and $b_0^{(k)}$. Next, the terms of (2.20) can be rearranged to produce

$$B_{k,1}(S_k) = \sum_{j=0}^{N-2} a_{j+1}^{(k)} \left[(T_c - S_k) a_j^{(1)} + S_k a_{j+1}^{(1)} \right] \tag{2.21}$$

$$+ S_k a_0^{(k)} a_0^{(1)} + (T_c - S_k) a_N^{(k)} a_{N-1}^{(1)} .$$

At this point, we can simplify notation by introducing the *symmetric Bernoulli trial* **b**, which has outcomes uniform on the set $\{-1,1\}$. Note that **b** has zero mean and unit variance, and that each $a_j^{(k)}$, and the product of any two or more independent $a_j^{(k)}$, may be represented by an appropriately indexed **b**. We also condition on the desired sequence $a_j^{(1)} = \hat{a}_j$ for $j \in \{0, 1, \ldots, N-1\}$. By using the fact that $[\hat{a}_j]^2 = 1$, (2.21) becomes

$$B_{k,1}(S_k) = \sum_{j=0}^{N-2} \mathbf{b}_{j+1} \left[(T_c - S_k) + S_k \hat{a}_j \hat{a}_{j+1} \right] \tag{2.22}$$

$$+ S_k \mathbf{b}_0 + (T_c - S_k) \mathbf{b}_N .$$

To gain more insight into the nature of (2.22), we note that $\hat{a}_j \hat{a}_{j+1} \in \{-1,1\}$, so we can let

$$\alpha = \{ j : \hat{a}_j \hat{a}_{j+1} = 1 \}, \tag{2.23}$$

and

$$\beta = \{ j : \hat{a}_j \hat{a}_{j+1} = -1 \} \tag{2.24}$$

for $j \in \{0, 1, \ldots, N-2\}$. After rearranging terms, we have

$$B_{k,1}(S_k) = P_k S_k + Q_k (T_c - S_k) + X_k T_c + Y_k (T_c - 2S_k), \tag{2.25}$$

where $P_k = \mathbf{b}_0$ and $Q_k = \mathbf{b}_N$ are uniform on $\{-1,1\}$, with

$$X_k = \sum_{j \in \alpha} \mathbf{b}_j \tag{2.26}$$

and

$$Y_k = \sum_{j \in \beta} \mathbf{b}_j . \tag{2.27}$$

Equation (2.25) is identical to a result derived in [2] for interfering users which select a signature sequence at random at the beginning of a transmission, but

then repeat this sequence for each data bit in the message.

If we denote the cardinalities $A = |\alpha|$ and $B = |\beta|$, then X_k and Y_k are produced by the sum of A and B symmetric Bernoulli trials, respectively, and thus have densities

$$p_{X_k}(j) = \binom{A}{\frac{j+A}{2}} 2^{-A} \; ; \quad j \in \{-A, -A+2, \ldots, A-2, A\} \tag{2.28}$$

and

$$p_{Y_k}(j) = \binom{B}{\frac{j+B}{2}} 2^{-B} \; ; \quad j \in \{-B, -B+2, \ldots, B-2, B\} . \tag{2.29}$$

From (2.23) and (2.24), we see that $A+B=N-1$. Furthermore, if we define the discrete aperiodic autocorrelation of the signature sequence of receiver 1, offset by one chip, by

$$C \triangleq \sum_{j=0}^{N-2} a_j^{(1)} a_{j+1}^{(1)} , \tag{2.30}$$

then we also have $A-B=C$. Therefore,

$$A = \frac{N-1+C}{2} \tag{2.31}$$

and

$$B = \frac{N-1-C}{2} . \tag{2.32}$$

From (2.30), we find that, for random desired sequences, C is distributed as the sum of $N-1$ symmetric Bernoulli trials, so the density of C is given by

$$p_C(j) = \binom{N-1}{\frac{j+N-1}{2}} 2^{1-N} \; ; \quad j \in \{1-N, 3-N, \ldots, N-3, N-1\} . \tag{2.33}$$

Note that if any two of the four quantities A, B, C, N are known, the other two may be found by using (2.31) and (2.32).

Finally, by substituting (2.25) and (2.10) into (2.9), we determine the output statistic of receiver 1, with all signals at received power $P=2$, and given $K-1$ interfering users, rectangular chip pulses, desired data bit $b_0^{(1)}=1$, and normalized to the chip duration $T_c=1$, to be

$$Z_1 = N + \sum_{k=2}^{K} W_k \cos\Phi_k \tag{2.34}$$

where

$$W_k = P_k S_k + Q_k(1-S_k) + X_k + Y_k(1-2S_k); \quad 0 \leq S_k < T_c = 1 . \tag{2.35}$$

Since the random variables P_k, Q_k, X_k, and Y_k are composed of disjoint sets of symmetric Bernoulli trials for a particular desired signature sequence, they are conditionally independent given C. In general, the MAI is not unconditionally independent, as we can show via a counterexample.† Suppose $N=2$, so the desired sequence has C uniform on $\{-1,1\}$, and that a single interfering user has a signature sequence of $[1,1]$ and is chip- and phase-synchronized to the desired signal. In this situation, when $C=1$ the MAI is uniform on the set $\{-2,2\}$, and when $C=-1$ the MAI is 0. Averaging over the values of C at this point produces a MAI density function with impulses at -2, 0, and 2. If the MAI were unconditionally independent, then convolving this density function with itself should generate the MAI density for two interfering users. However, from the given information we know that it is impossible for two interfering users to produce MAI values of either -2 or 2, but our convolution result has impulses at -4, -2, 0, 2, and 4. We therefore conclude that the MAI produced by multiple users is not independent unless we condition on a specific C.

A signature sequence of length N has $N-1$ chip boundaries, at which the sequence may or may not change to a different value. The quantity B represents the number of chip boundaries at which a transition to a different value occurs. As a consequence, B can be treated as a measure of the amount of "spreading" given to the desired signal. For example, B is minimized when C is at a maximum of $N-1$, which is equivalent to a signature sequence of all ones (minimum spreading). Conversely, when B is maximized, C is at its minimum value of $-(N-1)$, and thus the desired signature sequence is composed entirely of chips alternating between $+1$ and -1 (maximum spreading).

† This narrative is, by necessity, elementary; the general case is given at the end of the next section.

2.4.2. Distribution of the Multiple-Access Interference

We begin the calculation of the distribution of the MAI in (2.34) by letting $K=2$ so that there is only one interfering user, and we drop the subscripts k on the affected random variables. Next, we condition on C so that the random variables P, Q, X, Y in (2.35) are conditionally independent. The density of $\hat{W} \triangleq [W \,|\, C=c]$ is perhaps most easily constructed by the "brute force" method, where we perform further conditioning upon the discrete random variables $P=p$, $Q=q$, $X=x$, and $Y=y$. The further conditioned $\hat{W}$ now becomes an affine function of S, so S uniform on $[0,1]$ implies that the conditional distribution of $\hat{W}$ is uniform on $[a,b]=[\min\{a',b'\},\max\{a',b'\}]$, where $a'=q+x+y$ and $b'=p+x-y$. After averaging over the distributions of P, Q, X, and Y, we have a collection of $f_{W|C}(w)$ which can, in turn, be averaged over the distribution of C to produce $f_W(w)$. This density is shown in Figure 2.2 for $N=31$. Note that $f_W(w)$ consists of a component with a "wedding cake" appearance (produced when the $[a,b]$ are valid intervals), coupled with a set of impulses (produced when $[a,b]$ is degenerate; that is, when $a=b$).

Our next step is to find the distribution of $W\cos\Phi$, which we designate as the random variable D, for Φ uniform on $[0,2\pi]$. Separate cases for N even and odd are avoided by assuming that N is odd. We now split $f_W(w)$ into a set of $N+1$ conditional densities, $(N+1)/2$ of which are uniform on the *set* $\{-a,a\}$, and $(N+1)/2$ of which are uniform on the *interval* $[-a,a]$, where $a \in \{1,3,\ldots,N\}$.

If a random variable $\mathbf{x}$ is uniform on $\{-a,a\}$, then $\mathbf{y}=\mathbf{x}\cos\Phi$ has the "arc-sine" density [18]

$$f_{\mathbf{y}}(y) = \frac{1}{\pi\sqrt{a^2-y^2}}; \qquad -a<y<a \tag{2.36}$$

and is 0 elsewhere. (All density functions are defined to be 0 outside their specified support intervals.) The distribution function for $\mathbf{y}$ is found by integrating (2.36) directly, giving

$$F_{\mathbf{y}}(y) = \frac{1}{2} + \frac{1}{\pi}\sin^{-1}\left[\frac{y}{a}\right]. \tag{2.37}$$

If $\mathbf{x}$ is uniform on $[-a,a]$, then $\mathbf{y}=\mathbf{x}\cos\Phi$ has density [2]

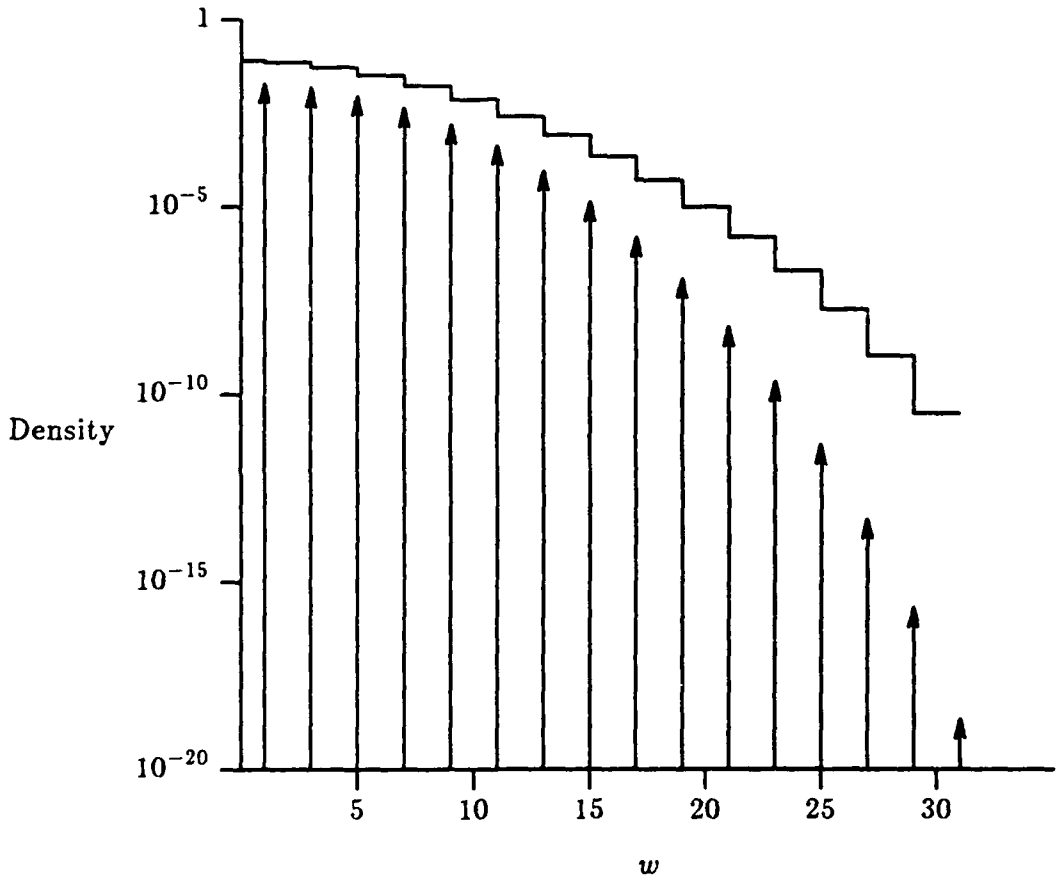

Figure 2.2. The density function of W ($N=31$, $K=2$).

$$f_{\mathrm{y}}(y) = \frac{1}{\pi a}\log\left[\frac{a+\sqrt{a^2-y^2}}{|y|}\right]; \qquad \begin{matrix} -a<y<a \\ y\neq 0 \end{matrix} \tag{2.38}$$

and distribution function

$$F_{\mathrm{y}}(y) = \frac{1}{2} + \frac{1}{\pi a}\left\{ y\log\left[\frac{a+\sqrt{a^2-y^2}}{|y|}\right] + a\sin^{-1}\left[\frac{y}{a}\right]\right\}; \tag{2.39}$$

where $\log = \log_e$. After taking an expectation over the possible values of a in the densities given by (2.36) and (2.38), the result is $f_D(d)$, which is shown in Figure 2.3. The figure also includes a plot of a Gaussian density function with the same variance for comparison.

To find the MAI density when $K \geq 3$, which we denote by $f_{\Xi}(x)$, we make use of the fact that the MAI produced by each interfering user is identically distributed and conditionally independent given C. Therefore, we must once again condition on C and find $f_{D|C}(x)$ for each of the N possible values for C. Next, each density is convolved with itself $K-2$ times and an expectation is performed over C; thus:

$$f_{\Xi}(x) = \mathrm{E}[f_{D|C}(x) * \cdots * f_{D|C}(x)]\,. \tag{2.40}$$

This function is not, in general, equal to $\mathrm{E}[f_{D|C}(x)] * \cdots * \mathrm{E}[f_{D|C}(x)] = f_D(x) * \cdots * f_D(x)$, which represents the MAI density if each interfering user produced a MAI value which was indeed unconditionally independent from that generated by the others.

2.4.3. Performing the Bounds Calculations

Since the random variable Ξ, representing the MAI produced by $K-1$ interfering users, is zero mean, symmetry in the receiver output statistic given by (2.34) allows us to find the probability of data bit error P_e by performing the integration

$$P_e = \int_{-\infty}^{-N} f_{\Xi}(x)dx\,. \tag{2.41}$$

To obtain numerical results, we are restricted to discrete representations of $f_{\Xi}(x)$, so we must be satisfied with finding either bounds on or an

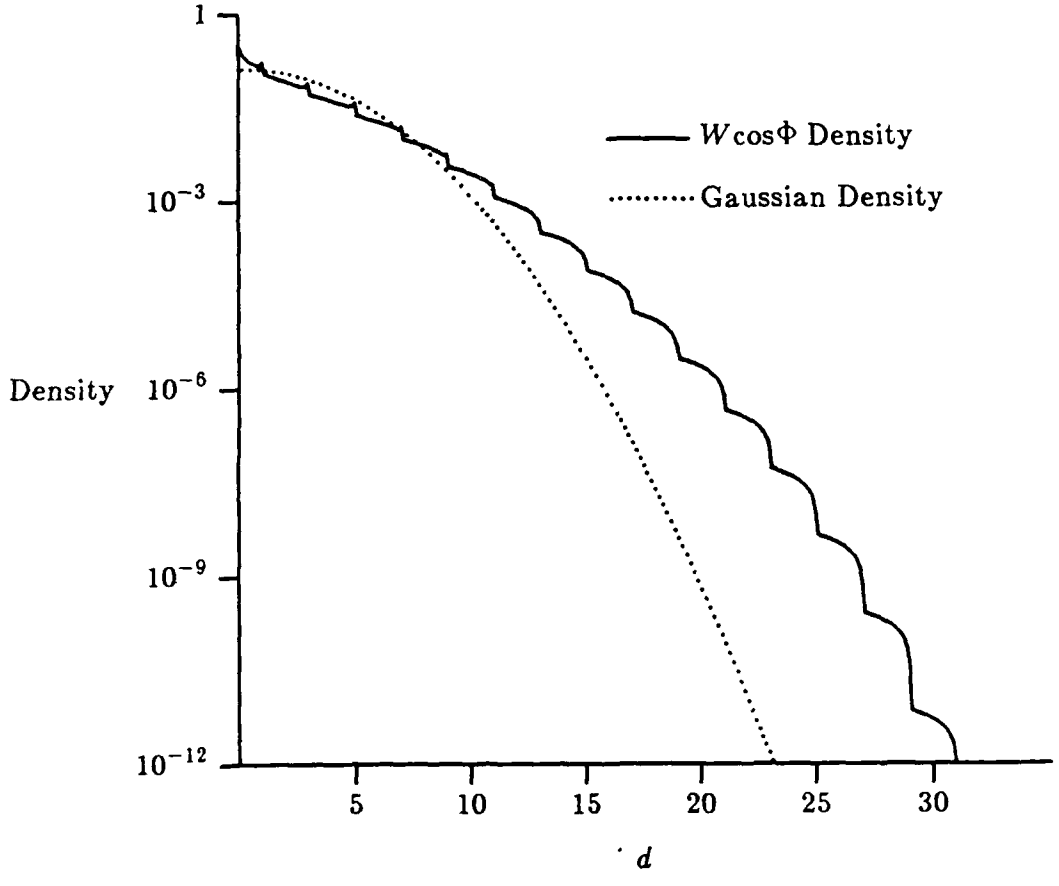

Figure 2.3. The density function of $D = W\cos\Phi$ compared with a Gaussian density having the same variance ($N = 31$, $K = 2$).

approximation to P_e. Fortunately, the bounds may be made arbitrarily tight (at the expense of increased computation time and memory requirements), so we pursue this course here. Since $K-2$ convolutions are performed on each of N densities $f_{D|C}(x)$, we avoid notational distractions by using $f(x)=f_{D|C}(x)$ with cumulative distribution function $F(x)=F_{D|C}(x)$.

To prepare $f(x)$ computationally for $K-2$ convolutions, we divide its support interval $[-N,N]$ into $2NM$ subintervals, each of length $1/M$, which we index by $0,1,\ldots,2NM-1$. The probability that the MAI is between $a=\lfloor i/M \rfloor - N$ and $b=\lfloor (i+1)/M \rfloor - N$ is $F(b)-F(a)$, which we set equal to $\tilde{f}(i)$. Note that

$$\sum_{i=0}^{2NM-1} \tilde{f}(i)=1\,. \tag{2.42}$$

After performing the convolutions and averaging over C, we obtain the discrete density $\tilde{f}_{\Xi}(i)$, $i\in\{0,1,\ldots,(K-1)(2NM-1)\}$, for the total MAI produced by $K-1$ interfering users. Upper and lower bounds on the probability of data bit error are now found by

$$P_e^{(u)} = \sum_{i=0}^{I_u} \tilde{f}_{\Xi}(i)\,; \qquad I_u = (K-2)NM+1\,, \tag{2.43}$$

and

$$P_e^{(l)} = \sum_{i=0}^{I} \tilde{f}_{\Xi}(i)\,; \qquad I_l = (K-2)(NM-1)\,. \tag{2.44}$$

We obtain (2.43) by effectively concentrating the probability mass in each subinterval of $f(x)$ onto the subinterval's *leftmost* point prior to performing the convolutions [2]. This maximizes the total probability mass in $\tilde{f}_{\Xi}(i)$ on the "wrong" side of the receiver threshold, producing an *upper bound* on P_e. If the mass is instead effectively concentrated on the *rightmost* point of its corresponding subinterval, then summing the values on the "wrong" side of the receiver detection threshold after performing the convolutions produces a *lower bound* on P_e, given by (2.44).

The procedure of calculating bounds on the probability of data-bit error can now be summarized. We first condition the desired signal on C and then perform the following steps (computational complexity order is shown in

parentheses):

1. Construct the density of W for each C (N^3);
2. Find the density for $W\cos\Phi$ for each C (N^3M);
3. Convolve the density of $W\cos\Phi$ for each C with itself $K-2$ times (KN^3M^2);
4. Average the set of densities over C (KN^2M);
5. Calculate bounds on P_e (KNM).†

We conclude that arbitrarily tight bounds on the probability of data-bit error in a DS/SSMA communication system may be determined by using a five-step procedure of computational complexity which is of order KN^3M^2.

2.5. The Standard Gaussian Approximation

In a narrow-band communication system with additive noise present at a correlation receiver, a data bit error occurs when the integrated amplitude of the noise exceeds the integrated amplitude of the desired signal in the opposite direction, causing a decision block error at the receiver. If the noise is a zero-mean Gaussian process, then the probability of bit error may be calculated by first finding the signal-to-noise ratio (SNR). Next, Q[SNR], defined by

$$Q[x] = \frac{1}{\sqrt{2\pi}} \int_x^\infty e^{-u^2/2} du, \tag{2.45}$$

is used to evaluate the probability that a wrong decision is made at the receiver and a data bit error occurs. Additionally, if the noise is white, then its autocorrelation function is impulsive, and the process produces values which are uncorrelated (and hence independent) from instant to instant in time. Thus channel errors are also independent from data bit to data bit.

One may wonder whether it is possible to model multiple-access interference in a DS/SSMA system as an additive white Gaussian noise process with variance equal to the MAI variance. It is obvious from (2.34) that the

† Actual computation time may be reduced by omitting step 4, performing step 5 for each conditional density, and then averaging the conditional P_e over C.

MAI is additive, but the plot in Figure 2.3 shows that modeling the MAI as a Gaussian random variable may not be accurate. Since we have a method to calculate bounds on the probability of data bit error caused by the MAI, we can check the accuracy of the Gaussian approximation by finding the MAI variance, calculating the SNR, evaluating (2.45), and comparing the results to the actual probability of data bit error. Testing whether or not the MAI is white (or almost white), so that data bit errors may be treated as essentially independent, is a bit more difficult. To do this, we must examine the effect of the MAI on a collection of data bits called a "packet", a task which is postponed until Chapter 3.

One of the advantages of using a Gaussian approximation to the MAI produced by a single interfering user is that we gain unconditional independence from the MAI generated by the other interfering users within a single desired data bit. Recall from Section 2.4.2 that the actual MAI from each interfering user is only conditionally independent given C, but we now show that the MAI is, in fact, uncorrelated.

From the structure of the density functions for the random variables P_k, Q_k, X_k, and Y_k from (2.35), we find that, for $k \in \{2, \ldots, K\}$ and $\Gamma_k \in \{P_k, Q_k, X_k, Y_k\}$,

$$\mathrm{E}[\Gamma_k | C] = 0 \tag{2.46}$$

for any C. Combining (2.46) and (2.35), we have

$$\mathrm{E}[W_k \cos\Phi_k | C] = 0. \tag{2.47}$$

We also know that the MAI is conditionally independent given C, which allows us to write

$$\mathrm{E}[W_j \cos\Phi_j W_k \cos\Phi_k | C] = \mathrm{E}[W_j \cos\Phi_j | C]\,\mathrm{E}[W_k \cos\Phi_k | C] \tag{2.48}$$

for $j,k \in \{2, \ldots, K\}$ and $j \neq k$. Taking expectations of both sides of (2.48) over C and substituting values from (2.47) gives

$$\mathrm{E}[W_j \cos\Phi_j W_k \cos\Phi_k] = \mathrm{E}[W_j \cos\Phi_j]\,\mathrm{E}[W_k \cos\Phi_k] = 0 \tag{2.49}$$

and thus the MAI produced by each interfering user is uncorrelated (and orthogonal) to that from the others. If we model the MAI as a Gaussian random variable, then the MAI components are also unconditionally independent.

2.5.1. Variance of the Multiple-Access Interference

Calculating a general expression for the multiple-access interference variance is facilitated by conditioning on C (or, equivalently, B) and by conditioning on the relative delays and phases of all interfering signals. For notational convenience, we express the delays and phases of the interfering signals as random vectors $\underline{S}=(S_2, \ldots, S_K)$ and $\underline{\Phi}=(\Phi_2, \ldots, \Phi_K)$. We also assume that N, the number of chips per bit, and K, the number of simultaneous users, are fixed.†

Since the random variables P_k, Q_k, X_k, and Y_k in (2.35) are zero mean and conditionally independent (given B), we conclude that the MAI term in (2.34) is zero-mean and each term of the summation is conditionally independent. By using the fact that the variance of the sum of zero mean independent random variables is the sum of their second moments, the conditional variance Ψ of the MAI is given by

$$\begin{aligned}\Psi \triangleq \mathrm{Var}\left[\mathrm{MAI}\middle|\underline{S},\underline{\Phi},B\right] &= \mathrm{E}\left[\left(\sum_{k=2}^{K} W_k\cos\Phi_k\right)^2\middle| S_k,\Phi_k,B\right] \\ &= \sum_{k=2}^{K}\mathrm{E}\left[W_k^2\middle|S_k,B\right]\mathrm{E}\left[\cos^2\Phi_k\middle|\Phi_k\right] \\ &= \sum_{k=2}^{K}\tfrac{1}{2}\left[1+\cos(2\Phi_k)\right]\mathrm{Var}\left[W_k\middle|S_k,B\right].\end{aligned} \tag{2.50}$$

The conditional variance of $W = W_k$ is calculated as follows:

$$\begin{aligned}\mathrm{Var}[W\,|S,B] = \mathrm{E}[P^2S^2|S] + \mathrm{E}[Q^2(1-S)^2|S] + \mathrm{E}[X^2|B] \\ + \mathrm{E}[Y^2(1-2S)^2|S,B].\end{aligned} \tag{2.51}$$

Since P and Q are uniform on $\{-1,1\}$, their variance is 1. The variance of X can be found by expressing X as a sum of $A=N-B-1$ symmetric Bernoulli trials and noting that

† In a later chapter, K will be treated as a random variable.

$$\mathrm{Var}[X|B] = \sum_{j=1}^{N-B-1} \mathrm{Var}[\mathbf{b}_j] = N-B-1 . \tag{2.52}$$

By similar reasoning,

$$\mathrm{Var}[Y(1-2S)|S,B] = B(1-2S)^2. \tag{2.53}$$

Combining the above yields

$$\Psi = \sum_{k=2}^{K} Z_k \tag{2.54}$$

where the Z_k are identically distributed and conditionally independent given B, and $Z = Z_k$ is specified by

$$Z = UV, \tag{2.55}$$

with

$$U = 1+\cos(2\Phi) , \tag{2.56}$$

$$V = (2B+1)(S^2-S)+N/2 . \tag{2.57}$$

Now we can determine the average MAI variance and use it to find an estimate for the average probability of data bit error. If the interfering signals are not chip and phase synchronous with the desired signal, then the average MAI variance is found by substituting expected values for S^2-S and $\cos(2\Phi)$ into (2.56) and (2.57). Since Φ is uniform on $[0,2\pi]$ it follows that $\mathrm{E}[\cos(2\Phi)] = 0$, and S uniform on $[0,1]$ implies that

$$\mathrm{E}[S^2-S] = \mathrm{E}[S^2] - \mathrm{E}[S] = \int_0^1 s^2 ds - \int_0^1 s ds \tag{2.58}$$

$$= -\frac{1}{6} .$$

Substituting into (2.55) gives

$$\mathrm{E}[Z|B] = \frac{3N-2B-1}{6} . \tag{2.59}$$

If the desired signature sequence is known, then B is also known and can be substituted into (2.59). Note that as B varies from 0 (minimum spreading) to $N-1$ (maximum spreading), the MAI variance ranges from a maximum value

of $(3N-1)/6$ to a minimum value of $(N+1)/6$.

If the desired sequence is random, then $\mathrm{E}[C]=0$, which implies that $\mathrm{E}[B]=(N-1)/2$, giving

$$\mathrm{E}[Z] = \mathrm{E}[\mathrm{E}[Z|B]] = \frac{N}{3} . \tag{2.60}$$

Since the MAI from each interfering user is uncorrelated to that produced by the other interfering users, the variances add, so that the total MAI variance from $K-1$ interfering users is $(K-1)N/3$. To find the probability of data bit error using the Gaussian approximation for the MAI, we treat Z_1 from (2.34) as a Gaussian random variable with mean N and variance $(K-1)N/3$. The average signal-to-noise ratio is then

$$\overline{\mathrm{SNR}} = \frac{\mu}{\sqrt{\mathrm{E}[\Psi]}} = \frac{N}{\sqrt{(K-1)N/3}} = \left(\frac{3N}{K-1}\right)^{1/2}, \tag{2.61}$$

which is identical to a result stated, but not derived, in [4]. The probability of data bit error is then approximated by

$$\hat{P}_e = \mathrm{Q}[\overline{\mathrm{SNR}}]. \tag{2.62}$$

At this point we digress for a moment and show the utility of using (2.55) to find the MAI variance under various chip and phase situations. For random desired sequences, substituting $\mathrm{E}[B] = (N-1)/2$ into (2.57) produces

$$\mathrm{E}[Z|S,\Phi] = N(S^2-S+1/2)[1+\cos(2\Phi)] . \tag{2.63}$$

If interfering signals are chip and phase aligned with the desired signal, for example, then $\mathrm{E}[Z|S=0,\Phi=0] = N$, resulting in

$$\mathrm{SNR}_1 = \left(\frac{N}{K-1}\right)^{1/2}, \tag{2.64}$$

which also represents a worst-case SNR [19]. Using similar reasoning, interfering signals that are chip aligned with random phases have

$$\mathrm{SNR}_2 = \left(\frac{2N}{K-1}\right)^{1/2}, \tag{2.65}$$

while phase aligned interfering signals with random chip delays produce

$$\mathrm{SNR}_3 = \left(\frac{3N}{2(K-1)} \right)^{1/2}. \tag{2.66}$$

2.5.2. Accuracy of the Standard Gaussian Approximation

Returning once again to interfering signals with random delays and phases, we can now compare the results of the Standard Gaussian Approximation to the bounds on P_e (Figure 2.4), and we note that the approximation seems to be accurate only for rather large K. Large K implies a high P_e and poor system performance, so a designer will be more interested in accurate values for P_e when K is small and the bit error rate is low. Unfortunately, the Standard Gaussian Approximation is not only inaccurate in this region, but becomes very optimistic as N grows; consequently, using this approximation to model multiple-access interference could result in a bit error rate that is higher than expected. The alternative is to use the bounds derived in [2] and Section 2.3 at the expense of higher computational complexity.

The above results show that, in general, multiple-access interference cannot be accurately modeled as a Gaussian random variable when $\mathcal{S}$ and Φ are random unless the number of simultaneous users is large. To discover why this is so, it will be useful to study how the Central Limit Theorem is used to justify the Standard Gaussian Approximation, and perhaps we can discover a way to improve the accuracy of this approximation for smaller values of K.

2.6. Multiple-Access Interference and the Central Limit Theorem

The Central Limit Theorem is often quoted as justification for using some form of a Gaussian approximation for the multiple-access interference density function when N is large (see, for example, [20]). However, we just showed that a large number of simultaneous users K seems to be necessary for the Standard Gaussian Approximation to be accurate, regardless of the number of chips per data bit N. Fortunately, though, there are specific conditions under which the Central Limit Theorem does allow us to accurately approximate the

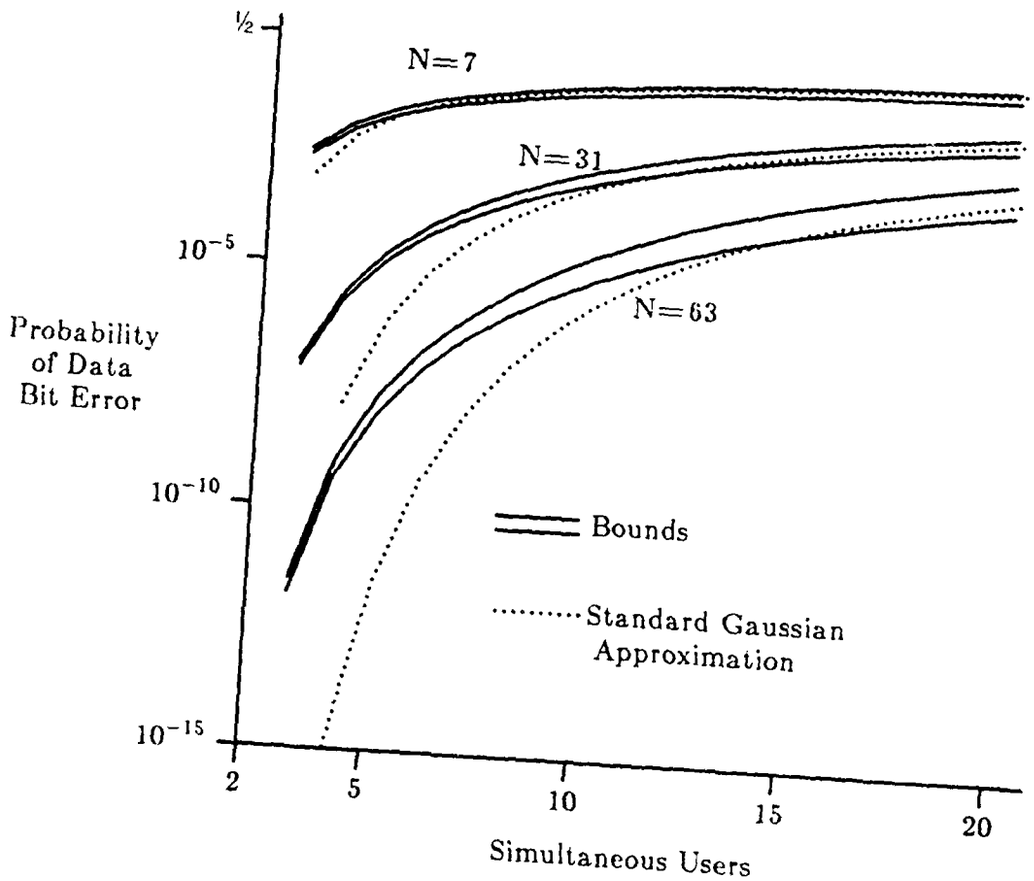

Figure 2.4. Bounds on the probability of data bit error vs the number of simultaneous users for $N=7$, 31, and 63, compared to results from the Standard Gaussian Approximation.

multiple-access interference by a Gaussian random variable for large N and for any value of K. We will then use this intermediate result to derive the Improved Gaussian Approximation for the probability of data bit error, and we show that this approximation is more accurate than the Standard Gaussian Approximation and more computationally efficient than calculating bounds on P_e.

We begin by stating without proof a form of the Central Limit Theorem which is useful for our applications [21]:

Theorem 2.1 (Central Limit). Let $X_1, X_2, \ldots, X_n, \ldots$ be a sequence of zero mean iid random variables, each with finite variance σ^2. Let

$$Z_n = \frac{S_n}{\sqrt{n}}, \qquad n = 1, 2, \ldots \tag{2.67}$$

be the normalized sequence, where $S_n = \sum_{j=1}^{n} X_j$. Then

$$\lim_{n\to\infty} Z_n \sim \tilde{N}(0,\sigma^2) \tag{2.68}$$

where $\tilde{N}(\mu,\sigma^2)$ denotes a Gaussian random variable with mean μ and variance σ^2, and "$\sim$" means "is distributed as".

To examine the effect of the Central Limit Theorem on the multiple-access interference, we normalize the receiver output statistic in (2.34) by N and K as follows:

$$\begin{aligned} \zeta_1 \triangleq \frac{1}{\sqrt{N(K-1)}} Z_1 &= \frac{1}{\sqrt{N(K-1)}} \left(N + \sum_{k=2}^{K} W_k \cos\Phi_k \right) \\ &= \left(\frac{N}{K-1} \right)^{1/2} + \frac{1}{\sqrt{N(K-1)}} \sum_{k=2}^{K} W_k \cos\Phi_k \ . \end{aligned} \tag{2.69}$$

The first term on the right side of (2.69) is deterministic and represents the mean value of the normalized receiver output statistic, while the terms in the summation express the MAI as a zero mean random variable.

2.6.1. Many Simultaneous Users

We begin our investigation into the effect of a large number of simultaneous users by fixing N and allowing $K \rightarrow \infty$. The Central Limit Theorem may be applied directly, giving

$$\lim_{K\rightarrow\infty} \zeta_1 = \lim_{K\rightarrow\infty} \left(\frac{N}{K-1} \right)^{1/2} + \frac{1}{\sqrt{N}} \lim_{K\rightarrow\infty} \frac{1}{\sqrt{K-1}} \sum_{k=2}^{K} W_k \cos\Phi_k \qquad (2.70)$$

$$\sim \tilde{N}(0, 1/3).\dagger$$

Since the MAI converges in distribution to a Gaussian random variable, the $Q[x]$ function given by (2.45) may be used to accurately find the probability of data bit error for large K. The mean of the normalized receiver output statistic is $\sqrt{N/(K-1)}$ from (2.69), but this value converges to 0 as $K \rightarrow \infty$, leading to the result

$$\lim_{K\rightarrow\infty} P_e = Q[0] = 1/2 \, . \qquad (2.71)$$

This is not surprising, since increasing the number of simultaneous users for fixed finite N eventually results in a useless channel.

We conclude that for a large but finite K, the normalized receiver output statistic can be accurately modeled as a Gaussian random variable with mean $\sqrt{N/(K-1)}$ and variance 1/3, producing an average SNR of $\sqrt{3N/(K-1)}$. This result holds even for a relatively small N. For a large N and small K, however, the applicability of the Central Limit Theorem is a bit more subtle, a situation which we examine next.

† At first, it seems odd that the variance of this random variable does not depend upon N. However, by multiplying both sides of (2.69) by $\sqrt{N}$, the normalization by N is removed and the MAI then converges in distribution to $\tilde{N}(0, N/3)$, which agrees with the MAI variance given by (2.60).

2.6.2. Many Chips per Data Bit

To analyze the effect of a large N on the distribution of the multiple-access interference, we must use care because N acts differently upon each of the various terms of W_k given by (2.35). We begin by fixing K, B, $\underline{S}=\underline{s}$, and $\underline{\Phi}=\underline{\phi}$, and by bringing the normalization factor $1/\sqrt{N}$ into the summation of (2.69), giving

$$\zeta_1 = \left(\frac{N}{K-1}\right)^{1/2} + \frac{1}{\sqrt{K-1}} \sum_{k=2}^{K} W'_k \cos\phi_k \ , \tag{2.72}$$

where

$$W'_k = \frac{P_k s_k}{\sqrt{N}} + \frac{Q_k(1-s_k)}{\sqrt{N}} + \frac{X_k}{\sqrt{N}} + \frac{Y_k(1-2s_k)}{\sqrt{N}} . \tag{2.73}$$

At this point, we find it convenient to introduce a quantity called the *spreading factor* $\eta \in [0,1]$, defined as

$$\eta \triangleq \frac{B}{N-1} . \tag{2.74}$$

Holding η constant as N varies has the same effect as allowing B to vary in proportion to $N-1$. For notational convenience, we drop the subscripts k and rewrite (2.73) as

$$W' = \frac{s}{\sqrt{N}}\mathbf{b}_P + \frac{1-s}{\sqrt{N}}\mathbf{b}_Q + \frac{1}{\sqrt{N}} \sum_{i=1}^{(1-\eta)(N-1)} \mathbf{b}_i + \frac{1-2s}{\sqrt{N}} \sum_{j=1}^{\eta(N-1)} \mathbf{b}_j \ , \tag{2.75}$$

where we have expressed A and B in terms of the spreading factor η, and P, Q, X, and Y have been represented as an appropriate sum of symmetric Bernoulli trials. As N becomes large, the first two terms on the right side of (2.75) vanish and the limit becomes, for $\eta \in (0,1)$,

$$\begin{aligned} \lim_{N\to\infty} W' &= \lim_{N\to\infty} \frac{1}{\sqrt{N}} \sum_{i=1}^{(1-\eta)(N-1)} \mathbf{b}_i + \lim_{N\to\infty} \frac{1-2s}{\sqrt{N}} \sum_{j=1}^{\eta(N-1)} \mathbf{b}_j \\ &= \sqrt{1-\eta} \lim_{N\to\infty} \frac{1}{\sqrt{(1-\eta)N}} \sum_{i=1}^{(1-\eta)(N-1)} \mathbf{b}_i + \sqrt{\eta}(1-2s) \lim_{N\to\infty} \frac{1}{\sqrt{\eta N}} \sum_{j=1}^{\eta(N-1)} \mathbf{b}_j \\ &= \sqrt{1-\eta} \lim_{n\to\infty} \frac{1}{\sqrt{n}} \sum_{i=1}^{n} \mathbf{b}_i + \sqrt{\eta}(1-2s) \lim_{n\to\infty} \frac{1}{\sqrt{n}} \sum_{j=1}^{n} \mathbf{b}_j \ . \end{aligned} \tag{2.76}$$

The Central Limit Theorem can now be employed to show that the first term

in (2.76) converges in distribution to $\tilde{N}(0, 1-\eta)$, and the second term converges in distribution to $\tilde{N}(0, \eta(1-2s)^2)$. For $\eta=0$, (2.76) converges in distribution to $\tilde{N}(0,1)$, and when $\eta=1$, (2.76) converges to $\tilde{N}(0,(1-2s)^2)$. The two terms on the right side of (2.76) represent a normalized form of the random variables X_k and Y_k in (2.35), which are conditionally independent when given B.

Now the reason for fixing Φ and S becomes clear: under these conditions, as $N\longrightarrow\infty$, equation (2.69) becomes a *linear combination* of independent Gaussian random variables, and hence the normalized receiver output statistic ζ_1 is also Gaussian with mean $\sqrt{N/(K-1)}\longrightarrow\infty$ and variance

$$\sigma^2 = \frac{1}{K-1}\sum_{k=2}^{K}\left[1+4\eta(s_k^2-s_k)\right]\cos^2\phi_k\,. \tag{2.77}$$

Once again, we employ the $Q[x]$ function to find the probability of data bit error as $N\longrightarrow\infty$, giving for finite K,

$$\lim_{N\to\infty} P_e = Q[\infty] = 0. \tag{2.78}$$

This result leads to the logical conclusion that as the number of chips per data bit increases for fixed finite K, the communication channel eventually becomes noiseless.

We now make the important observation that for large but finite N, *provided* relative delays S_k and phases Φ_k are fixed, and for a particular η and hence a particular B, the normalized receiver output statistic can be closely approximated by a Gaussian random variable with mean $\sqrt{N/(K-1)}$ and variance given by (2.77). This observation provides the basis for a new technique, called the Improved Gaussian Approximation, for finding the probability of data bit error in a DS/SSMA communication system. This technique is very accurate even for small K, and has computational complexity equivalent to that of finding bounds on P_e. In addition, the Improved Gaussian Approximation lays the groundwork for calculating the effect of bit-to-bit error dependence, the details of which are in Chapter 3.

2.7. The Improved Gaussian Approximation

Returning to equation (2.50), we note that the conditional MAI variance Ψ is a function of the delays and phases of all interfering signals and of the desired sequence structure expressed through the quantity B; consequently, each outcome $\Psi=\psi$ is produced by specific outcomes of $\mathcal{S}$, Φ, and B. In addition, results from the previous section show that as N becomes large, $Q[N/\sqrt{\psi}]$ gives an accurate approximation of P_e for a particular ψ. Therefore, if we can find the distribution of Ψ, then the approximate probability of data bit error can be calculated directly by

$$\hat{P}_e = \mathrm{E}\left[\mathrm{Q}\left[\frac{N}{\sqrt{\Psi}}\right]\right] = \int_0^\infty \mathrm{Q}\left[\frac{N}{\sqrt{\psi}}\right] f_\Psi(\psi)\,d\psi\,. \tag{2.79}$$

At first, the task of finding $f_\Psi(\psi)$ appears extremely complex, since there may be numerous interfering signals, each of which has an infinite number of possible values for S and Φ. However, the k-th user's signal variance Z_k given by (2.54)-(2.57) is independent of and identically distributed to the variance of the other users, so we can proceed by first finding the distribution of the variance produced by a single user.

2.7.1. Distribution of the Multiple-Access Interference Variance

The distribution of Z from (2.55) is found as follows. Since Φ is uniform on $[0,2\pi]$, U has a form of arc-sine distribution [18] with density

$$f_U(u) = \frac{1}{\pi\sqrt{u(2-u)}}\,; \qquad 0 < u < 2. \tag{2.80}$$

(As before, all density functions are defined to be 0 outside their specified support intervals.) The conditional density of V is determined to be†

$$f_{V|B}(v) = \frac{1}{\sqrt{\tilde{B}(2v+\tilde{B}-N)}}\,; \qquad \frac{N-\tilde{B}}{2} < v < \frac{N}{2}, \tag{2.81}$$

where $\tilde{B} = B+\frac{1}{2} = (N-C)/2$. Finally, we note that U and V are

† The derivations of (2.81), (2.82), and (2.84) are given in the Appendix.

independent, allowing us to construct the density of $Z = UV$ as

$$f_{Z|B}(z) = \frac{1}{2\pi\sqrt{\tilde{B}z}} \log \left| \frac{\sqrt{N-z} + \sqrt{\tilde{B}}}{\sqrt{N-z} - \sqrt{\tilde{B}}} \right|; \qquad \begin{matrix} 0 < z \leq N \\ z \neq N-\tilde{B} \end{matrix} \tag{2.82}$$

where $\log = \log_e$. Next, we remove the conditioning on B and obtain the result

$$f_Z(z) = \mathrm{E}[f_{Z|B}(z)] = 2^{1-N} \sum_{j=0}^{N-1} \binom{N-1}{j} f_{Z|j}(z). \tag{2.83}$$

This density is plotted in Figure 2.5 for $N = 31$. The cumulative distribution function of $Z|B$ may be found by integrating (2.82), giving

$$\begin{aligned} F_{Z|B}(z) = 1 + \frac{1}{\pi\sqrt{\tilde{B}}} \Bigg\{ & \sqrt{N-\tilde{B}} \log \left| \frac{b(a^2+c^2)}{a(b^2+c^2)} \right| \\ & - 2\sqrt{\tilde{B}} \sin^{-1} \left[\left| \frac{N-z}{N} \right|^{1/2} \right] \\ & + \sqrt{z} \log \left| \frac{a}{b} \right| \Bigg\}; \qquad 0 \leq z \leq N, \end{aligned} \tag{2.84}$$

where

$$\begin{aligned} a &= \sqrt{N-z} + \sqrt{\tilde{B}}\,; \\ b &= \sqrt{N-z} - \sqrt{\tilde{B}}\,; \\ c &= \sqrt{N-\tilde{B}} + \sqrt{z}\,. \end{aligned}$$

Since the Z_k in (2.54) are conditionally independent given B, the density of the total MAI variance Ψ is

$$f_\Psi(z) = \mathrm{E}[f_{Z|B}(z) * \cdots * f_{Z|B}(z)] \tag{2.85}$$

with $K-2$ convolutions being performed. $\hat{P}_e$ is now found by evaluating (2.79).

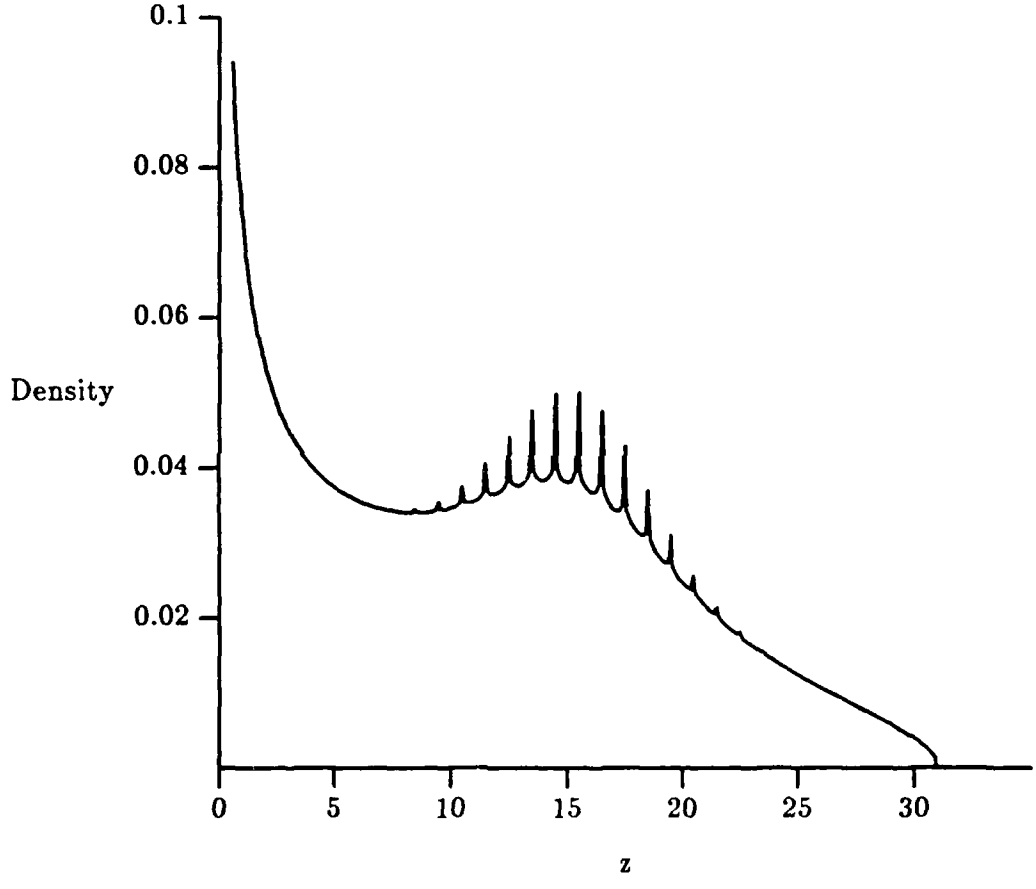

Figure 2.5. The density function of Z ($N=31$, $K=2$).

2.7.2. Computation Methods and Accuracy

To prepare $f_{Z|B}(z) = f(z)$ computationally for $K-2$ convolutions, we divide the interval $[0,N]$ into NM subintervals, each of length 1/M, and note that the probability that the MAI variance is between i/M and $(i+1)/M$ is $F((i+1)/M) - F(i/M)$, which we set equal to $\tilde{f}(i)$. By concentrating the probability mass in each subinterval onto its center point, we approximate the continuous $f(z)$ with a discrete $\tilde{f}(i)$ that is still a valid density; i.e.,

$$\sum_{i=0}^{NM-1} \tilde{f}(i) = 1. \tag{2.86}$$

However, while the support of $f(z)$ is $[0,N]$, the domain of $\tilde{f}(i)$ only extends from $1/(2M)$ to $N-[1/(2M)]$. Therefore, we must use care after performing the discrete convolutions of $\tilde{f}(i)$ and averaging over B to insure that each value of the new discrete density is subsequently matched to the proper MAI variance when evaluating (2.62). Specifically,

$$\tilde{f}_{\psi}(i) = \Pr\left\{\psi = \frac{2i+K-1}{2M}\right\}; \quad i \in \{0, 1, \ldots, (K-1)(NM-1)\}, \tag{2.87}$$

thus

$$\hat{P}_e = \sum_{i=0}^{I} Q\left[\frac{N}{\sqrt{y(i)}}\right] \tilde{f}_{\psi}(i), \tag{2.88}$$

where

$$I = (K-1)(NM-1) \tag{2.89}$$

and

$$y(i) = \frac{2i+K-1}{2M}. \tag{2.90}$$

In summary, calculating P_e using the Improved Gaussian Approximation requires the following steps (as before, computational complexity order is shown in parentheses):

1. Construct the density of the variance of $W\cos\Phi$ for each C (N^2M);
2. Convolve the density of the MAI variance for each C with itself $K-2$ times (KN^3M^2);

3. Average the set of densities over the distribution of C (KN^2M);

4. Perform an expectation to obtain an approximation for P_e (KNM).

Thus the Improved Gaussian Approximation is a four-step procedure with an order KN^3M^2 computational complexity.† Figure 2.6 compares the Improved Gaussian Approximation to bounds on P_e, showing that this approximation is quite accurate for all values of K, even when N is surprisingly small.

2.7.3 Deterministic Desired Sequences

The final step in calculating the density function for the random variable Ψ is to average over all possible values of B, shown in (2.85). However, the performance of a specific desired sequence in a multiple-access environment where all interfering sequences are random may be found by simply finding the density $f_{Z|B}(z)$ for the value of B associated with the signature sequence, and then evaluating (2.85) and (2.88). At the end of Section 2.4.1 we pointed out that B may be treated as a measure of the amount of "spreading" given to a desired signal, so we would expect that the bit error rate improves as B increases. Figure 2.7 shows this effect as B progresses from 0 (minimum spreading) to $N-1$ (maximum spreading) for $N=31$. The plot for $B=0$ is especially interesting; this represents the performance of a narrow-band signal in a direct-sequence spread-spectrum environment where the interfering signals have random signature sequences.

2.8. Conclusion

We have shown that the multiple-access interference can be modeled as an additive Gaussian process for all practical values of N, as long as all interfering signals have fixed delay and phase relative to the desired signal.

† Since we have shown that both Gaussian approximations converge to the actual P_e for large K, one could reduce computation time still further by comparing P_e obtained by the Standard Gaussian Approximation to that produced by the Improved Gaussian Approximation as K increases. Once the two values were within a specified error bound, the Standard Gaussian Approximation could be used exclusively for computations involving larger K.

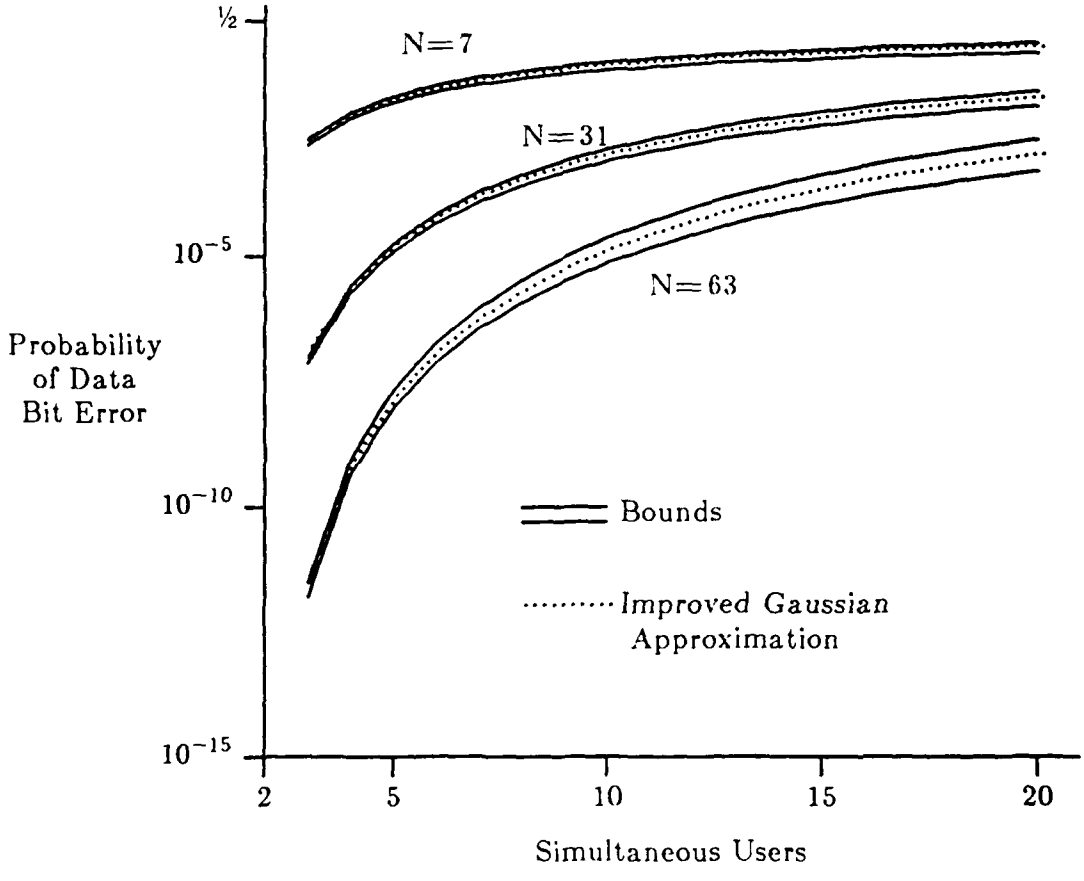

Figure 2.6. Bounds on the probability of data bit error vs the number of simultaneous users for $N=7$, 31, and 63, compared to results from the Improved Gaussian Approximation.

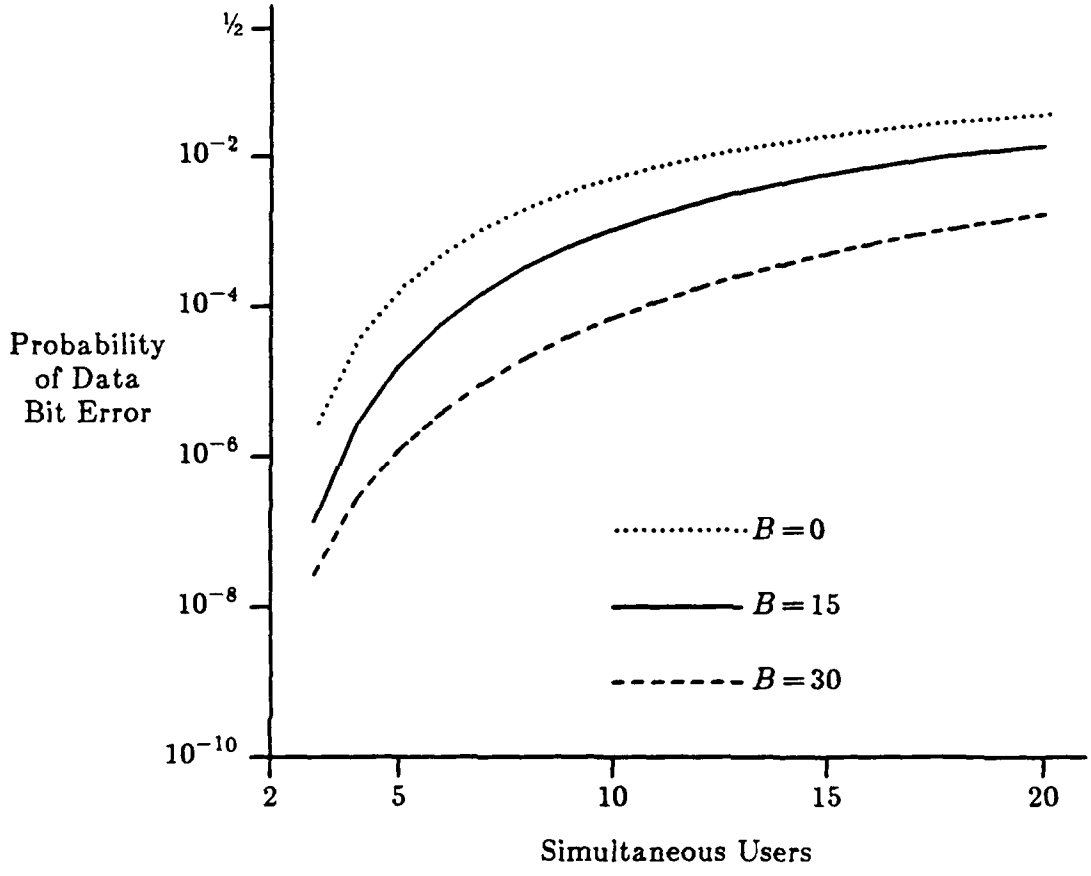

Figure 2.7. Probability of data bit error using the Improved Gaussian Approximation for various values of B ($N=31$).

The MAI variance can be expressed as a function of the delay and phase values, and thus is itself a random variable. We found the distribution of this random variable and discovered that an accurate approximation to the probability of data bit error may be calculated by averaging the $Q[x]$ function over this distribution. In the next chapter, we show that, in general, multiple-access interference does not produce independent error events within a packet of transmitted bits, and hence cannot be treated as a white noise process. However, if we again fix the delays and phases of all interfering signals, independent bit errors result, and the probability of packet success can be found by using some of the techniques developed in this chapter.

CHAPTER 3
THE DATA LINK LAYER: PROBABILITY OF PACKET SUCCESS

3.1. Introduction

The purpose of the *data link layer* is to provide the functional and procedural means to transfer data between network entities and to detect and possibly correct errors which may occur in the physical layer [1]. One method of accomplishing this task is to divide a message into one or more sets of data bits called a "packet", and to transmit each packet separately. A packet normally consists of a *preamble,* used for initial receiver synchronization, followed by the *header,* which contains routing and destination information. Next, the *data* is sent, and finally, some type of *error control* is appended to allow the receiver to determine if the packet was received correctly [16]. Error control may also be incorporated into the packet in such a way to allow a number of data errors to be corrected as well, thus improving packet throughput in situations where the bit error rate is greater than zero.

For a packet to be successful, the destination receiver must not be busy, correct synchronization must occur, and the data portion of the packet must be received error-free or, if error correction capability exists, the packet must not have more errors than the error control code can correct. Analysis in this chapter is directed toward finding the probability of packet success given that the desired receiver is not busy and has already synchronized to the desired signal containing the packet. As before, we let multiple-access interference cause all of the data bit errors in the desired signal, and all interfering signals have random signature sequences which are different for each consecutive data bit.

Because of the special nature of DS/SSMA signals, error dependence exists from bit-to-bit, and finding the probability of a successful packet is not particularly straightforward. The theory of moment spaces allows us to gain valuable insight into packet performance when bit-to-bit error dependence produces a communication channel with memory. We do this by examining three general cases: packets with no error correction capability, and packets using block error correcting codes over both lightly and heavily loaded channels. The utility of moment space bounds is limited, however, since these bounds cannot be made arbitrarily tight. We therefore turn to the Improved Gaussian Approximation, developed in Chapter 2, for numerical results. These results are then compared with other methods which employ various "short cuts", such as using the Standard Gaussian Approximation and ignoring bit-to-bit error dependencies.

Some of the analysis techniques used in this chapter require treating the probability of data bit error P_e and other related quantities as *random variables,* where we eventually calculate their expectation. In most cases, it will be obvious out of context whether the random variable or its corresponding expectation is being used. In places where ambiguity may be present, we use an overbar for the average value; i.e., $\bar{P}_e = \mathrm{E}[P_e]$.

3.2. Mapping Successful Bits to Successful Packets

Suppose a packet of length L bits is transmitted over a memoryless binary symmetric communication channel with average probability of data bit error P_e. Assuming no error correction capability, the average probability of packet error is

$$P_E = 1 - (1-P_e)^L. \tag{3.1}$$

To simplify notation, we define the probability of a successful data bit as $Q_e = 1 - P_e$ and the probability of a successful packet as

$$Q_E = 1 - P_E = (Q_e)^L. \tag{3.2}$$

If the packet includes block error control capability that can correct t or fewer errors, the probability of packet success becomes

$$Q_E = \sum_{i=0}^{t} \binom{L}{i} (1-Q_e)^i (Q_e)^{L-i} \tag{3.3}$$

which is simply the sum of the first $t+1$ terms of the binomial expansion of $[(1-Q_e)+Q_e]^L$. Under multiple-access interference in the direct-sequence spread-spectrum environment, however, the channel now has memory due to the nature of the interfering signals, and using (3.3) to find the probability of a successful packet may not be accurate.

3.3. The Origins of Bit-to-Bit Error Dependence

One of the analytical challenges presented by the nature of the multiple-access interference on the communication channel is bit-to-bit error dependence. Although the data sequence $b(t)$ and the chip sequence $a(t)$ are modeled as random and independent from bit to bit (chip to chip), error event dependence stems partly from the fact that the relative delays S_k of the interfering signals, while randomly selected at the start of a transmission, may be essentially constant over the duration of a desired packet. It is also possible that the r-f carrier stability of each transmitted signal may be such that the phases Φ_k of all interfering signals are also essentially constant over the duration of the packet. (On the other hand, since the desired receiver is not phase-locked to any of the interfering signals, we may find that phase jitter in the interfering signals allows us to perform some degree of phase averaging at the data bit level.) We consider two cases of dependency: interfering signals that have constant phases and delays over the duration of the packet, and interfering signals which produce constant delays but random phases from bit-to-bit relative to the desired signal. Since the duration of a chip is assumed large compared to that of a single r-f carrier cycle, random bit-to-bit phases can coexist with delays which are essentially constant over a desired packet. The magnitudes of the interfering terms in (2.9) depends on the $\underline{S} = (S_2, \ldots, S_K)$ through the cross-correlation functions, and on the $\underline{\Phi} = (\Phi_2, \ldots, \Phi_K)$ through the cosine terms. There is, however, no dependence upon the term l in (2.17) since the signature sequence changes for consecutive data bits in each interfering signal. As a result, if both delays and phases of

all interfering signals are random from bit-to-bit within the desired signal, then the error events are indeed independent.

For analysis to progress with reasonable effort, it is tempting to somehow assume independent bit error events within a packet. This can be done by working with the worst-case SNR shown in (2.64), which avoids dependencies by fixing $\Phi=\underline{0}$ and $S=\underline{0}$, or by merely using the average SNR in (2.61) and ignoring the dependencies. We now present a method which will allow a more accurate calculation of the average probability of packet success by incorporating into the analysis the effects of bit-to-bit error dependency. First, we apply the technique of moment spaces, developed by Dresher *et al* [22], to gain insight into the effect of dependent error events by constructing a convex hull on the function mapping the probability of a successful bit to the probability of a successful packet. Analytical results are then obtained by conditioning on the dependent random variables to obtain bit-to-bit error events that are conditionally independent, allowing us to directly map the conditional probability of a successful bit onto the conditional probability of a successful packet by using (3.3). We then perform an expectation operation over packets to obtain the average probability of packet success. The conditioning is performed on the random variables in the multiple-access interference which are essentially fixed during the transmission of a desired packet, such as the relative delays of the interfering packets and (possibly) the relative phases of the r-f carriers.

3.4. Moment Space Bounds on Packet Performance

Suppose we have a random variable X for which the distribution $F_X(x)$ is defined on the closed and finite interval $I=[a,b]$, but is otherwise unknown. In addition, suppose we wish to find a specific moment of X given by

$$\mathrm{E}[g(X)] = \int_I g(x)dF_X(x). \tag{3.4}$$

Given the above information, we can only make the obvious conclusion that $E[g(X)]$ is bounded by the minimum and maximum values that $g(x)$ assumes for $x\in[a,b]$. However, if other moments of X are known, these bounds may

be improved by using the theory of moment spaces. The theory is based upon interpreting an integral inequality as a condition that a specific point lie in a space determined by the convex hull of a given curve. The following theorem, originally developed in [23], formally states this relationship between the moments of a random variable.

3.4.1. The Moment Space Theorem

Theorem: Let X be a random variable with a probability distribution function $F_X(x)$ defined over a finite closed interval $I = [a,b]$. Let $g_1(x), g_2(x), \ldots, g_N(x)$ be a set of N continuous functions defined on I. The moment of the random variable X induced by the function $g_i(x)$ is

$$m_i = \mathrm{E}[g_i(x)] = \int_I g_i(x) dF_X(x). \tag{3.5}$$

Now denote the moment space M by

$$M = \{m = (m_1, \ldots, m_N) \in \mathbf{R}^N \,|\, m_i\}, \tag{3.6}$$

where F_X ranges over the set of probability distributions defined on I and $\mathbf{R}^N$ denotes N-dimensional Euclidean space. Then M is a closed, bounded, convex set. Now let C be the curve $r = (r_1, \ldots, r_N)$ traced out in $\mathbf{R}^N$ by $r_i = g_i(x)$ for x in I. Let H be the convex hull of C. Then

$$H = M. \tag{3.7}$$

In words, the convex hull of all the moment-defining functions traced out in Euclidean N-space contains all of the moments defined by (3.5) for any probability distribution $F_X(x)$. For a proof of this theorem, see [23].

Suppose we modify the hypothesis of the moment space theorem by considering 2-dimensional Euclidean space, removing the restriction that $I = [a,b]$ is finite, and letting $g_1(x) = x$ and $g_2(x)$ be convex. The resulting conclusion is Jensen's inequality: $g_2(\mathrm{E}[x]) \leq \mathrm{E}[g_2(x)]$. By forcing a finite interval $[a,b]$ for the support of $F_X(x)$, we strengthen this conclusion considerably by gaining the ability to fully bound the moments defined in higher dimensional Euclidean space, rather than producing the single inequality offered by Jensen.

The moment space theorem relates successful data bits to successful packets in the following way. Let the probability of successful bit transmission, conditioned on $K-1$ interfering users in the multiple access environment, be a function of the relative delays S_k and phases Φ_k, where $2 \leq k \leq K$. Then Q_e becomes a random variable expressed as

$$Q_e(\underline{S},\underline{\Phi}) = Q_e(S_2, \ldots, S_K, \Phi_2, \ldots, \Phi_K) \tag{3.8}$$

with distribution $F_Q(x)$. Now let $\mathbf{R}^N = \mathbf{R}^2$, $g_1(x) = x$, and

$$g_2(x) = \sum_{i=0}^{t} \binom{L}{i} (1-x)^i (x)^{L-i} \tag{3.9}$$

$$\triangleq g(x;L,t).$$

Equation (3.9) corresponds to the mapping of $x = Q_e(Sunder,\underline{\Phi})$, the probability of a successful data bit, to $g_2(x) = Q_E(Sunder,\underline{\Phi})$, the probability of a successful packet, given that up to t errors can be corrected within the packet and that the error events are independent from bit-to-bit. Also, the first moment

$$\mathrm{E}[Q_e(\underline{S},\underline{\Phi})] = \overline{Q}_e \tag{3.10}$$

may be bounded or closely approximated from techniques presented in Chapter 2. Once the endpoints of I are found, the theorem can be used to bound Q_E, the average probability of packet success. The left endpoint of the interval represents a lower bound, and the right endpoint represents an upper bound, on $Q_e(\underline{S},\underline{\Phi})$, the conditional probability of data bit success evaluated over all possible values of $\underline{S}$ and $\underline{\Phi}$. If $\underline{\Phi}$ is random from bit-to-bit, then the left and right endpoints of I represent lower and upper bounds on $Q_e(\underline{S}) = \mathrm{E}[Q_e(\underline{S},\underline{\Phi})|\underline{S}]$ evaluated over all possible values of $\underline{S}$.

Since the purpose of this discussion is to gain insight into the effect that dependent bit error events have on packet performance, we will present examples based upon both light and heavy channel loading with respect to the MAI present, and under varying amounts of error control capability at the desired receiver, without attempting to determine the endpoints for $I = [a,b]$ explicitly.

3.4.2. No Error Correction Capability

Figure 3.1 shows a plot of $g(x;L,t) = x^L$ corresponding to a packet of length $L = 1000$ data bits and no error correcting capability ($t = 0$). We begin by plotting a hypothetical $I = [a,b]$ on the abscissa. Then we construct the convex hull between the two points. Since $g(x;L,0)$ is itself convex, the hull is lower bounded by the function itself and upper bounded by the line segment connecting the points (a,a^L) and (b,b^L). Next, we plot $\overline{Q}_e$ on the abscissa and draw a line through the convex hull. Then the ordinate values on the boundaries of the hull represent the upper and lower bounds on Q_E. These values are labeled $Q_E^{(u)}$ and $Q_E^{(l)}$ in the figure.

We now note an interesting result. The quantity $(\overline{Q}_e)^L$ is the average probability of packet success if the data bit error events were independent. Since $g(x;L,0)$ is convex on [0,1] for $0 < L < \infty$, the independent error event (memoryless channel) assumption produces a *lower bound* on the probability of a successful packet; that is, $Q_E^{(l)} = (\overline{Q}_e)^L$. This is somewhat surprising, since error dependency is usually considered "bad" in communications, and yet we just showed that reliability may improve when the channel has memory. Recall, however, that we assumed no error correcting capability in the packet, so a single error results in packet destruction. Therefore, positively correlated bit-to-bit error events will tend to improve system performance by concentrating multiple bit errors within a few packets rather than spreading them uniformly among the packets. There is no analytical reason, then, to insist on a chip and phase synchronous worst-case assumption to force independent channel errors in a situation where no error control is used; a tighter lower bound on packet performance is obtained by simply using $Q_E^{(l)} = (\overline{Q}_e)^L$.

3.4.3. Light Channel Load with Error Correction

Figure 3.2 plots the function $g(x;L,t)$ for a packet of length $L = 1000$ with $t = 10$, showing possible values for $Q_E^{(u)}$ and $Q_E^{(l)}$ under light and heavy channel loading conditions. If the channel has a small number of simultaneous users relative to the spreading sequence length N and the power of the error control code, then $I = [a,b]$ will map to a concave part of $g(x;L,t)$. Now the situation is opposite to that which occurred with no error control; that is,

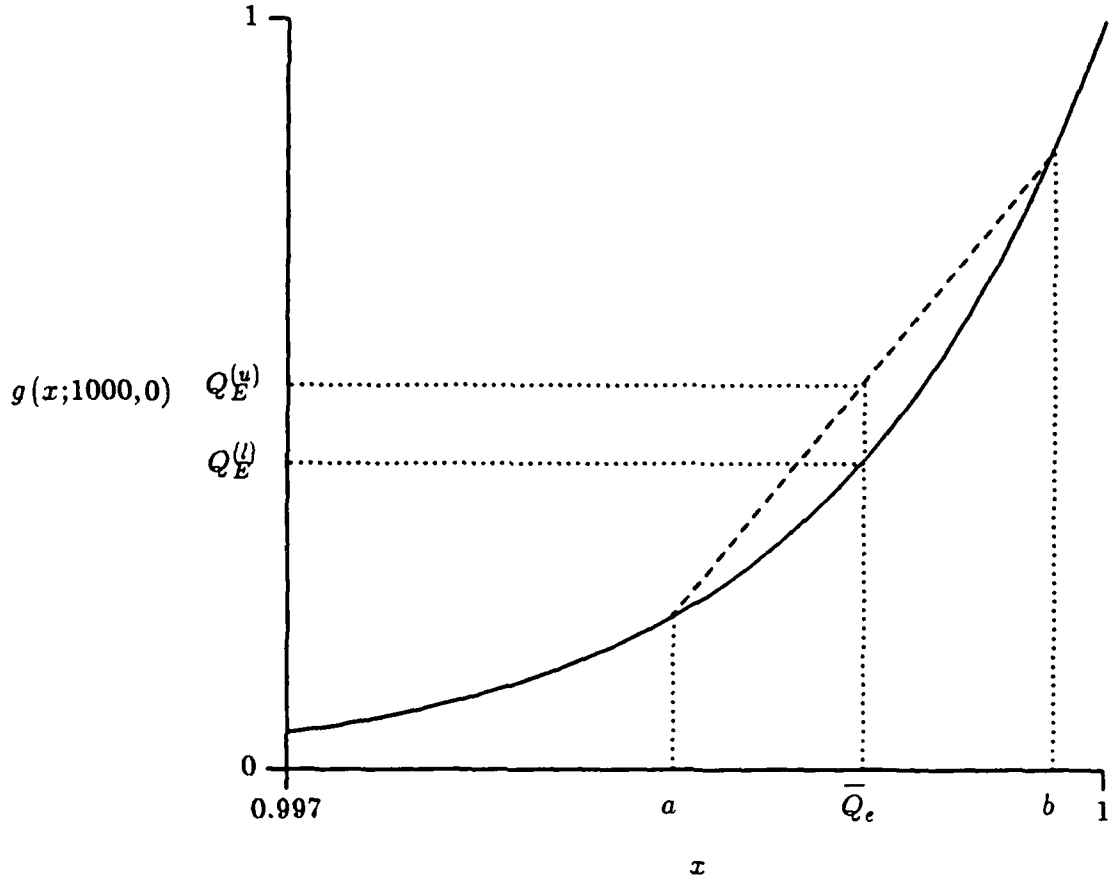

Figure 3.1. Plot of $g(x;L,t)=g(x;1000,0)$, showing the procedure for finding $Q_E^{(l)}$ and $Q_E^{(u)}$.

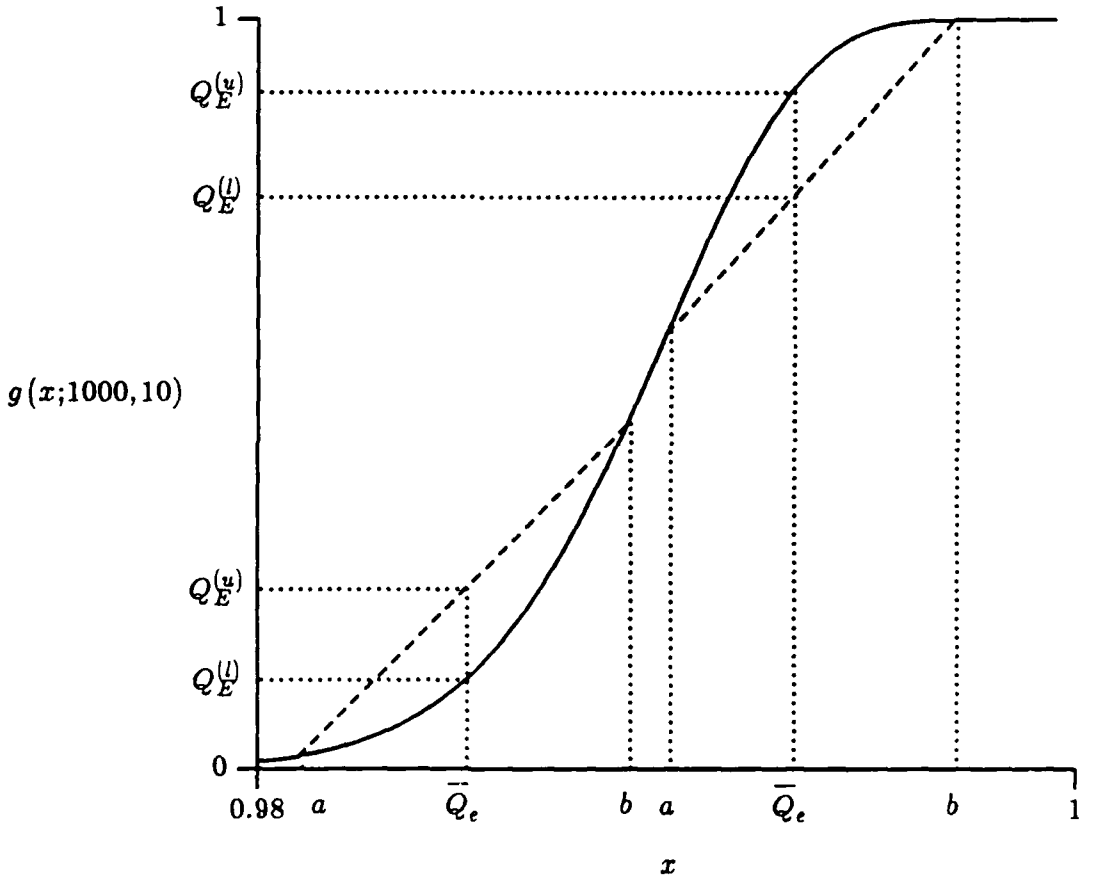

Figure 3.2. Plot of $g(x;L,t)=g(x;1000,10)$, showing the procedure for finding $Q_E^{(l)}$ and $Q_E^{(u)}$ on both convex and concave portions of the curve.

assuming independent error events yields an *upper bound* on the probability of packet success, and actual performance may be worse. This makes intuitive sense by noting that this situation is equivalent to a channel with a small amount of multiple-access interference relative to the ability of the error control code to correct errors. Therefore, if the errors that do occur are distributed uniformly among all packets, the error control code may be able to recover most or all of the packets transmitted. The situation changes when bit-to-bit error events are positively correlated, since we would now expect a few more packets to have too many errors for the error control code to handle, resulting in poorer average performance.

3.4.4. Heavy Channel Load with Error Correction

Under conditions of high MAI (large number of simultaneous users), $I = [a,b]$ may map to a convex part of $g(x;L,t)$, as shown in Figure 3.2. In this situation, assuming independent bit error events once again produces a lower bound on packet performance. This is because the bit error rate is so high that the error control code is overwhelmed, and a large number of packets are lost. Now the system performs better when the channel has memory, perhaps producing a few more packets that can be recovered via error control than would have occurred under memoryless conditions.

3.4.5. Bounds Using the Standard Gaussian Approximation

A similar procedure may be used to estimate packet performance within the framework of the Standard Gaussian Approximation to the probability of bit error given by (2.62). Since (2.62) uses SNR, which is directly related to the MAI variance Ψ by $\mathrm{SNR} = \mu/\sqrt{\Psi}$, we can map MAI variance to successful packets through the composition

$$Q_E(\Psi;L,t) = g\left(\Phi\left[\frac{\mu}{\sqrt{\Psi}}\right];\, L,t\right) \tag{3.11}$$

where

$$\Phi[x] \;=\; 1-Q[x] \;=\; \frac{1}{\sqrt{2\pi}}\int_{-\infty}^{x} e^{-u^2/2}du\,. \tag{3.12}$$

A plot of $g(\Phi[\mu/\sqrt{\Psi}];L,t)$ vs Ψ for $L = 1000$, $t = 0$, and $\mu = N = 31$ is shown in

Figure 3.3. Unlike Figure 3.1, the curve is no longer convex in the region of light channel loading (few simultaneous users); consequently, the quantity $(\Phi[\overline{SNR}])^L$ will *not* produce a lower second moment bound on the probability of packet success when no error control is used.

3.5. Probability of Packet Success

We begin this section by referring to (2.34) and (2.35) and noting that if we condition on the interfering signal delays S_k and, if necessary, the phases Φ_k, then the multiple-access interference would be independent from bit-to-bit within a packet. The independent data bit assumption enables us to use (3.3) directly to find the (conditional) probability of packet success. If we could do this for all possible combinations of S_k and Φ_k for $2 \leq k \leq K$ by finding $Q_E = g(Q_e; L, t)$ for each $Q_e(\underline{S}, \underline{\Phi})$, we would have a collection of conditional probability of packet success values which could be averaged to find $\overline{Q}_E$.

One possible analytic approach is to divide the interval $[0, T_c/2]$ into M_S equal regions, and the interval $[0, \pi/2]$ into M_Φ equal regions, and calculate Q_e for every possible combination of $K-1$ users in $M_S M_\Phi$ regions. (Symmetry present in (2.34) and (2.35) allows us to examine delays between 0 and $T_c/2$ rather than between 0 and T_c, and phases between 0 and $\pi/2$ rather than between 0 and 2π.) From these results, an approximation to the distribution of $Q_e(\underline{S}, \underline{\Phi})$ is obtained, from which $Q_E = \mathrm{E}[g(Q_e; L, t)]$ may be found. The disadvantage to this approach is that the number of computations grows as $(M_S M_\Phi)^{K-1}$, which quickly becomes intractable, even for modest values of K and $M_S M_\Phi$. Instead, we take a second moment approach which does not exhibit an exponential growth in computational complexity.

In Chapter 2, we developed the Improved Gaussian Approximation by conditioning on the delay vector $\underline{S}$ and phase vector $\underline{\Phi}$, and we showed that the resulting probability of data bit error after averaging over $\underline{S}$ and $\underline{\Phi}$ was a close approximation to the actual $P_e = 1 - Q_e$ found by the bounding procedure. Since conditioning on $\underline{S}$ and $\underline{\Phi}$ also causes bit error events to become independent, the Improved Gaussian Approximation provides the ability to accurately calculate the probability of packet success while

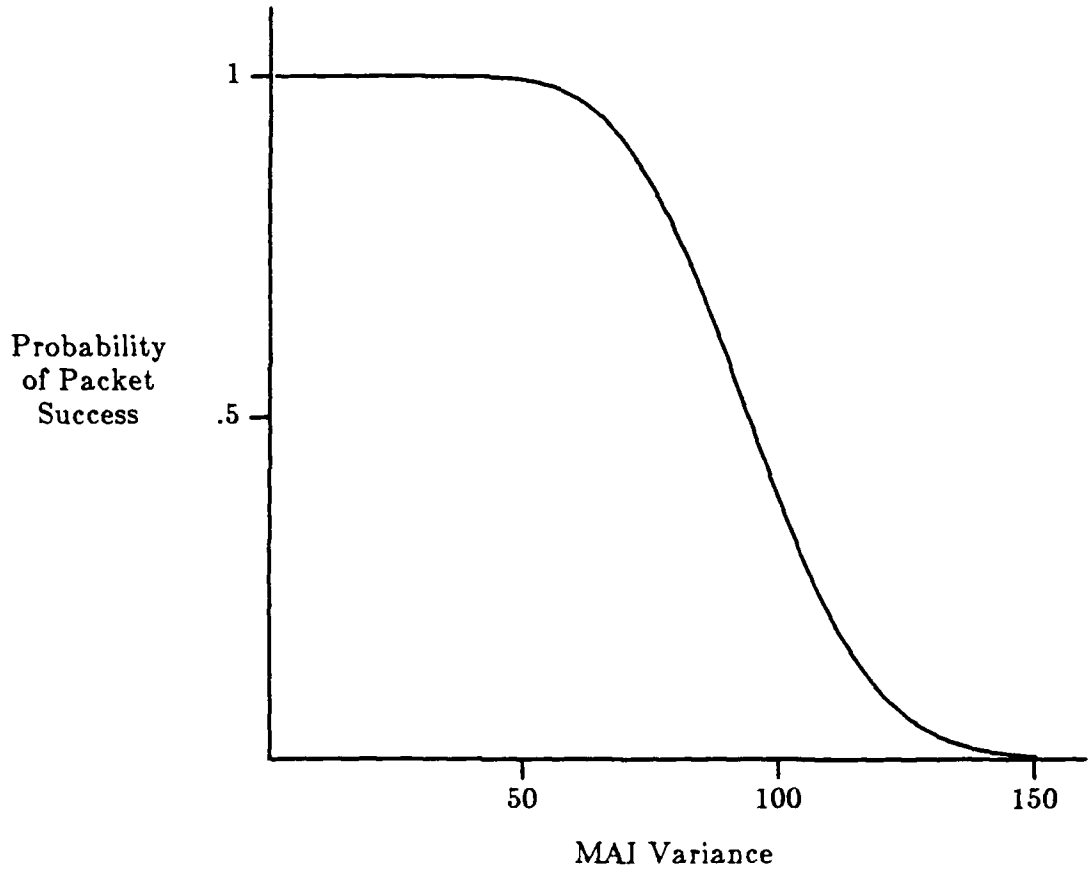

Figure 3.3. The probability of packet success vs MAI variance ($N=31$, $L=1000$, $t=0$).

accounting for the effects of bit-to-bit error dependence.

3.5.1. Fixed Delay and Phase

In this section we assume that all transmitted carriers are *phase stable;* that is, each phase Φ_k is selected from a distribution uniform on $[0,2\pi]$ at the start of a desired packet, and then remains constant over the duration of the transmission. The delays $\mathcal{S}_k$ are selected from distributions uniform on $[0,1]$ at the beginning of a desired packet, and also remain constant during the transmission. By following the same line of reasoning as that used in Section 2.7, we see that each outcome $\Psi=\psi$ of the MAI variance is produced by specific outcomes of $\mathcal{S}$, Φ, and B, so we can use $\Phi[N/\sqrt{\psi}]$ as an accurate approximation to $Q_e(\psi)$ for a particular ψ. Furthermore, since channel errors are now conditionally independent, $g(Q_e(\psi);L,t)$ is also an accurate estimate of the packet success probability $Q_E(\psi)$. We now realize that much of the work required for finding $Q_E=\mathrm{E}[Q_E(\Psi)]$ has already been accomplished in Chapter 2: since (2.85) gives the density function for the MAI variance for any particular K, we have

$$Q_E = \mathrm{E}\left[g\left[\Phi\left[\frac{N}{\sqrt{\Psi}}\right];L,t\right]\right] = \int_0^\infty g\left[\Phi\left[\frac{N}{\sqrt{\psi}}\right];L,t\right] f_\Psi(x)dx\,. \quad (3.13)$$

Perhaps the easiest method of computing (3.13) is to use the discrete density $\tilde{f}_\Psi(i)$ given by (2.81) and sum over the composition; thus

$$Q_E = \sum_{i=0}^{I} g\left[\Phi\left[\frac{N}{\sqrt{y(i)}}\right];L,t\right]\tilde{f}_\Psi(i)\,, \quad (3.14)$$

where

$$I = (K-1)(NM-1) \quad (3.15)$$

and

$$y(i) = \frac{2i+K-1}{2M}\,. \quad (3.16)$$

A plot of Q_E vs K for $N=31$ and $L=1000$ is shown as the solid line in Figure 3.4 for $t=0$ and in Figure 3.5 for $t=10$.

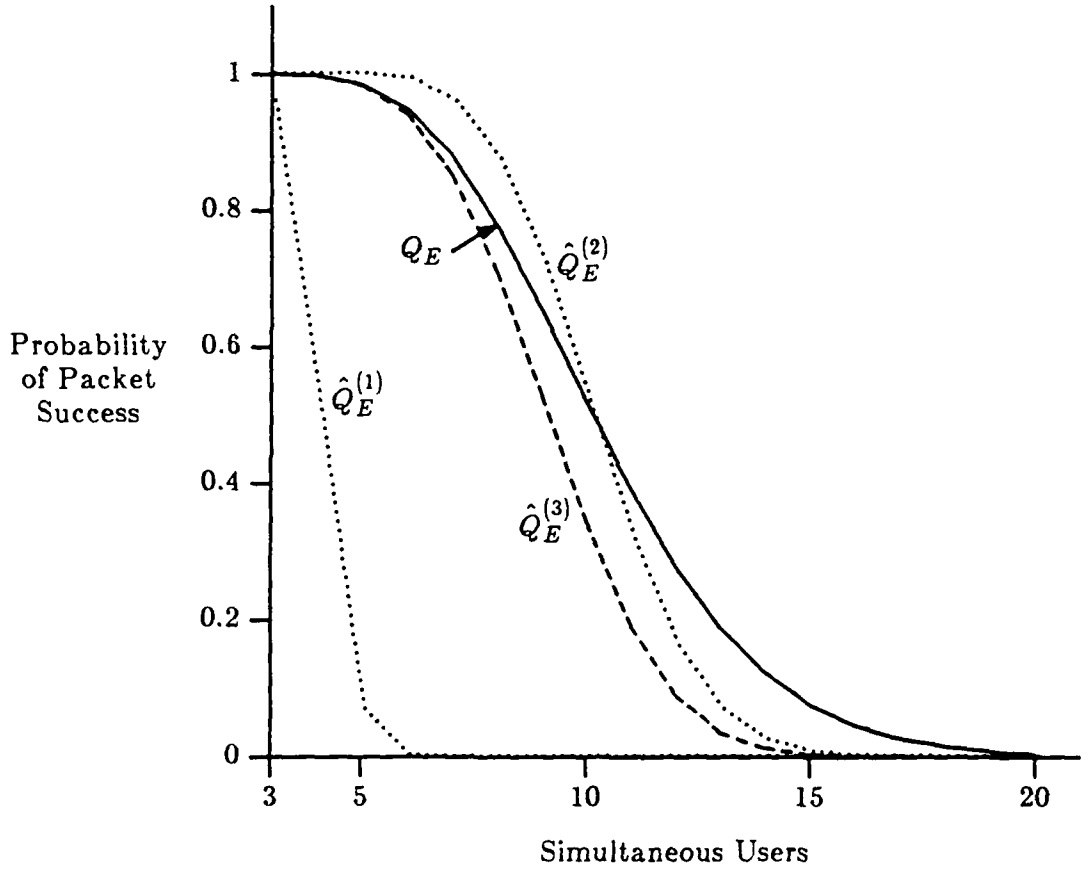

Figure 3.4. Average probability of packet success vs the number of simultaneous users for $\underline{\Phi}$ fixed during a desired packet ($N=31$, $L=1000$, $t=0$).

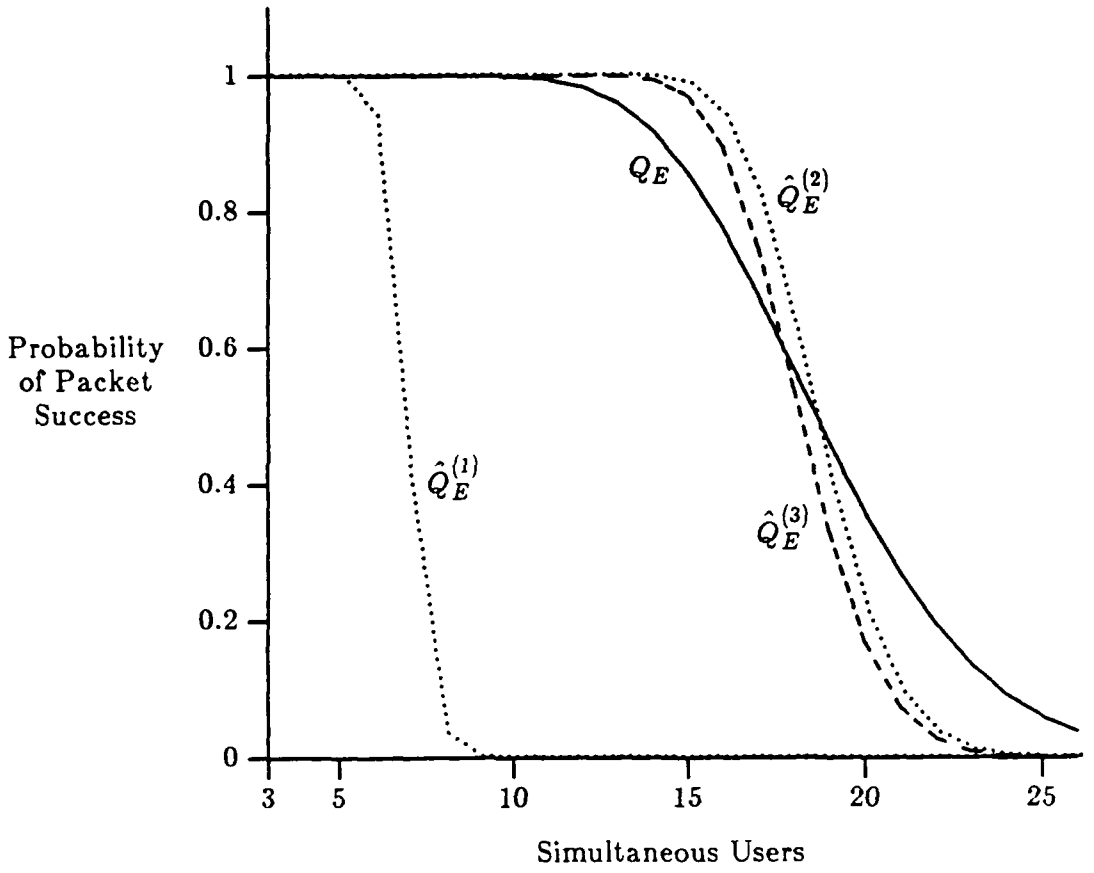

Figure 3.5. Average probability of packet success vs the number of simultaneous users for $\underline{\Phi}$ fixed during a desired packet ($N=31$, $L=1000$, $t=10$).

We can also obtain a discrete approximation $\tilde{f}_{Q_E}(j)$ to the distribution of the probability of packet success by using the following procedure. First, note that Q_E is a probability measure; as such, the support of the density function $f_{Q_E}(x)$ is [0,1]. We divide this interval into J subintervals, each of length $1/J$, and let

$$\tilde{f}_{Q_E}(j) = \Pr\left\{\frac{j}{J} \le Q_E \le \frac{j+1}{J}\right\}; \qquad j \in \{0, 1, \ldots, J-1\}. \tag{3.17}$$

Next, we let

$$A_j = \left\{i: \frac{j}{J} \le g\left(\Phi\left[\frac{N}{\sqrt{y(i)}}\right]; L, t\right) \le \frac{j+1}{J}\right\}; \tag{3.18}$$

$$i \in \{0, 1, \ldots, I\}.$$

Then

$$\tilde{f}_{Q_E}(j) = \sum_{i \in A} \tilde{f}_{\Psi}(i). \tag{3.19}$$

Knowing an approximation to $f_{Q_E}(x)$ may prove useful in calculating the distribution of packet delay in a communication network, since the "probability" that Q_E is at or below a certain value $x \in [0,1]$ is approximately

$$\sum_{j \le Jx} \tilde{f}_{Q_E}(j). \tag{3.20}$$

Figure 3.6 shows the distribution of Q_E for $N = 31$ and various values of K.

In Section 2.7 it was pointed out that each outcome $\Psi = \psi$ is produced by specific outcomes of S, Φ, and B. As a consequence, the value for Q_E given by (3.13) is based upon the assumption that C (and hence B) is selected from its distribution given by (2.33) at the start of each desired packet, and then remains constant over the duration of the packet. If C varies within a single desired packet, then we can find bounds on Q_E by using the following procedure. First, note that for any fixed $S = \underline{s}$ and $\Phi = \underline{\omega}$, if $B_1 \le B_2$ then $\psi | B_2 \le \psi | B_1$. Since $Q_E(\psi) = g(\Phi[N/\sqrt{\psi}]; L, t)$ is a decreasing composition of ψ, we conclude that $Q_E | B_1 \le Q_E | B_2$. This allows us to obtain bounds, in the context of the Improved Gaussian Approximation, on the probability of packet

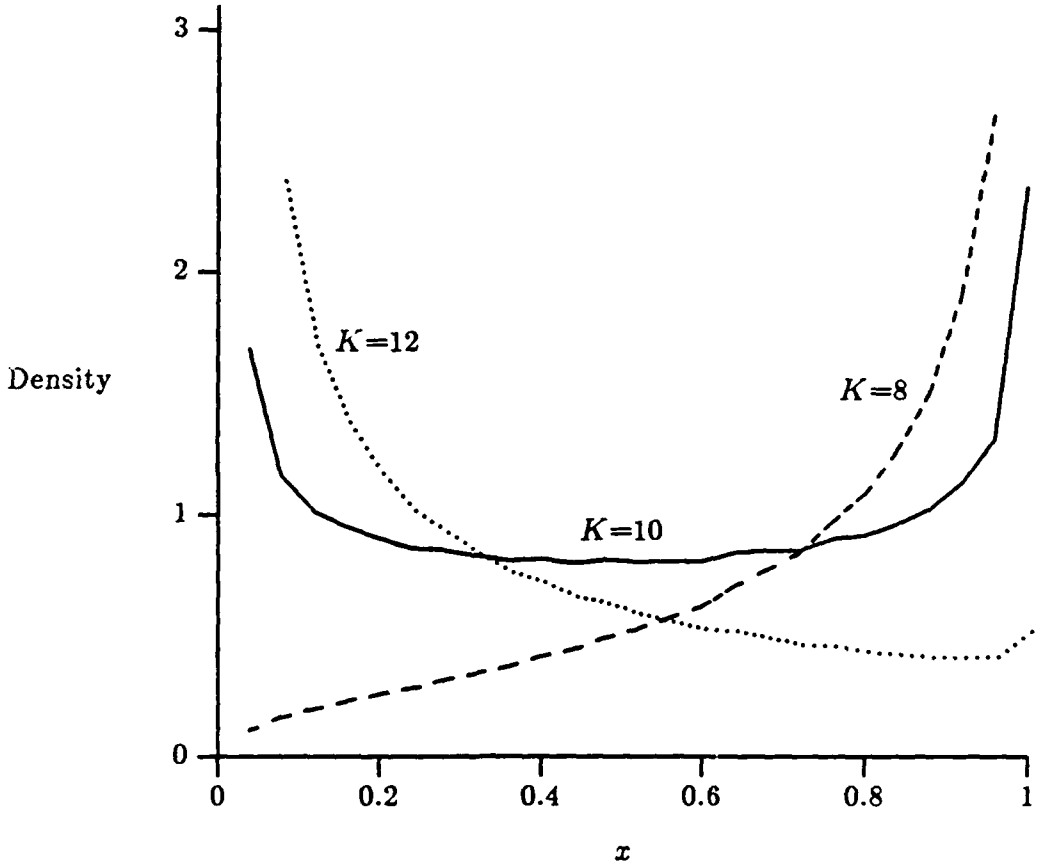

Figure 3.6. Density function for the probability of packet success for various values of K ($N=31$, $L=1000$, $t=0$).

success for any desired signature sequence structure. For example, if a desired packet has a $B = B_d$ which varies from bit-to-bit between a minimum B_L and a maximum B_U, then $Q_E|B_L \leq Q_E|B_d \leq Q_E|B_U$.

We now explore the possibility of using less accurate (but easier to calculate) methods of finding Q_E, and we compare the results with those given by (3.13) for various values of K. One approach, for example, is to assume that all interfering signals are in chip and phase alignment with the desired signal. Not only does this situation provide independent bit error events, but also results in a worst-case multiple-access interference situation when all signals have equal power at the desired receiver [7]. We also know from Section 2.6 that the Standard Gaussian Approximation is accurate for fixed delays and phases, so the probability of packet success under these conditions is given by

$$\hat{Q}_E^{(1)} = g\left(\Phi\left[\frac{N}{\sqrt{\mathrm{E}[\Psi|\underline{S}=\underline{0},\underline{\Phi}=\underline{0}]}}\right]; L,t\right) \tag{3.21}$$

$$= g\left(\Phi\left[\left(\frac{N}{K-1}\right)^{1/2}\right]; L,t\right).$$

Since the expectation can be expressed as a simple function of N and K, computational complexity of (3.21) is very low; however, Figures 3.4 and 3.5 show that this worst-case situation produces a very loose lower bound on packet performance.

A method which retains the low computational complexity of (3.21) while producing results closer to those given by (3.13) is to use the average SNR from (2.61) in a Standard Gaussian Approximation to the probability of packet success. If bit-to-bit error dependencies are also ignored, we have

$$\hat{Q}_E^{(2)} = g\left(\Phi\left[\frac{N}{\sqrt{\mathrm{E}[\Psi]}}\right]; L,t\right) \tag{3.22}$$

$$= g\left(\Phi\left[\left(\frac{3N}{K-1}\right)^{1/2}\right]; L,t\right).$$

Figure 2.2 showed that the Standard Gaussian Approximation yielded results that were optimistic for small K and accurate for large K. Also, from Figure 3.3 we see that $g(\Phi[\mu/\sqrt{x}\,]; L,0)$ begins as a concave function of x for small x, and then becomes convex when x is large. (The curve has a similar shape for $t>0$). We conclude from the theory of moment spaces that (3.22) will probably produce an optimistic estimate of packet success for a lightly-loaded channel and then become pessimistic as the MAI increases. This effect is shown in Figures 3.4 and 3.5.

As a third and final alternate method of calculating packet performance, we may wish to use the Improved Gaussian Approximation to produce accurate Q_e values, but again ignore bit-to-bit error dependence and estimate Q_E by

$$\hat{Q}_E^{(3)} = g\left(\mathrm{E}\left[\Phi\left[\frac{N}{\sqrt{\Psi}}\right]\right]; L,t\right). \tag{3.23}$$

The convexity of $g(x;L,0)$ in Figure 3.1 allows us to use (3.23) as a lower bound on packet performance, as shown in Figure 3.4, when there is no error correction capability. However, $g(x;L,t)$ for $t>0$ becomes concave as x approaches 1 (Figure 3.2); as a consequence, when error correction is used, (3.23) will be optimistic for small K and pessimistic for large K (Figure 3.5). An additional characteristic of bit-to-bit error dependence and its effect on packet performance is a more gradual roll-off of the curve given by Q_E compared to $\hat{Q}_E^{(2)}$ and $\hat{Q}_E^{(3)}$. This may reduce the accuracy of using a "noiseless-useless" channel approximation [14], where all packets are assumed successful if λ or fewer users transmit simultaneously, otherwise all packets are considered lost.

3.5.2. Fixed Delay, Random Phase

In certain situations, phase jitter from transmitter instability or changing channel characteristics may allow us to average the phase of each interfering signal over its distribution at the bit level within a desired packet. The probability of packet success becomes

$$\tilde{Q}_E = \mathrm{E}\left[g(\mathbf{x}\,;\,L,t)\right], \tag{3.24}$$

where

$$\mathbf{x} \;=\; \mathrm{E}\left[Q_e\,|\mathcal{S}\right] \;=\; \int_0^\infty \Phi\left[\frac{N}{\sqrt{\psi}}\right] f_{\Psi|\mathcal{S}}(x)dx\,. \tag{3.25}$$

The random variable $\mathbf{x}$ in (3.25) is obtained by averaging the probability of data bit success over the phase vector Φ, and is therefore a function of the delay vector $\mathcal{S}$. Next, $g(\mathbf{x};L,t)$ is averaged over $\mathcal{S}$ in (3.24) to determine the probability of packet success. Directly evaluating (3.25) is difficult, however, since we need to know the conditional density $f_{\Psi|\mathcal{S}}(x)$. Since an approximation to $f_{\Psi}(x)$ is calculated in Section 2.7.2 by performing discrete convolutions on $\tilde{f}_{Z|B}(i)$, we cannot express $f_{\Psi|\mathcal{S}}(x)$ as a simple function of $\mathcal{S}$ and x. Instead, we are forced to use the procedure described in the introduction to Section 3.5, where we divide the delay interval $[0,T_c/2]=[0,½]$ into M_S equal regions and calculate a specific $f_{\Psi|\mathcal{S}=\mathcal{s}}(i)$ for every possible combination of $K-1$ users in M_S regions. In order to avoid the exponential (in K) computational complexity associated with such a task, we will be content to find upper and lower bounds on $\tilde{Q}_E$ when no error correction capability exists, and an approximation to $\tilde{Q}_E$ otherwise.

If no error correction is used by the system, then we know that the function $g(x;L,0)=x^L$ is convex for $x\in[0,1]$, and Jensen's inequality (Section 3.4) allows us to write

$$\tilde{Q}_E^{(l)} = g\left(\mathrm{E}[\mathbf{x}]\,;\,L,0\right) \;\le\; \mathrm{E}\left[g(\mathbf{x}\,;\,L,0)\right] = \tilde{Q}_E\,, \tag{3.26}$$

where $\mathbf{x}$ is a random variable given by (3.25). However,

$$g\left(\mathrm{E}[\mathbf{x}]\,;\,L,0\right) = \hat{Q}_E^{(3)} \tag{3.27}$$

from (3.23). Therefore, a lower bound $\tilde{Q}_E^{(l)}$ on (3.24) may be found by ignoring

the effect of bit-to-bit error dependence altogether. An upper bound on (3.24) is produced by once again using Jensen's inequality to give

$$g\left(\mathrm{E}\left[Q_e\,|\underline{\mathcal{S}}\right];\,L,0\right) \leq \mathrm{E}\left[g(Q_e\,;\,L,0)|\underline{\mathcal{S}}\right]. \tag{3.28}$$

Note that both sides of (3.28) are random variables; taking an expectation of each side preserves the inequality [24]:

$$\tilde{Q}_E = \mathrm{E}\left[g(\mathbf{x};\,L,0)\right] \;\leq\; \mathrm{E}\left[g(Q_e\,;\,L,0)\right] = \tilde{Q}_E^{(u)}. \tag{3.29}$$

But

$$\mathrm{E}\left[g(Q_e\,;\,L,0)\right] = Q_E \tag{3.30}$$

from (3.13). Consequently, the probability of packet success with random interfering signal phases is upper bounded by assuming that the interfering signals have constant delays *and* phases throughout a desired packet. These bounds are plotted in Figure 3.7; note that they are reasonably tight when the probability of packet success is high, which is the performance region of greatest interest to a systems designer.

The upper and lower bounds given by (3.26) and (3.29) have two disadvantages: they cannot be made arbitrarily tight and, since $g(x;L,t)$ is no longer convex when $t>0$, they cannot be used as bounds when error correction capability exists. We can, however, loosely lower-bound $\tilde{Q}_E$ by allowing all interfering signals to be in worst-case chip alignment with the desired signal, and we can approximate $\tilde{Q}_E$ by averaging the MAI variance over all possible interfering signal delays.

The lower bound on $\tilde{Q}_E$ is easily obtained by using the Standard Gaussian Approximation where interfering signals have random phases and chip boundary alignment. In this case,

$$\tilde{Q}_E^{(l)} = g\left(\Phi\left[\frac{N}{\sqrt{\mathrm{E}[\Psi|\underline{\mathcal{S}}=\underline{0}]}}\right];\,L,t\right) \tag{3.31}$$

$$= g\left(\Phi\left[\left(\frac{2N}{K-1}\right)^{1/2}\right];\,L,t\right)$$

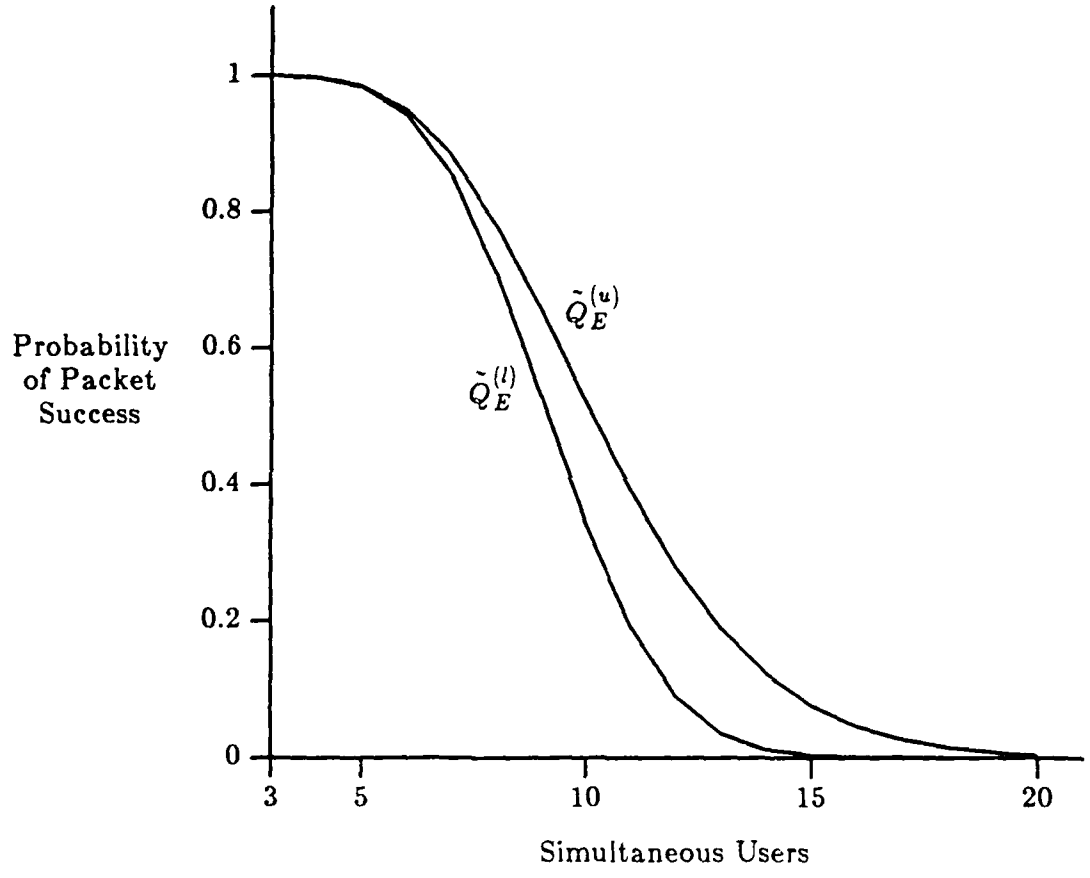

Figure 3.7. Bounds on the average probability of packet success vs the number of simultaneous users for $\underline{\Phi}$ random from bit-to-bit ($N=31$, $L=1000$, $t=0$).

from (2.65). To approximate $\tilde{Q}_E$ we can substitute $\mathrm{E}[U]=1$ into (2.55), giving $Z'=V$, which represents a phase-averaged MAI value produced by one interfering signal as a function of its delay S. The density of Z' is given by (2.81) which integrates to form

$$F_{Z'|B}(v) = \left(\frac{2v+\tilde{B}-N}{\tilde{B}} \right)^{1/2}; \qquad \frac{N-\tilde{B}}{2} \le v \le \frac{N}{2}. \tag{3.32}$$

The distribution of the total MAI variance Ψ is found using the techniques of Section 2.7, producing a probability of packet success

$$\tilde{Q}_E^{(2)} = \mathrm{E}\left[g\left(\Phi\left[\frac{N}{\sqrt{\Psi|\,U=1}} \right]; L,t \right) \right]. \tag{3.33}$$

A plot of $\tilde{Q}_E^{(1)}$ and $\tilde{Q}_E^{(2)}$ as a function of K for $N=31$, $L=1000$, and $t=10$ is shown in Figure 3.8.

3.6. Conclusion

From the results in this chapter, it is evident that the multiple-access interference cannot be modeled as a process producing values which are independent from bit-to-bit within a desired packet. The theory of moment spaces allows us to conclude that the dependent error events present in a desired packet actually improves performance under all channel traffic situations when no error control is used, and under heavy channel loading when error correction is possible. The error dependencies will cause poorer system performance when the desired packet includes error correction capability and is transmitted over a lightly-loaded channel. Since this latter situation is perhaps of greatest interest to a systems designer, the effect of error dependencies should be incorporated into the analysis to avoid overly optimistic estimates of network performance. In the next chapter, we examine the effect of error dependence on the performance of a direct-sequence spread-spectrum packet broadcast system using the slotted ALOHA protocol.

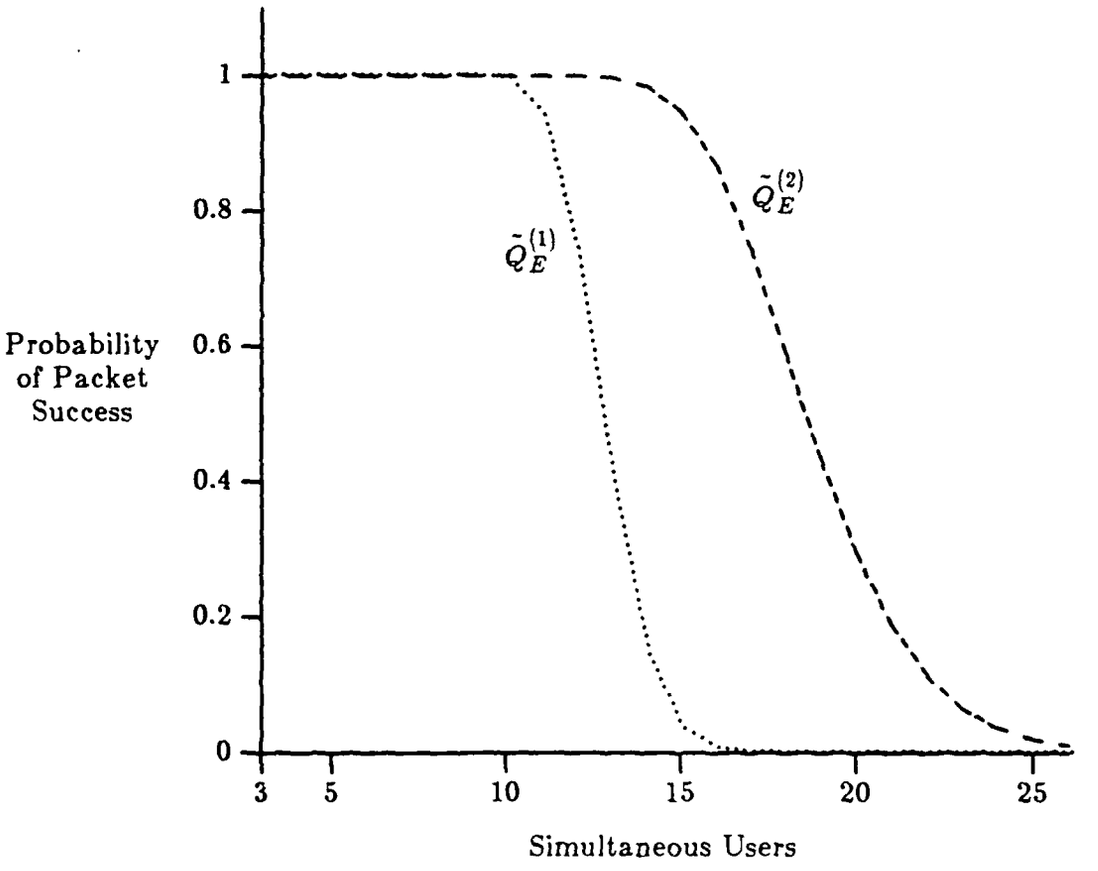

Figure 3.8. Lower bound and an approximation to the probability of packet success vs the number of simultaneous users for $\underline{\Phi}$ random from bit-to-bit ($N=31$, $L=1000$, $t=10$).

CHAPTER 4
THE NETWORK LAYER: SLOTTED ALOHA MODEL

4.1. Introduction

The *network layer* defines how packets of data bits are routed and relayed between user nodes, and regulates the flow of packets [1]. In Chapter 1 we discovered that many of the results in the literature concerning DS/SSMA communications were obtained by simplifying the physical and data link layers to enable fairly complicated networks to be analyzed. Our approach is just the opposite: we have endeavored in the last two chapters to produce an accurate estimate of the probability of data bit error without the inaccuracies of the Standard Gaussian Approximation, and we incorporated the effects of dependent bit error events into our estimate of the probability of packet success. We will now apply these results to a simplified network model to gain insight into the effect that a more accurate analysis of packet performance has on the network throughput.

Throughput this chapter, we make use of the "slotted ALOHA" network model, described in the next section. First, we derive the network throughput equations for an infinite-user network, and show how arbitrarily tight bounds on the throughput may be calculated. We then work mainly with the lower throughput bound and quantify the performance enhancement gained by incorporating error correction capability into the desired signal. Although throughput is increased by using error control, the required redundancy shortens the effective length of the actual message; we take this into account by calculating a quantity called the "effective throughput". Next, we define network capacity as the maximum effective throughput, and we compare the capacity of an infinite-user DS/SSMA slotted ALOHA packet network with a

number of narrow-band networks using an equivalent signal ban 'width.

Much of the effort in this thesis has been devoted to comparing the bit and packet error performance by using three different approximations in the calculations. These are, in order of increasing accuracy (and increasing computational effort), the Standard Gaussian Approximation (SGA) from equation (3.22), the Improved Gaussian Approximation (IGA) from (3.23), and the Improved Gaussian Approximation while accounting for bit-to-bit error dependence (IGA-D) given by (3.13). This chapter will explore the network performance under each of these three approximations, and will allow systems designers to decide if the increased accuracy of the IGA and IGA-D methods are worth the extra effort required over the SGA approach. In order to provide contrast between the IGA and IGA-D approaches, the IGA-D calculations are based upon phase stable transmitters, so that there is dependency from both delay $\mathcal{S}$ and phase Φ parameters between the desired and interfering signals.

4.2. Infinite User Model

Consider a large number of independent users (nodes) sharing a common communication channel and generating packets of length L bits. Each of the n users receives packets at a very slow rate S_i packets per time slot, and the time between packets is exponentially distributed with mean $1/S_i$ which is large relative to the packet length. Then the arrivals of all newly-generated packets are Poisson [25] with rate

$$S = \sum_{i=1}^{n} S_i .$$

When a packet arrives at a particular node, transmission begins at the start of the next slot (Figure 4.1). Each slot is long enough for a packet to be transmitted, and any associated guard time between slots is assumed short compared to the packet transmission time. It is also assumed that propagation delays and slot timing errors are suc' that the bit and packet error probabilities developed in the previous sections hold.

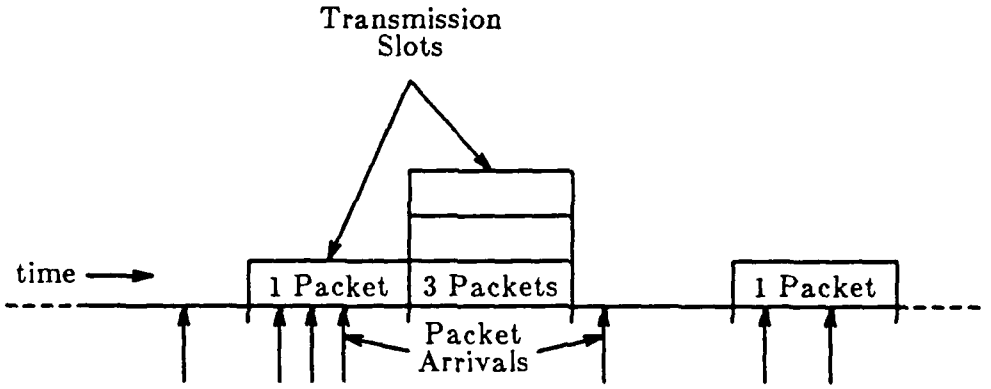

Figure 4.1. Typical channel activity of a spread-spectrum slotted ALOHA packet network.

In the previous chapter, we showed that multiple-access interference from two or more users in a particular slot could cause a packet error, requiring retransmission. Figure 4.2 shows this situation from a networking point of view: the channel receives both newly generated packets at rate S and previously unsuccessful packets at rate R, also assumed Poisson. The offered channel traffic is then Poisson with rate $G = S + R$. Of course, it is hoped that the channel throughput rate is S, so that all newly arrived packets will eventually be successfully transmitted. This will occur only if the channel is *stable;* that is, if the queue containing unsuccessful packets occasionally empties [25].

4.3. Network Throughput

The calculation of network throughput gives an indication of system performance by quantifying the average number of *successful* packets transmitted per unit time. Since some of the packets may be received in error, the throughput is at or below the channel "offered rate", or the average number of packets transmitted in the same unit of time. By defining a unit of time to be equivalent to the duration of a slot, both offered rate and throughput are specified in "packets per slot". Although K, the number of simultaneous users in a particular slot, is now a random variable, the relative probabilities of each value of $K \in \{0, 1, \ldots\}$ are determined by the channel offered rate G. When G is small, the probability is high that K will also be small, and the probability of a successful packet will be high. Throughput will be low because of the low offered rate. On the other hand, if G is large then a large K is also likely, but since the probability of packet success is now low, S may still be low. We therefore expect S to be approximately equal to the offered rate when G is small, reach a peak, and then eventually decrease as G continues to increase.

We begin our study of network performance by reviewing the derivation of the throughput equation for a narrow-band slotted ALOHA system, and then we expand the concept to allow more than one successful packet in a particular slot.

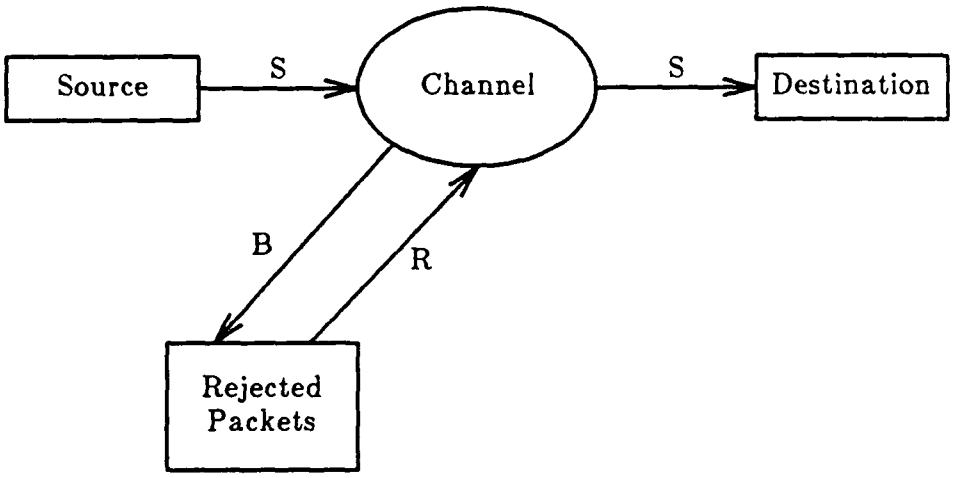

Figure 4.2. Network model for a packet radio system.

4.3.1. Derivation of the Throughput Equation

For traditional narrow-band packet broadcast systems (slotted or unslotted), throughput analysis is usually accomplished by ignoring errors caused by AWGN at the receiver and assuming a given packet is successful if and only if no part of it overlaps with another packet during transmission [25,26]. If an overlap (or "collision") does occur, all packets involved effectively jam each other and are lost. In the slotted ALOHA model with Poisson packet arrivals, a packet is successful if and only if a slot contains just one packet, which occurs with probability e^{-G}. The throughput is the offered rate times the probability that a single packet will be successful; thus

$$S = Ge^{-G} \leq 1 . \tag{4.1}$$

When spread-spectrum techniques are used, collisions are no longer catastrophic; instead, we must account for the degradation of the channel when two or more users occupy a slot simultaneously. We do this by turning to conditional probabilities.

Throughput may be viewed as the expected number of successful packets in a typical slot [13]; as such, we can define $S|k$ as the expected number of successful packets given k packets in a slot. Therefore

$$S|k = \sum_{m=1}^{k} m \binom{k}{m} [Q_E(k)]^m [1-Q_E(k)]^{k-m} , \tag{4.2}$$

where $Q_E(k)$ is the average probability of packet success with k total users in a slot. Since (4.2) is simply the expected value of a binomial distribution, we have

$$S|k = k\, Q_E(k) . \tag{4.3}$$

After averaging over the Poisson distribution of k, the result becomes

$$S = \sum_{k=1}^{\infty} e^{-G}\, k\, \frac{G^k}{k!}\, Q_E(k) \tag{4.4}$$

$$= \sum_{k=1}^{\infty} e^{-G}\, \frac{G^k}{(k-1)!}\, Q_E(k)$$

$$= Ge^{-G} \sum_{k=0}^{\infty} \frac{G^k}{k!}\, Q_E(k+1).$$

In the first two expressions for S in (4.4), the summation index k represents averaging over the total number of users in a slot; because of the limit change in the last expression, k now becomes the number of *interfering* users in a slot. Also, since $Q_E(k+1) \leq 1$ for all $k \in \{0, 1, 2, \ldots\}$, we have

$$S \leq Ge^{-G} \sum_{k=0}^{\infty} \frac{G^k}{k!} = G \tag{4.5}$$

and thus the series in (4.4) converges.

If the first term in the summation of (4.4) is separated from the remaining terms, we can write

$$S = Ge^{-G} + Ge^{-G} \sum_{k=1}^{\infty} \frac{G^k}{k!}\, Q_E(k+1). \tag{4.6}$$

The term Ge^{-G} represents the throughput when there is only one packet in a slot, which is identical to the throughput in a narrow-band slotted ALOHA channel given by (4.1). The remaining terms in (4.6) represent the additional throughput realized by using direct sequence spread-spectrum techniques.

4.3.2. Throughput Bounds

An exact evaluation of (4.4) is not possible because of the infinite sum, but we can use the fact that $Q_E(k)$ is a decreasing function of k to obtain arbitrarily tight upper and lower bounds on S. For example, the series may be lower bounded by simply truncating it after $Q_E(k+1)$ reaches some arbitrary minimum value; call it $Q_E(K_u)$:

$$S^{(l)} = Ge^{-G} \sum_{k=0}^{K_u - 1} \frac{G^k}{k!} Q_E(k+1). \tag{4.7}$$

Similarly, S may be upper bounded by letting $Q_E(k) = Q_E(K_u)$ for all $k \geq K_u$.

giving

$$S^{(u)} = Ge^{-G}\sum_{k=0}^{K_u-1}\frac{G^k}{k!}Q_E(k+1) + Ge^{-G}\sum_{k=K_u}^{\infty}\frac{G^k}{k!}Q_E(K_u) \tag{4.8}$$

$$= S^{(l)} + Q_E(K_u)Ge^{-G}\sum_{k=K_u}^{\infty}\frac{G^k}{k!}$$

$$= S^{(l)} + Q_E(K_u)\left[G - Ge^{-G}\sum_{k=0}^{K_u-1}\frac{G^k}{k!}\right].$$

It follows from (4.7) and (4.8) that

$$S^{(u)} - S^{(l)} = Q_E(K_u)\left[G - Ge^{-G}\sum_{k=0}^{K_u-1}\frac{G^k}{k!}\right]. \tag{4.9}$$

The quantity $S^{(u)} - S^{(l)}$ represents the relative tightness of the bounds, and is shown in Figure 4.3 for various values of $Q_E(K_u)$ when using the Standard Gaussian Approximation for $Q_E(k)$. Although the difference between $S^{(u)}$ and $S^{(l)}$ increases with G, a proper choice for $Q_E(K_u)$ will insure tight bounds for all reasonable values of G. To avoid excessively busy plots by showing both bounds, we will instead use only $S^{(l)}$ with $Q_E(K_u) \leq 10^{-3}$ for most of the throughput results in this chapter.

We can now compare the SGA, IGA, and IGA-D methods of calculating the probability of packet success in the network throughput equation. Figure 4.4 shows these three methods when there is no error correction capability in the desired packet. In Chapter 3 we discovered that the IGA-D method produces the most accurate results, but it is lower bounded by using the Improved Gaussian Approximation while ignoring the effect of bit-to-bit error dependence. This bound also manifests itself in the throughput curve; indeed, the bound is quite pessimistic under heavy channel loading (high offered rates). On the other hand, the SGA analysis technique gives optimistic throughput values under low offered rates and pessimistic values when G is high.

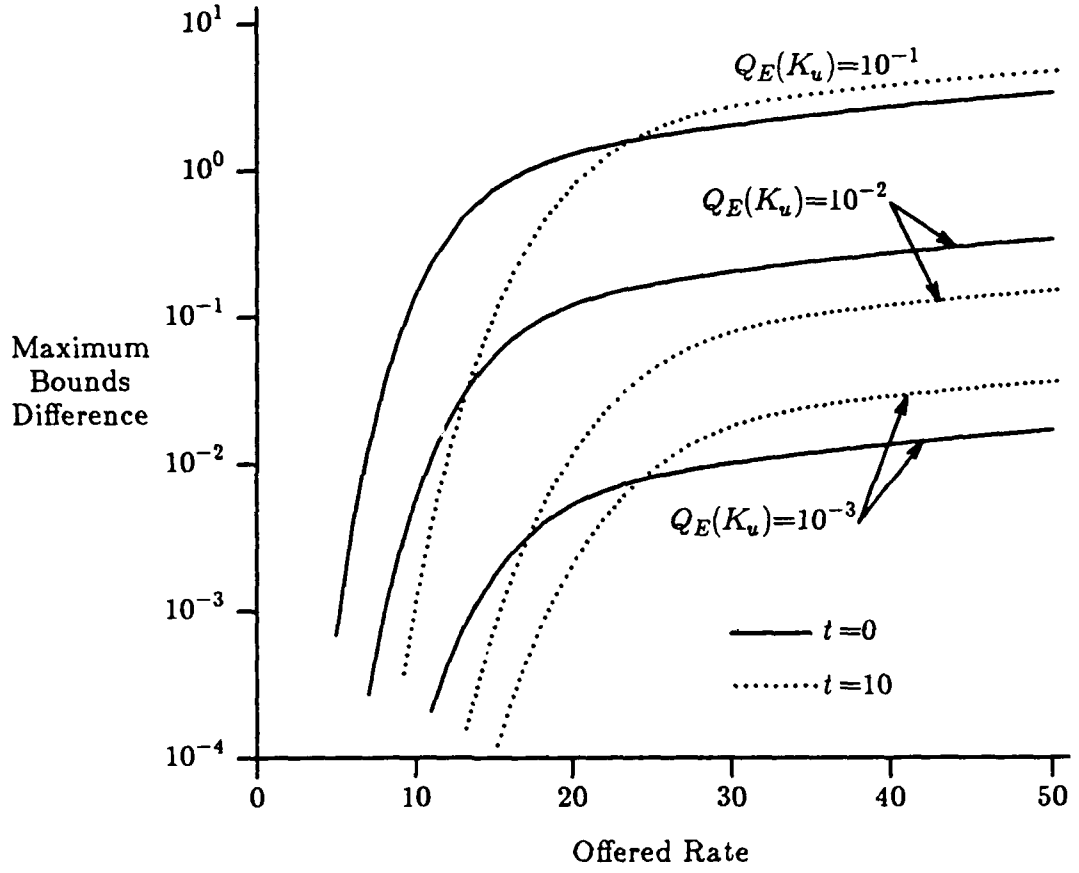

Figure 4.3. Maximum difference between upper and lower bounds on throughput vs offered rate for the Standard Gaussian Approximation ($N=31$, $L=1000$).

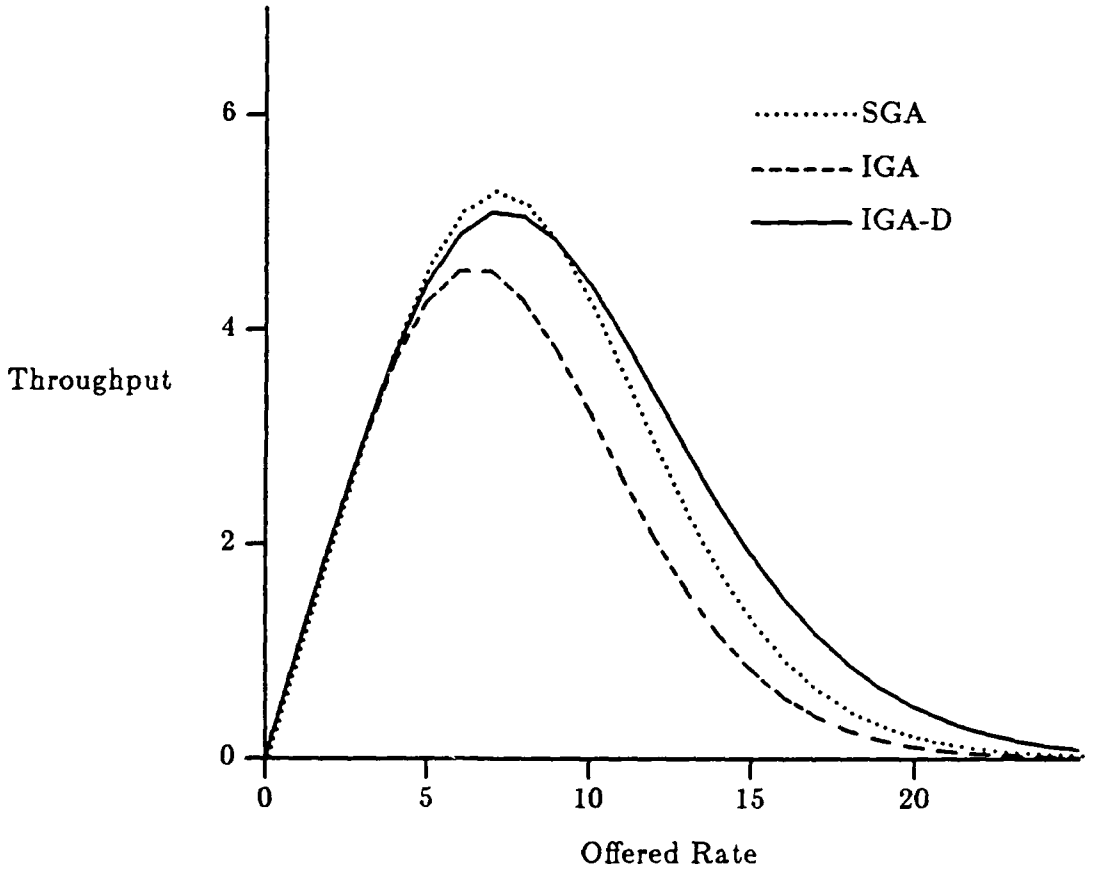

Figure 4.4. Throughput vs offered rate for SGA, IGA, and IGA-D analysis techniques ($N=31$, $L=1000$, $t=0$).

4.4. Packet Error Control and Network Throughput

In traditional narrow-band packet system analysis [12], packets are usually assumed to possess some form of error control, so that only error-free data is "accepted" by the receiver. Error control (error detection) allows the receiver to identify packets which have been involved in a collision and reject the packets accordingly. Traditional analysis still assumes a noiseless channel, so that a packet not involved in a collision will be received correctly with probability 1. Conversely, if two or more narrow-band transmitters operate simultaneously, the communication channel is considered useless during this time; consequently, no amount of error control (error correction) will recover the affected packets, which are then assumed lost.

As shown in the preceding chapters, multiple-access interference in a spread-spectrum communications system can be modeled as additive channel noise; as a result, we can no longer assume that successful packets were transmitted across a noiseless channel. But, at the expense of additional signal bandwidth, we no longer have the unfortunate consequence of a useless channel when two or more transmitters occupy a single time slot. We can conclude, then, that most packets adversely affected by multiple-access interference were not totally destroyed from transmission across a useless channel, but merely contain a few bit errors here and there which can be corrected by an appropriate error control code.

Figure 4.5 shows the effect on network throughput when a packet of length $L = 1000$ bits can have up to 10 errors corrected at the destination node. Although the throughput in "packets per slot" increases over the case where $t = 0$, the redundancy added by the error control code means that each packet has fewer than L information bits in it, with a corresponding reduction in actual data throughput. We can account for this data reduction per packet by defining a quantity called the *effective throughput* and using it in throughput calculations when $t > 0$.

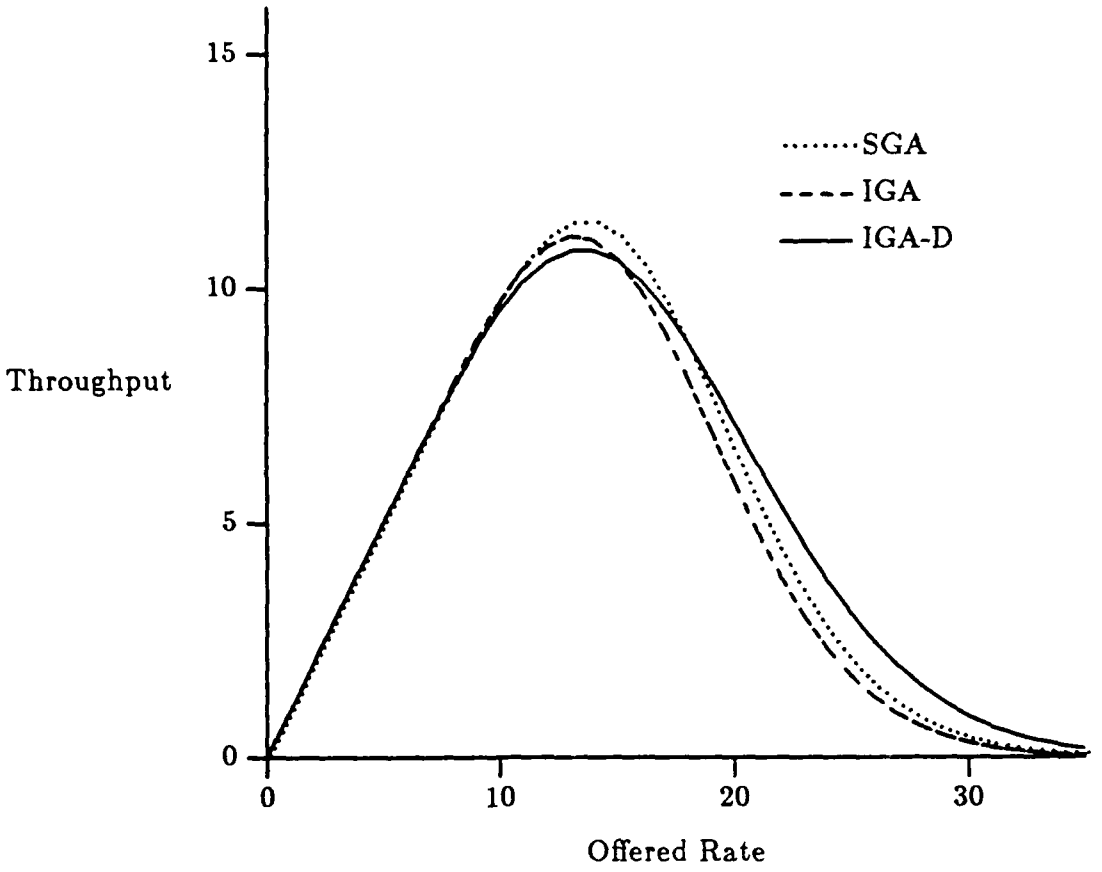

Figure 4.5. Throughput vs offered rate for SGA, IGA, and IGA-D analysis techniques ($N=31$, $L=1000$, $t=10$).

4.4.1. Effective Throughput: Upper Bound

Suppose M message bits are to be encoded with a block error control code into a packet of length L bits, where $M \leq L$. Then the quantity $L-M$ represents the redundancy added to the information to gain some form of error correction capability. It is logical to assume that a higher redundancy results in the ability to correct more bit errors in the packet at the cost of having fewer message bits within the packet; this fact is quantified in the *Hamming bound* [27], which states that to correct t errors in a block of length L bits, the number of message bits M within the block is upper bounded by

$$M \leq L - \left\lceil D \right\rceil \tag{4.10}$$

where

$$D = \log_2 \left[\sum_{i=0}^{t} \binom{L}{i} \right]. \tag{4.11}$$

The quantity M/L is defined as the *rate* R_c of the code, which is simply the fraction of the packet devoted to the message.

Since each packet of length L bits now contains only $M \leq L$ bits of actual data, we can define the *effective throughput* T as

$$T = SR_c = \frac{SM}{L} \leq \frac{S\left(L - \left\lceil D \right\rceil\right)}{L}, \tag{4.12}$$

where the units for T are "data blocks per slot". Obviously, $S \geq T$ with equality when $t = 0$. Note that T is just the number of equivalent packets of L message bits required to obtain the same information throughput as S packets of M message bits and $L-M$ additional bits for error control. Equations (4.10) and (4.12) are met with equality if and only if the error control code employed is a *perfect code,* defined in [27]. Such a code, however, may not exist for arbitrary L and M.

Actual computations are hindered when (4.12) is used directly because $\left|\binom{L}{t}\right|$ is large for reasonable values of L and t; for example, $\left|\binom{10^4}{10}\right| \cong 10^{38}$. The Appendix shows a way to directly calculate a lower bound on D, yielding the following result:

$$T \leq \frac{S\left[L - \left\lceil C(L,t)\right\rceil\right]}{L} \tag{4.13}$$

where

$$C(L,t) = (L+\tfrac{1}{2})\log_2(L) - (t+\tfrac{1}{2})\log_2(t) - (L-t+\tfrac{1}{2})\log_2(L-t) \tag{4.14}$$
$$+ (12L+1)^{-1} - \tfrac{1}{2}\log_2(2\pi) - (12t)^{-1} - 12(L-t)^{-1}.$$

4.4.2. Effective Throughput: Lower Bound

Obtaining a lower bound on T is slightly more involved. First, we must relate S to T by finding a minimum performance limit on block codes in general; then using (4.7) as a lower bound on the packet throughput S for a given G will produce a lower bound on the effective throughput T. We begin by stating the *Gilbert-Varsharmov lower bound* on block code performance [27].

Consider a block code of arbitrary length L. The minimum distance d_m is the smallest Hamming distance between any two codewords in the code. It follows that the Hamming distance is related to the maximum number of errors that the code is guaranteed to correct by the formula

$$d_m = 2t + 1. \tag{4.15}$$

For a code that is not a perfect code, *some* codewords will still decode correctly even though they may contain more than t errors; however, *all* codewords with t or fewer bit errors will decode into the correct information word. It can be shown [28] that binary block codes exist which have a normalized minimum distance that satisfies

$$\frac{d_m}{L} \geq A, \tag{4.16}$$

where A and the code rate R_c are related by

$$R_c = 1 + A\log_2 A + (1-A)\log_2(1-A); \qquad 0 \leq A \leq \tfrac{1}{2}. \tag{4.17}$$

Equations (4.16) and (4.17) represent the Gilbert-Varsharmov bound, where A is plotted as a function of R_c in Figure 4.6.

Now we are in a position to determine a lower bound on the effective throughput T as a function of channel offered rate G for a given packet

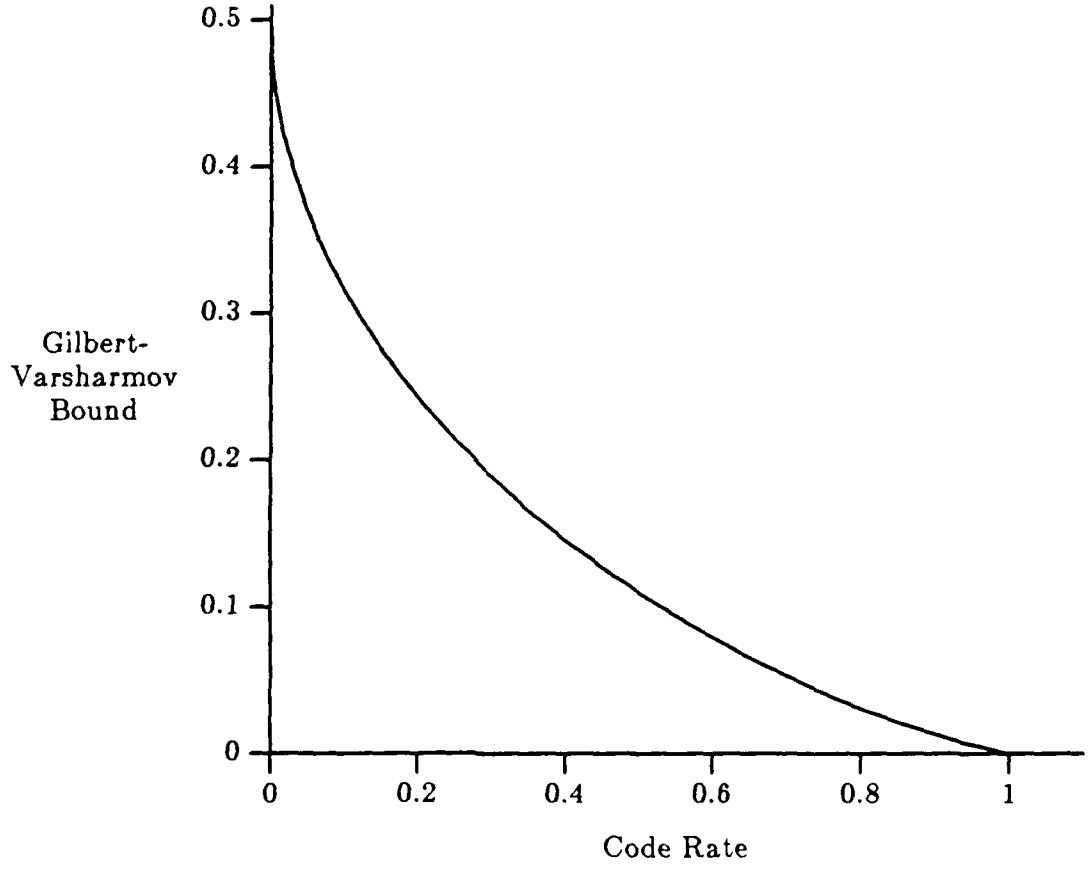

Figure 4.6. Gilbert-Varsharmov lower bound on the normalized asymptotic minimum distance of a block code vs its corresponding rate.

length L, signature sequence length N, and error correction performance t. First, we use (4.7) to lower bound S as a function of G. Next, (4.15) finds d_m for the desired t. Although the quantity A in (4.17) is usually treated as a (decreasing) function of R_c, the mapping is one-to-one, so we can also treat R_c as a decreasing function of A. Substituting (4.15) and (4.16) into (4.17), we have

$$T = SR_c \geq S\left[1+\tilde{A}\log_2\tilde{A}+(1-\tilde{A})\log_2(1-\tilde{A})\right], \tag{4.18}$$

where

$$\tilde{A} = \frac{2t+1}{L}. \tag{4.19}$$

Since we are guaranteed that at least t errors can be corrected with our code (some subset of the collection of codewords may do better), the values for $Q_E(k)$ used in (4.7) will lower bound S directly by assuming that a *maximum* of t errors can be corrected by any codeword.

At this point we are not yet certain whether the addition of error correcting capability to the packets will increase or decrease the effective throughput of the network. Increasing t will increase the average number of successful packets in a slot given that K packets are transmitted, but each packet now contains fewer information bits. Figure 4.7 shows a comparison of the lower bound on T, which we call $T^{(t)}$, vs G for various values of t. (For $t=0$, we set $T^{(t)}=S^{(t)}$.) Note that as t increases, the peak effective throughput exceeds that of a system with larger N and no error correction capability, but without the additional bandwidth penalty incurred by increasing N. However, since the addition of error control reduces the portion of a packet which is devoted to the message, we see that as t increases for a given N, the effective throughput curve peaks more slowly. For example, if $G=5$ and $N=31$, then a network of packets using $t=5$ produces a higher effective throughput than that given by the more powerful $t=20$ error control code. As a consequence, if the offered rate is low, then increasing the error correcting capability for each node in the network actually *reduces* the effective throughput. As the offered rate increases, however, the situation eventually reverses and the more powerful error control code produces the greater effective throughput.

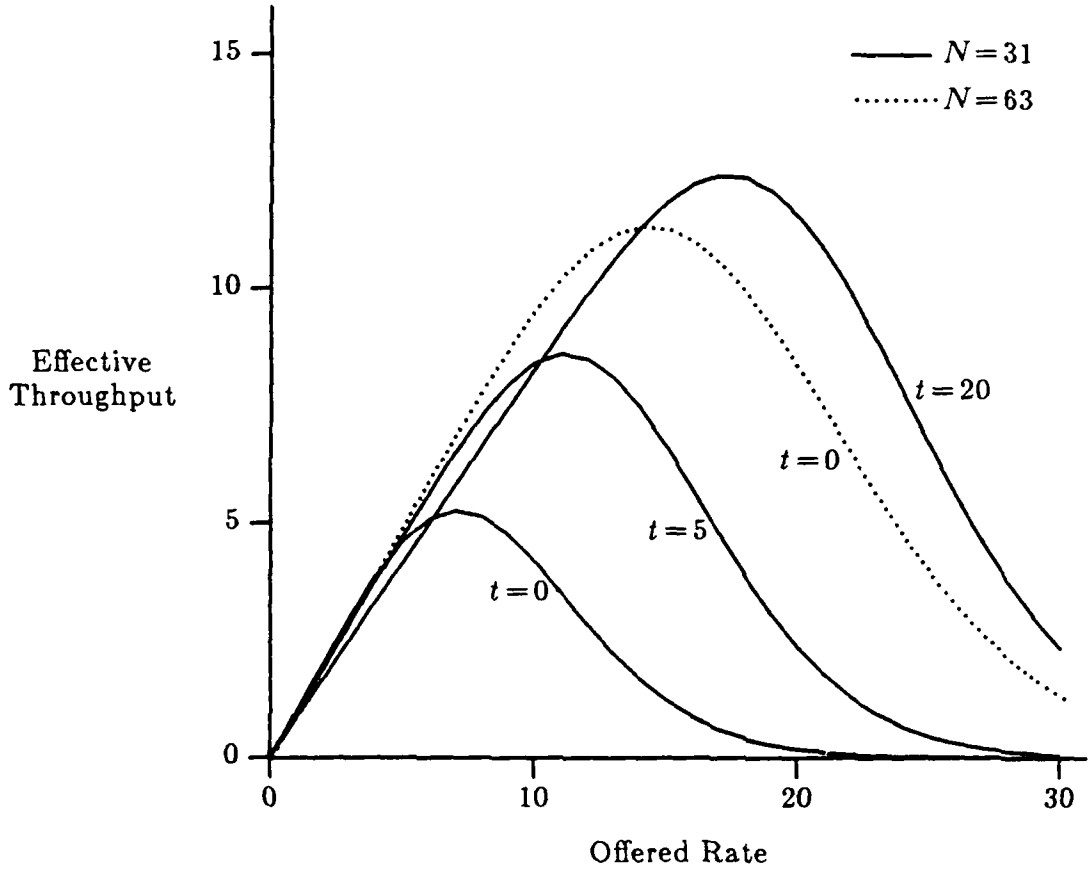

Figure 4.7. A comparison of effective throughput (lower bounded) vs offered rate for different error correction capabilities.

If we plot the peaks of the effective throughput curves in Figure 4.7 as a function of t, the result is the solid line in Figure 4.8. The dotted line in the Figure is a plot of the actual throughput $S^{(l)}$; as t increases, the corresponding reduction in actual information carried by each packet widens the difference between $S^{(l)}$ and $T^{(l)}$. The peak throughput is related to the network capacity, which we define in the next section.

4.5. Network Capacity

When designing a packet communications system, determining network capacity (maximum effective throughput) is an important consideration to avoid instability from an offered rate which exceeds the traffic-handling capability of the channel. In fact, if network capacity greatly exceeds the required throughput, the network's retransmission policy becomes less important to system stability. Figure 4.9 shows this in more detail. Suppose for a given network the required effective throughput is T_0. The capacity of scheme A barely exceeds T_0, and therefore the retransmission rate R must be carefully regulated so that $G = S + R$ falls within the interval a to avoid operating in the unstable region above the curve. Scheme B has a capacity exceeding T_0 by a greater amount, allowing much more variation in the packet retransmission rate (interval b) before instability results.

4.5.1. Effect of Error Control and Sequence Length

In the last section we calculated a lower bound on the effective throughput, which we called $T^{(l)}$, and used it to examine the effect of error control on network performance. For notational consistency, we define network capacity T_C as the maximum value for $T^{(l)}$; that is, $T_C \triangleq \sup\{T^{(l)}\}$. Plots of the network capacity as a function of N for the SGA, IGA, and IGA-D analysis methods are given in Figure 4.10. When $t = 0$, using the IGA method without accounting for bit-to-bit error dependencies gives a slightly pessimistic result for T_C for all values of N, which is consistent with the bit and packet error performance given in Chapters 2 and 3. However, as N increases with $t > 0$, the SGA and IGA methods produce results that are

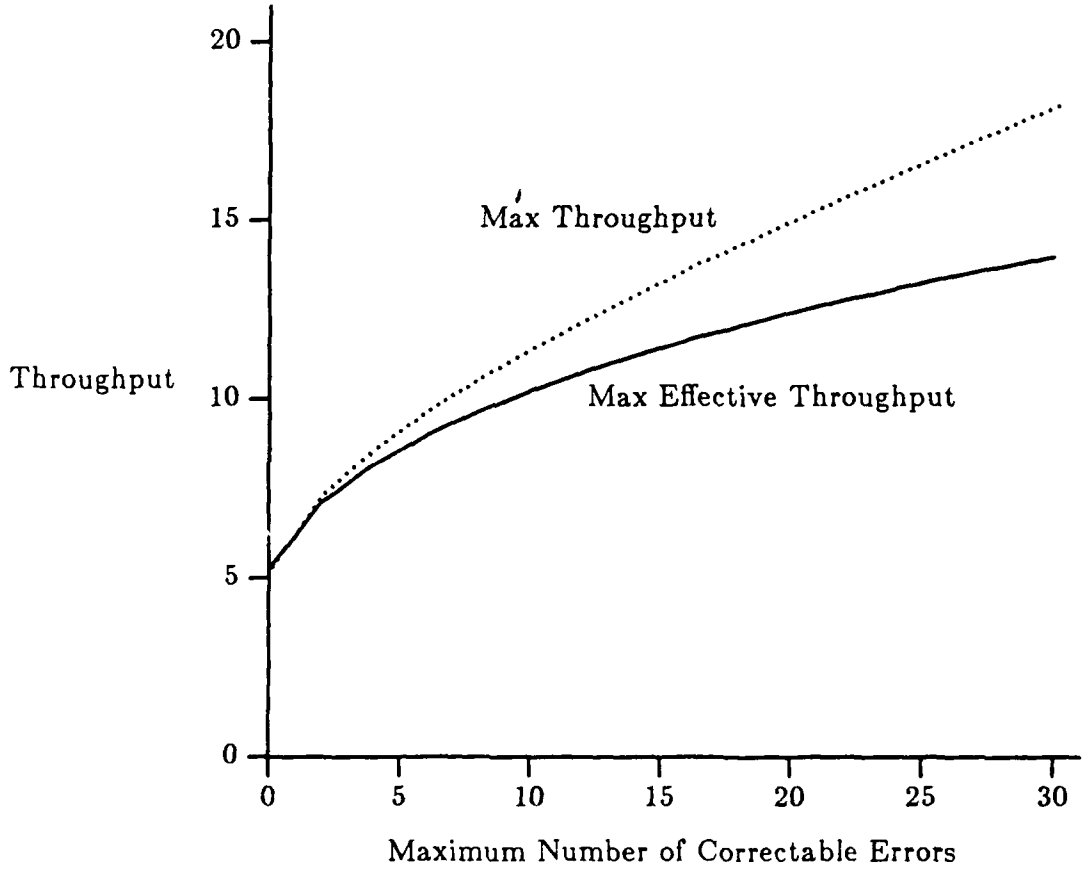

Figure 4.8. Maximum throughput and maximum effective throughput vs number of correctable packet errors ($N=31$, $L=1000$).

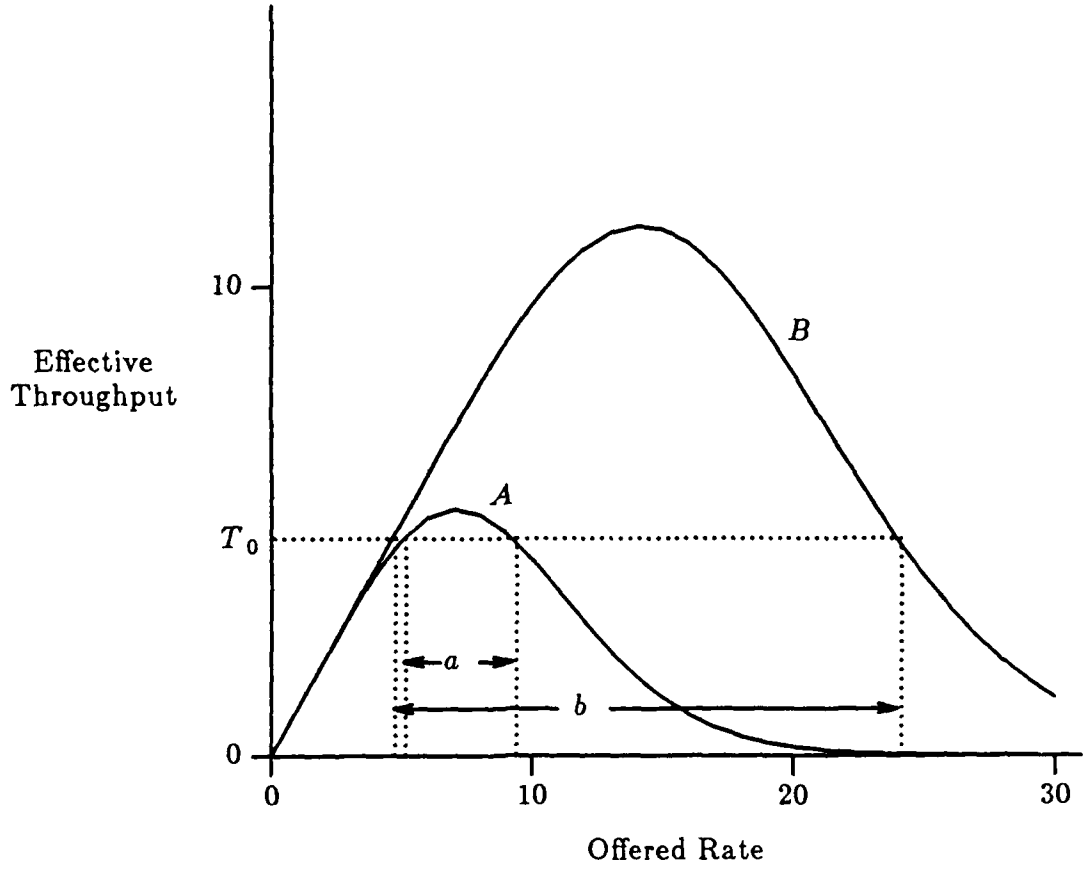

Figure 4.9. The effect of network capacity on the retransmission policy.

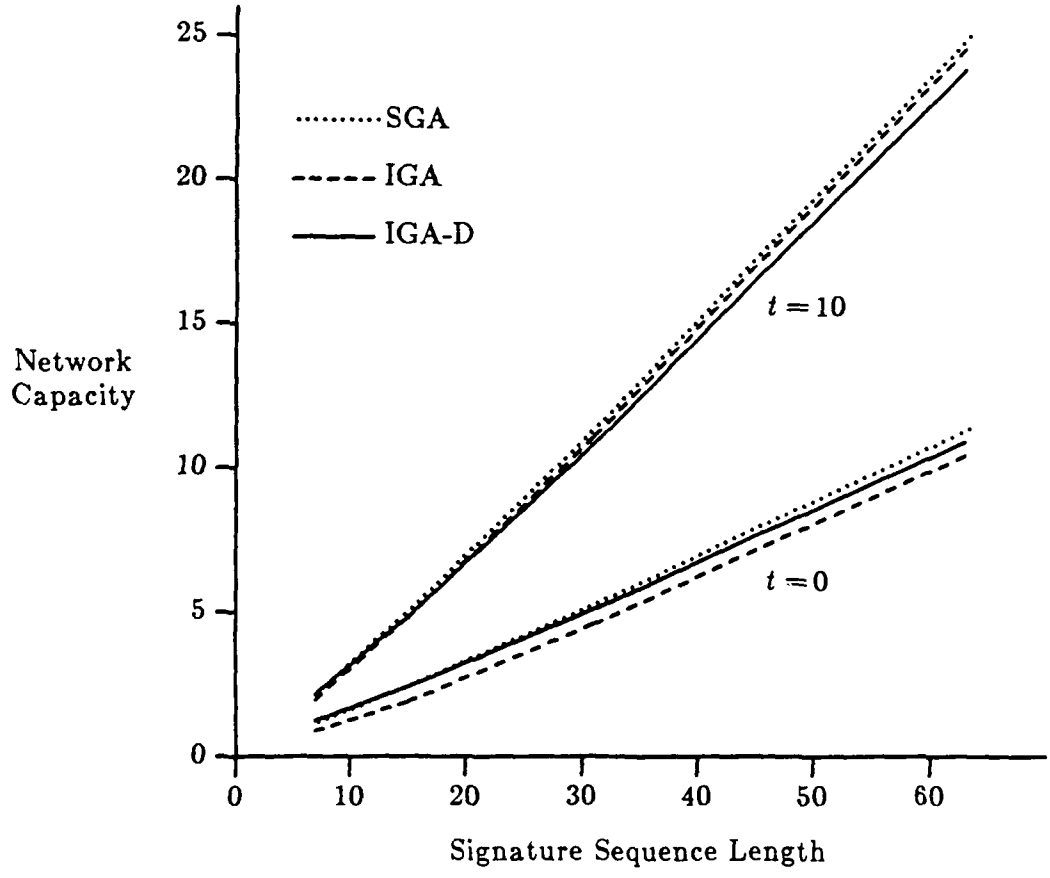

Figure 4.10. Network capacity vs signature sequence length ($L = 1000$).

slightly optimistic compared to those from the IGA-D procedure.

It is also interesting to examine the effect that error control alone has on T_C. Figure 4.11 shows T_C as a function of t for fixed N and L. Note that a small amount of error correction capability increases effective throughput at capacity substantially; then the improvement settles to a fairly linear function of t as t increases further. Also, the SGA and IGA methods seem to converge to the same value for T_C as t increases. This is because higher error control capability means that network capacity occurs at a larger offered rate G. As the offered rate becomes large, the probability that K is small is also small. We discovered in Chapter 2 that the SGA and IGA converge to the same values for the probability of data bit error as K increases for fixed N, so it is reasonable to expect that the packet success rates and network effective throughput performance will become identical as well. One of the main advantages of error control is that added throughput is realized without a corresponding increase in signal bandwidth. Given adequate error control, then, one may wonder if the capacity of a DS/SSMA packet network compares favorably to that of an ordinary narrow-band slotted ALOHA packet network with respect to bandwidth efficiency. This issue is addressed in the next section.

4.5.2. Throughput/Bandwidth Comparisons

The advantages of using spread-spectrum in a packet radio system must be compared to the cost of this signaling technique in terms of increased bandwidth. It is certainly apparent from results in this chapter that the throughput at channel capacity of a direct-sequence spread-spectrum slotted packet network is high because multiple packets can be successfully transmitted in a single slot. However, to gain insight into whether spread-spectrum signaling really offers any throughput advantage over narrow-band signals, we must normalize the throughput by the signal bandwidth; this will enable us to compare the performance of a single spread-spectrum system to a number of narrow-band networks with the same total bandwidth. In order to avoid arbitrary cutoff limits on the (theoretically infinite) bandwidths of the signals in question, we note that N, the number of chips per data bit in the spectral-spreading signal, is also approximately the ratio of the bandwidth of

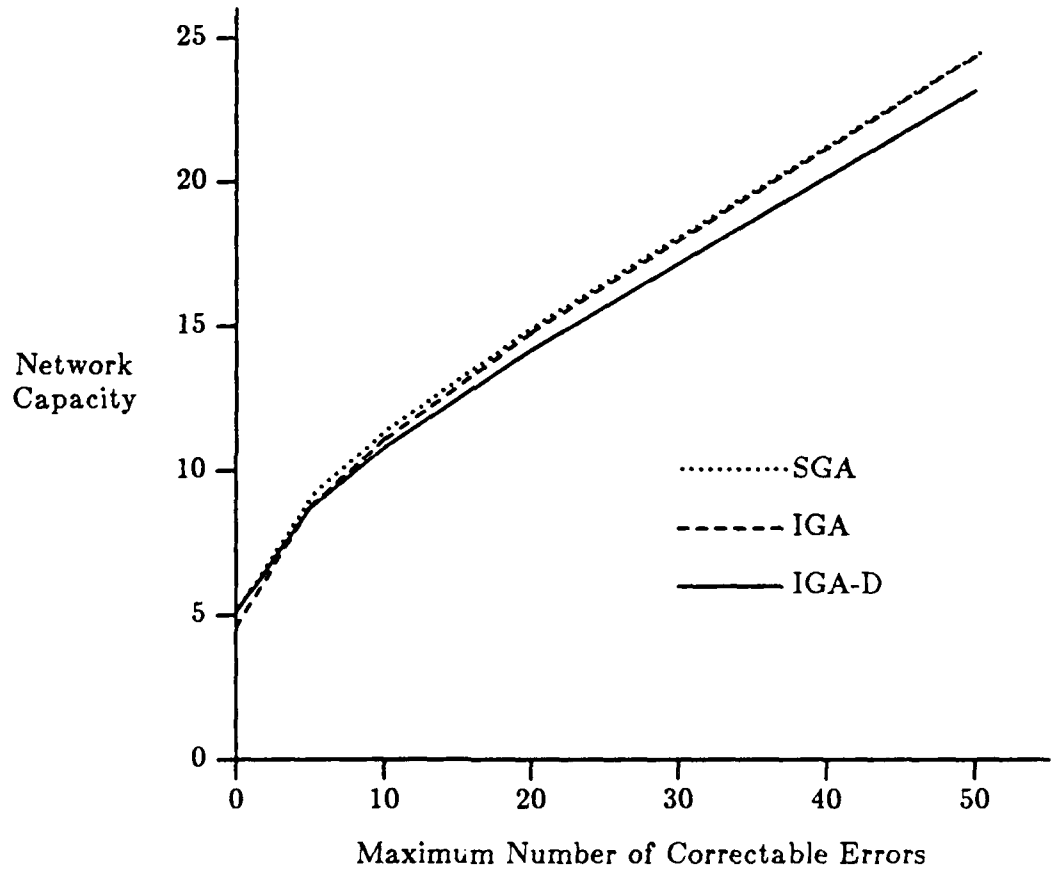

Figure 4.11. Network capacity vs maximum number of correctable errors ($N=31$, $L=1000$).

the spread-spectrum signal to that of the narrow-band signal.

The network capacity of a narrow-band slotted ALOHA system can be found by taking the derivative of (4.1) with respect to G and setting the result to zero, giving

$$\frac{dS}{dG} = e^{-G}(1-G) = 0; \tag{4.20}$$

thus maximum throughput of $S = 1/e \cong 0.368$ is produced at an offered rate of $G = 1$. We now define the *capacity/bandwidth factor* $\mathcal{B}$ by

$$\mathcal{B} = \frac{eT_C}{N} \tag{4.21}$$

which is the ratio of the maximum effective data throughput of the spread-spectrum packet system to the data capacity of N narrow-band slotted ALOHA packet networks. Using the results derived in the previous sections, we can find values of $\mathcal{B}$ for various values for N and t (Figure 4.12). It is apparent that a direct-sequence spread-spectrum packet system with no error control makes poorer use of channel bandwidth for a particular T_C than using N narrow-band slotted ALOHA systems. However, when a sufficient amount of error control is employed to correct some of the packet errors caused by multiple-access interference, the network capacity increases beyond that of N narrow-band systems.†

4.6. Conclusion

By allowing the total number of users K to become a random variable with a Poisson distribution, we can derive arbitrarily tight bounds on the network throughput of a slotted ALOHA packet system using DS/SSMA signaling. Since each slot can carry more than one packet successfully, the throughput measured in "packets per slot" can exceed unity at the expense of a greater transmission bandwidth compared to ordinary narrow-band phase-

† Under our assumption of a useless channel during narrow-band collisions, slotted ALOHA systems under traditional analysis will not realize any additional throughput from error correction.

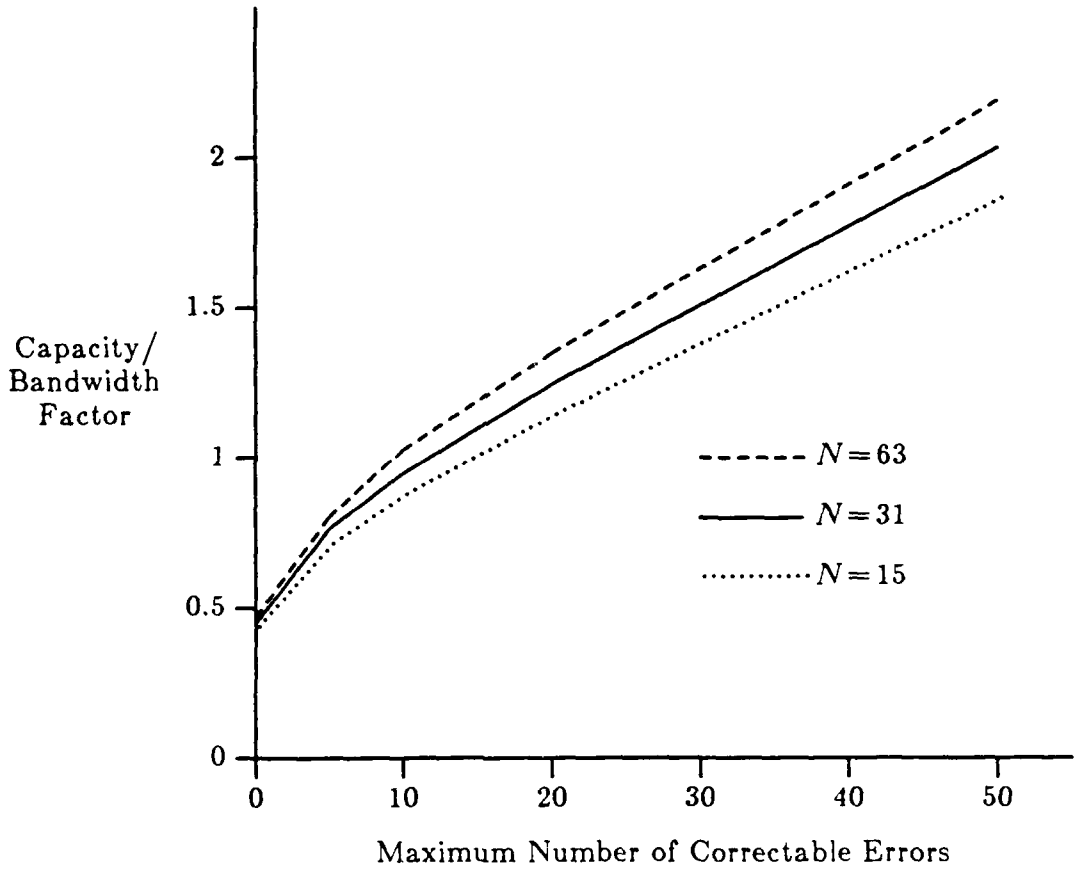

Figure 4.12. Capacity/bandwidth factor (IGA-D) vs number of correctable errors ($L = 1000$).

shift keying techniques. When no error control is used, the IGA method (Improved Gaussian Approximation without accounting for bit-to-bit error dependencies) produces a lower bound on the throughput of the network obtained with the IGA-D (Improved Gaussian Approximation incorporating error dependencies) technique. The SGA (Standard Gaussian Approximation) method is easy to calculate and has lower computational complexity than the other two methods, but provides only an approximation to the actual throughput. If the bit-to-bit error events were truly independent, then the SGA approach is quite optimistic over most of the throughput curve shown in Figure 4.4.

When error correction capability is incorporated into the packets, then the IGA technique no longer lower-bounds the IGA-D results (Figure 4.5). Also, since error control adds redundancy to the data in a packet, the throughput S is no longer an accurate indication of network performance. Instead, we must account for the reduction in packet data by using the effective throughput T, which is the average number of packets consisting entirely of information bits corresponding to S packets comprised of fewer information bits coupled with an error control code. By using the Gilbert-Varsharmov lower bound on block error control code performance, we can calculated a lower bound on T.

The capacity of a network, which we define as the maximum effective throughput, is an important design criterion. For example, if we insure that the network capacity is significantly higher than the required effective throughput, then the retransmission rate associated with failed packets can fall between two widely-spaced limits. We can also compare the capacity of the DS/SSMA packet network to that of N narrow-band slotted ALOHA systems which occupy the same bandwidth. When no error control is used, DS/SSMA is only about half as efficient as the (relatively inefficient) narrow-band signals, but as the error control code becomes more powerful, the capacity/bandwidth factor of the wide-band signaling technique eventually exceeds that of N narrow-band networks.

CHAPTER 5
CONCLUSIONS

5.1. Summary of Results

In Chapter 2, we compared bounds on the probability of data bit error in a direct-sequence spread-spectrum multiple-access communication system with random signature sequences to the results given by the Standard Gaussian Approximation. Although it is tempting to use this approximation for all bit error rate calculations because of its simplicity, we discovered that under some conditions the approximation is inaccurate. Specifically, if the relative delays and phases of the interfering signals are random, then the Standard Gaussian Approximation produces *optimistic estimates* of the bit error rate when K, the number of simultaneous transmitters, is small and the bit error rate is relatively low. If the interfering signal delays and phases are fixed, however, then the Standard Gaussian Approximation is quite accurate for all values of K. By finding the distribution of the multiple-access interference variance over all possible delay and phase values, we can use the Gaussian approximation over the support of the distribution and average the results for a much more accurate representation of the probability of data bit error. This technique, called the Improved Gaussian Approximation, also allows us to account for the bit-to-bit error dependencies produced by the relative constant delays and (possibly) phases of the interfering signals over the transmission time of a desired packet.

The effect of bit-to-bit error dependence on the probability of a successful packet is analyzed in Chapter 3. If no error control is used, then error dependence improves average packet performance by concentrating the bit errors that do occur within a few packets, increasing the number of packets that are error-free. When error control is employed and the channel is lightly

loaded, then performance diminishes when bit error dependencies exist, since concentrating multiple bit errors within a few packets may exceed the capability of the error control code to correct those errors. If the channel is heavily loaded, then performance improves when there is bit-to-bit error dependence. In this situation, some packets are effectively sacrificed by receiving many more than their share of errors, while other packets now have far fewer than the average number of errors and can thus be rescued via error control.

The results in Chapter 4 show that a slotted direct-sequence spread-spectrum packet radio network possesses a significant throughput advantage over that of an equivalent narrow-band ALOHA system; and, provided a reasonable amount of error control is used to further combat multiple-access interference, the throughput per unit bandwidth is also higher. We conclude that the advantages of the direct-sequence spread-spectrum signaling technique in terms of multipath resolution, multiple-access capability, and communications security, along with increased bandwidth efficiency over that of a conventional narrow-band slotted ALOHA network, may be obtained at the expense of a more complicated transmitter and receiver design.

5.2. Future Research

Following the structure of this thesis, there are a number of exciting topics to be worked in the physical, data link, and network layers to gain further insight into the general performance of a spread-spectrum multiple-access packet network.

The physical layer provides the foundation for any communication network, so accurate analysis here is essential for obtaining correct values for packet success and network throughput. We have concentrated on DS/SSMA signaling using rectangular signature sequence pulses with phase-shift keying and coherent detection. Non-coherent detectors are usually cheaper and less complicated, and other chip pulse shapes (such as the raised sine pulse) may increase bandwidth efficiency. The near-far problem, where a strong interfering signal prevents the reception of a weaker desired signal, is an

important consideration in finding the probability of data bit error, but incorporating different signal amplitudes into the results requires some knowledge of the topology of the network being analyzed.

Bit-to-bit error dependence effects are more difficult to analyze if the interfering signals have signature sequences that repeat at the beginning of each data bit, since there are now additional dependencies associated with the particular signature sequence patterns. One of the remaining challenges at the data link layer, then, is to work this problem without (hopefully) producing expressions that are of exponential computational complexity. Like the near-far problem, the analysis of specific signature sequences assigned to specific nodes requires a knowledge of the network topology.

At the network layer, we have shown that it is possible to obtain accurate results for network throughput while avoiding many of the crude approximations sometimes used at the physical and data link layers. Additional work is required to produce accurate throughput results when the network is unslotted. The unslotted network is much easier to implement, since we avoid the difficult task of providing a means to time-synchronize a number of independent nodes. In narrow-band signaling, one motivation for providing time slots in an ALOHA scheme was a doubling of network capacity over the unslotted case [12], but because of the multiple-access nature of spread-spectrum, it is not clear what effect the lack of time slotting will have on network throughput under this signaling scheme. It is obvious, however, that the unslotted case is more difficult to analyze.

Throughput may be considered as a "macroscopic" measure of the performance of a specific packet network; at the "microscopic" level a designer may need to know the average delay (or its distribution) required for a specific packet to reach its destination. Indeed, there are many applications (such as industrial robot control and digitized voice transmission) where minimizing packet delay is an extremely important design criterion. Future work should therefore concentrate on developing a method for finding the distribution of packet delay in a spread-spectrum multiple-access network.

As a final note, we briefly compare the frequency-hopped (FH) method of spread-spectrum signaling to the direct-sequence (DS) technique. Since FH avoids interference from other users by changing the actual r-f carrier

frequency according to some pseudo-random pattern, there are no bit-to-bit error dependencies to influence performance. Also, the near-far effect is reduced because of the isolation provided by the different frequency slots. Frequency synthesizer design factors place a limit on the hopping rate of a FH system, however, so the DS method with a short chip duration provides superior multipath rejection. Eventually, however, the hopping rate of synthesizers may be fast enough to combat multipath interference by allowing the receiver to change frequency before the arrival of multipath components in a specific frequency slot.

LIST OF REFERENCES

LIST OF REFERENCES

[1] John D. Day and Hubert Zimmermann "The OSI reference model," in *Proc. IEEE,* pp. 1334-1340, Dec. 1983.

[2] J. S. Lehnert and M. B. Pursley, "Error probabilities for binary direct-sequence spread-spectrum communications with random signature sequences," *IEEE Transactions on Communications,* vol. COM-75, pp. 87-98, Jan 1987.

[3] K. Yao, "Error probability of asynchronous spread spectrum multiple-access communication systems," *IEEE Transactions on Communications,* vol. COM-25, pp. 803-809, Aug. 1977.

[4] M. B. Pursley, "Performance evaluation for phase-coded spread-spectrum multiple-access communication—Part I: System analysis," *IEEE Transactions on Communications,* vol. COM-25, pp. 795-799, Aug. 1977.

[5] M. B. Pursley, D. V. Sarwate, and W. E. Stark, "Error probability for direct-sequence spread-spectrum multiple-access communications—Part 1: Upper and lower bounds," *IEEE Transactions on Communications,* vol COM-30, PP. 975-984, May 1982.

[6] E. A. Geraniotis and M. B. Pursley, "Error probability for direct-sequence spread-spectrum multiple-access communications—Part 2: Approximations," *IEEE Transactions on Communications,* vol COM-30, PP. 985-995, May 1982.

[7] M. B. Pursley and D. J. Taipale, "Error probabilities for spread-spectrum packet radio with convolutional codes and Viterbi decoding," *IEEE Transactions on Communications,* vol. COM-75, pp.1-12, Jan. 1987.

[8] D. H. Davis and S. A. Gronemeyer, "Performance of slotted ALOHA random access with delay capture and randomized time of arrival," *IEEE Transactions on Communications,* vol. COM-28, pp. 703-710, May 1980.

[9] E. S. Sousa and J. A. Silvester, "A spreading code protocol for a distributed spread spectrum packet radio network," in *Proc. IEEE Global Communications Conf.,* pp. 481-486, Nov. 1984.

[10] E. S. Sousa and J. A. Silvester, "A code switching technique for distributed spread spectrum packet radio networks," in *Proc. IEEE Global Communications Conf.,* pp. 1093-1095, June 1985.

[11] Y. Birk and F. A. Tobagi, "Code-assignment policies for multi-receiver nodes in CDMA packet radio networks," in *Proc. of IEEE INFOCOM '86,* pp. 415-423, Apr. 1986.

[12] N. Abramson "The throughput of packet broadcasting channels," *IEEE Transactions on Communications,* vol. COM-25, pp. 117-128, Jan. 1977.

[13] D. Raychaudhuri, "Performance analysis of random access packet-switched code division multiple access systems," *IEEE Transactions on Communications,* vol. COM-29, pp. 895-901, June 1981.

[14] J. M. Musser and J. N. Daigle, "Throughput analysis of an asynchronous code division multiple-access (CDMA) system," in *Proc. ICC,* Philadelphia, July 1982, pp. 2F.2.1-2F.2.7.

[15] A. Polydoros and J. Silvester, "An analytical framework for slotted random access spread spectrum networks," in *Proc. IEEE Military Communications Conf.,* pp. 461-467, Oct. 1985.

[16] J. M. Brazio and F. A. Tobagi, "Throughput analysis of spread spectrum multihop packet radio networks," in *Proc. of IEEE INFOCOM '85,* pp. 256-265, March 1985.

[17] J. Brazio, "Capacity analysis of multihop packet radio networks under a general class of channel access protocols and capture modes," Ph.D. dissertation, Department of Electrical Engineering, Stanford University, California, 1986.

[18] W. Feller, *An Introduction to Probability Theory and Its Applications.* Vol. I. New York: John Wiley & Sons, 1968, pp. 52-54, 79-82.

[19] M. B. Pursley, "Spread-spectrum multiple-access communications," in *Multi-User Communications,* G. Longo (ed.), Springer-Verlag, Vienna and New York, pp. 139-199, 1981.

[20] P. K. Enge and D. V. Sarwate, "Spread-spectrum multiple-access performance of orthogonal codes: linear receivers," *IEEE Transactions on Communications,* vol. COM-35, pp. 1309-1319, December 1987.

[21] H. J. Larson and B. O. Shubert, *Probabilistic Models in Engineering Sciences, Vol. I.* New York: John Wiley & Sons, Inc., 1979, pp. 123, 244, 358.

[22] M. Dresher, "Moment spaces and inequalities," *Duke Math. Journal,* Vol. 20, pp. 261-271, June 1953.

[23] M. Dresher, S. Karlin, and L. S. Shapley, "Polynomial games," in *Contributions to the Theory of Games,* vol. I., (H. W. Kuhn and A. W. Tucker, editors), Annals of Mathematics Studies, no. 24, pp. 161-180, 1950.

[24] R. B. Ash, *Real Analysis and Probability.* New York: Academic Press, Inc., 1972, pp. 254.

[25] J. F. Hayes, *Modeling and Analysis of Computer Communications Networks.* New York: Plenum Press, 1984, Chapter 8.

[26] F. A. Tobagi, "Random access techniques for data transmission over packet switched radio networks," Ph.D. dissertation, Department of Electrical Engineering, University of California, Los Angeles, 1974.

[27] J. G. Proakis, *Digital Communications.* New York: McGraw-Hill, Inc., 1983, Chapter 5.

[28] W. W. Peterson and E. J. Weldon, *Error-Correcting Codes.* Cambridge: MIT Press, 1972.

[29] A. Papoulis, *Probability, Random Variables, and Stochastic Processes.* New York: McGraw-Hill, Inc., 1965, p. 126.

APPENDIX

Appendix

A.1. Derivation of (2.81)

Given the random variable S which is uniform on $[0,1]$, we wish to find the distribution of

$$V = (2B+1)(S^2-S) + \frac{N}{2}. \tag{A.1.1}$$

We begin by finding the density function of $X = S^2-S$ as follows. From [29], for $X = g(S)$ quadratic in S the density of X is

$$f_X(x) = \frac{f_S(s_1)}{|g'(s_1)|} + \frac{f_S(s_2)}{|g'(s_2)|}, \tag{A.1.2}$$

where s_1 and s_2 are the solutions to $g(s)-x=0$ and $g'(s_i)$ is the first derivative of $g(s)$ evaluated at s_i. Substituting

$$s_{1,2} = \frac{1 \pm \sqrt{1+4x}}{2} \tag{A.1.3}$$

along with $g'(s) = 2s-1$, into (A.1.2) gives

$$f_X(x) = \frac{2}{\sqrt{1+4x}}; \qquad -\frac{1}{4} < x \leq 0. \tag{A.1.4}$$

We now note that the random variable V in (A.1.1) is of the form $V = aX+b$, where a and b are constants; therefore

$$f_V(v) = \frac{1}{|a|} f_X\left(\frac{v-b}{a}\right). \tag{A.1.5}$$

Finally, substituting $a = 2B+1$ and $b = N/2$ into (A.1.5) gives, for a specific B,

$$f_V(v) = \frac{1}{\sqrt{\tilde{B}(2v+\tilde{B}-N)}}; \qquad \frac{N-\tilde{B}}{2} < v < \frac{N}{2}, \tag{A.1.6}$$

where $\tilde{B} = B+\frac{1}{2}$.

A.2. Derivation of (2.82)

The random variable $Z = UV$ is the product of two independent random variables; as such, we have [21]

$$f_Z(z) = \int_{-\infty}^{\infty} \frac{1}{|v|} f_U\left(\frac{z}{v}\right) f_V(v)dv\,, \tag{A.2.1}$$

where

$$f_U(u) = \frac{1}{\pi\sqrt{u(2-u)}}; \qquad 0 < u < 2 \tag{A.2.2}$$

and, for a particular B, $f_V(v)$ is given by (A.1.5).

The quantity inside the integral in (A.2.1) is the joint density of Z and V; i.e.

$$f_{Z,V}(z,v) = \frac{1}{|v|} f_U\left(\frac{z}{v}\right) f_V(v)\,, \tag{A.2.3}$$

which, after substituting the appropriate values from (A.1.6) and (A.2.2), becomes

$$f_{Z,V}(z,v) = \frac{1}{2\pi\sqrt{\tilde{B}z}} \frac{1}{\sqrt{v^2-bv+c}} \tag{A.2.4}$$

where

$$b = \frac{N-\tilde{B}+z}{2} \tag{A.2.5}$$

and

$$c = \frac{z(N-\tilde{B})}{4}\,. \tag{A.2.6}$$

From a standard table of integrals, we find that

$$\int \frac{dv}{\sqrt{v^2-bv+c}} = \log\left[2v - b + 2\sqrt{v^2-bv+c}\right] \tag{A.2.7}$$

where $\log = \log_e$.

To determine the limits of integration in (A.2.1) we must find the support of $f_{Z,V}(z,v)$. We know that $0 < U < 2$ and $(N-\tilde{B})/2 < V < N/2$, so $Z = UV$ is the product of two positive numbers and $0 < Z < N$. If we let U vary

between 0 and 2, then for $V=(N-\tilde{B})/2$ we have $0<Z<N-\tilde{B}$ and for $V=N/2$ we have $0<Z<N$. If $U=0$, then $Z=0$ for all V, and if $U=2$ then $Z=2V$ for all V. We have thus completely defined the boundaries of the support for $f_{Z,V}(z,v)$, which are shown in Figure A.1. Now the integral in (A.2.1) may be split into two parts, giving

$$f_Z(z) = \begin{cases} \int_{\frac{N-\tilde{B}}{2}}^{N/2} f_{Z,V}(z,v)dv\,; & 0<z<N-\tilde{B} \\ \\ \int_{z/2}^{N/2} f_{Z,V}(z,v)dv\,; & N-\tilde{B}<z<N \end{cases} \tag{A.2.8}$$

After substituting the appropriate values for b and c into the top integral in (A.2.8), we obtain for $0<z<N-\tilde{B}$

$$\begin{aligned} f_Z(z) &= \frac{1}{2\pi\sqrt{\tilde{B}z}}\log\left[\frac{(N-z)+2\sqrt{\tilde{B}(N-z)}+\tilde{B}}{(N-z)-\tilde{B}}\right] \\ &= \frac{1}{2\pi\sqrt{\tilde{B}z}}\log\left[\frac{\left(\sqrt{N-z}+\sqrt{\tilde{B}}\right)\left(\sqrt{N-z}+\sqrt{\tilde{B}}\right)}{\left(\sqrt{N-z}+\sqrt{\tilde{B}}\right)\left(\sqrt{N-z}-\sqrt{\tilde{B}}\right)}\right] \\ &= \frac{1}{2\pi\sqrt{\tilde{B}z}}\log\left[\frac{\sqrt{N-z}+\sqrt{\tilde{B}}}{\sqrt{N-z}-\sqrt{\tilde{B}}}\right]. \end{aligned} \tag{A.2.9}$$

Similarly, the lower integral in (A.2.8) evaluates as

$$f_Z(z) = \frac{1}{2\pi\sqrt{\tilde{B}z}}\log\left[\frac{\sqrt{N-z}+\sqrt{\tilde{B}}}{\sqrt{\tilde{B}}-\sqrt{N-z}}\right] \tag{A.2.10}$$

for $N-\tilde{B}<z<N$. Finally, combining (A.2.9) and (A.2.10) yields

$$f_Z(z) = \frac{1}{2\pi\sqrt{\tilde{B}z}}\log\left|\frac{\sqrt{N-z}+\sqrt{\tilde{B}}}{\sqrt{N-z}-\sqrt{\tilde{B}}}\right|; \quad 0<z<N. \tag{A.2.11}$$

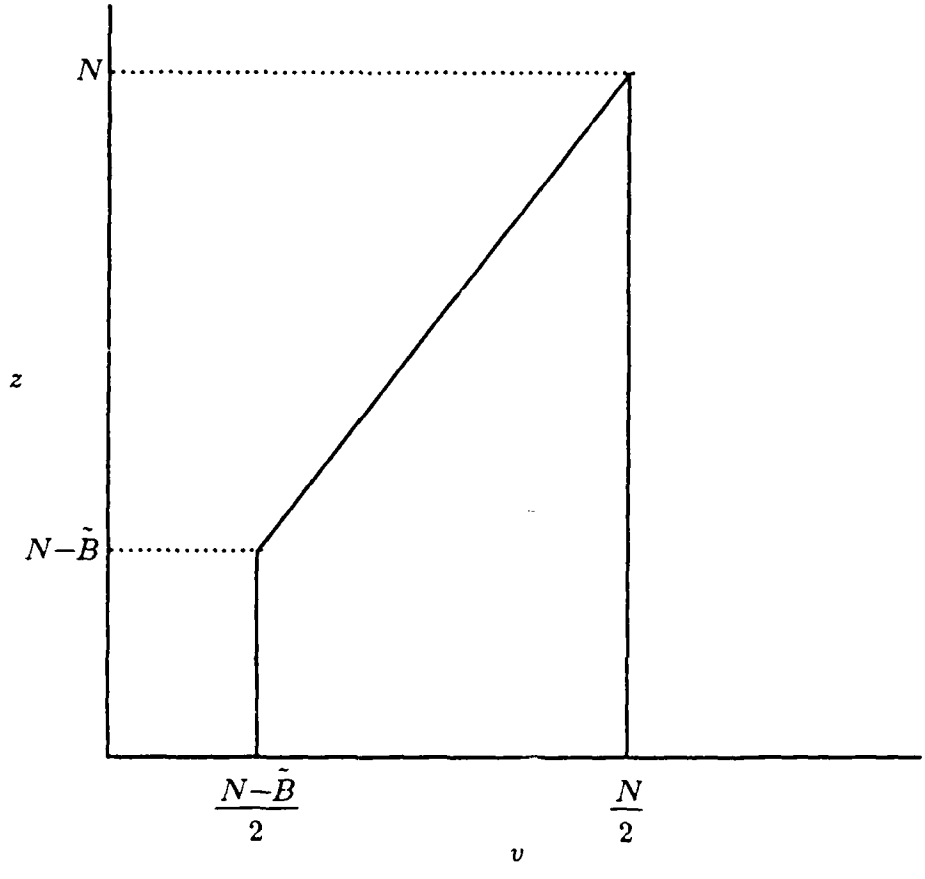

Figure A.1. Support of $f_{Z,V}(z,v)$.

A.3. Derivation of (2.84)

To obtain the cumulative distribution function of the random variable Z for a particular B, we integrate (A.2.11) directly, remembering to find an appropriate constant of integration to produce a valid distribution function. First, we restrict z to be between 0 and $N-\tilde{B}$ and we separate the log terms in (A.2.11) to produce

$$F_Z(z) = \frac{1}{2\pi\sqrt{\tilde{B}}}\left\{\int \frac{1}{\sqrt{z}} \log\left[\sqrt{N-z}+\sqrt{\tilde{B}}\right]dz - \int \frac{1}{\sqrt{z}} \log\left[\sqrt{N-z}-\sqrt{\tilde{B}}\right]dz\right\}. \tag{A.3.1}$$

The two integrals in (A.3.1) will be called (1) and (2), respectively. Next, for z between $N-\tilde{B}$ and N, we have

$$F_Z(z) = \frac{1}{2\pi\sqrt{\tilde{B}}}\left\{\int \frac{1}{\sqrt{z}} \log\left[\sqrt{N-z}+\sqrt{\tilde{B}}\right]dz - \int \frac{1}{\sqrt{z}} \log\left[\sqrt{\tilde{B}}-\sqrt{N-z}\right]dz\right\}. \tag{A.3.2}$$

The first integral in (A.3.2) is identical to integral (1), and we call the second integral (3).

The following integral from a standard table of integrals will prove useful. If we let $X = N-\tilde{B} \pm 2\sqrt{\tilde{B}}x - x^2$ then

$$\int \frac{\sqrt{X}}{x}dx = \sqrt{X} \pm \sqrt{\tilde{B}}\sin^{-1}\left[\frac{x \mp \sqrt{\tilde{B}}}{\sqrt{N}}\right] - \sqrt{N-\tilde{B}}\log\left[\frac{2\left|\sqrt{(N-\tilde{B})X} \mp \sqrt{\tilde{B}}x + N-\tilde{B}\right|}{x}\right]. \tag{A.3.3}$$

Integral (1): Performing a change of variable by letting $z = N-y^2$ we obtain

$$\frac{1}{2}(1) = \int \frac{-y}{\sqrt{N-y^2}} \log\left[y+\tilde{B}\right]dy \,. \tag{A.3.4}$$

Integrating by parts with

$$u = \sqrt{N-y^2}; \qquad du = \frac{-y\,dy}{\sqrt{N-y^2}}, \tag{A.3.5}$$

and

$$v = \log\left[y+\sqrt{\tilde{B}}\right]; \qquad dv = \frac{dy}{y+\sqrt{\tilde{B}}}, \tag{A.3.6}$$

produces

$$\frac{1}{2}(1) = \sqrt{N-y^2}\log\left[y+\sqrt{\tilde{B}}\right] - \int \frac{\sqrt{N-y^2}}{y+\sqrt{\tilde{B}}}dy \,. \tag{A.3.7}$$

If we let $y = x-\sqrt{\tilde{B}}$ in the integral in (A.3.7), which we call integral (A), we have

$$(A) = \int \frac{\left[N-\left(x-\sqrt{\tilde{B}}\right)^2\right]^{1/2}}{x}dx \tag{A.3.8}$$

$$= \int \frac{\sqrt{X}}{x}dx$$

which is given by (A.3.3) for $X = N-\tilde{B}+2\sqrt{\tilde{B}}x-x^2$. We now back-substitute $x = y+\sqrt{\tilde{B}}$ into (A), substitute (A) into (A.3.7), and then back-substitute $z = N-y^2$, which gives

$$\frac{1}{2}(1) = \sqrt{z}\left[\log\left[\sqrt{N-z}+\sqrt{\tilde{B}}\right]-1\right] \tag{A.3.9}$$

$$-\sqrt{\tilde{B}}\sin^{-1}\left[\left(\frac{N-z}{N}\right)^{1/2}\right]$$

$$+\sqrt{N-\tilde{B}}\log\left[\frac{2\left[\sqrt{(N-\tilde{B})z}+\sqrt{\tilde{B}(N-z)}+N\right]}{\sqrt{N-z}+\sqrt{\tilde{B}}}\right].$$

Integral (2): The procedure for evaluating integral (2) is identical (except for sign changes) to that used for integral (1) through the integration by parts, producing

$$\frac{1}{2}(2) = \sqrt{N-y^2}\log\left[y-\sqrt{\tilde{B}}\right]-\int\frac{\sqrt{N-y^2}}{y-\sqrt{\tilde{B}}}dy\,. \tag{A.3.10}$$

After a change of variables, evaluating the integral in (A.3.10) by using (A.3.3), and back-substituting, we obtain

$$\begin{aligned}\frac{1}{2}(2) = \sqrt{z}\left(\log\left[\sqrt{N-z}-\sqrt{\tilde{B}}\right]-1\right) \\ +\sqrt{\tilde{B}}\,\sin^{-1}\left[\left(\frac{N-z}{N}\right)^{1/2}\right] \\ +\sqrt{N-\tilde{B}}\,\log\left[\frac{2\left(\sqrt{(N-\tilde{B})z}-\sqrt{\tilde{B}(N-z)}+N\right)}{\sqrt{N-z}-\sqrt{\tilde{B}}}\right].\end{aligned} \tag{A.3.11}$$

Integral (3): While carefully monitoring sign changes, integral (3) is evaluated by using a procedure of integrating by parts, applying (A.3.3), and back substituting, which gives

$$\begin{aligned}\frac{1}{2}(3) = \sqrt{z}\left(\log\left[\sqrt{\tilde{B}}-\sqrt{N-z}\right]-1\right) \\ +\sqrt{\tilde{B}}\,\sin^{-1}\left[\left(\frac{N-z}{N}\right)^{1/2}\right] \\ +\sqrt{N-\tilde{B}}\,\log\left[\frac{2\left(\sqrt{(N-\tilde{B})z}-\sqrt{\tilde{B}(N-z)}+N\right)}{\sqrt{N-z}-\sqrt{\tilde{B}}}\right].\end{aligned} \tag{A.3.12}$$

Now we can assemble integrals (1), (2), and (3) into (A.3.1) and (A.3.2) to obtain

$$F_Z(z) = \begin{cases} \dfrac{1}{2\pi\sqrt{\tilde{B}}}\, 2\left[\dfrac{1}{2}(1)-\dfrac{1}{2}(2)\right]+C\,; & 0 \le z \le N-\sqrt{\tilde{B}} \\ \dfrac{1}{2\pi\sqrt{\tilde{B}}}\, 2\left[\dfrac{1}{2}(1)-\dfrac{1}{2}(3)\right]+C\,; & N-\sqrt{\tilde{B}} \le z \le N \end{cases} \tag{A.3.13}$$

where C is a constant of integration. To evaluate C, note that $F_Z(0) = -1 + C$ which implies that $C = 1$. Finally, by substituting the actual values for integrals (1), (2), and (3) into (A.3.13) we have, for a specific B,

$$\begin{aligned} F_Z(z) = 1 + \frac{1}{\pi\sqrt{\tilde{B}}} \Bigg\{ & \sqrt{N-\tilde{B}}\, \log\left|\frac{b(a^2+c^2)}{a(b^2+c^2)}\right| \\ & - 2\sqrt{\tilde{B}}\, \sin^{-1}\left[\left(\frac{N-z}{N}\right)^{1/2}\right] \\ & + \sqrt{z}\, \log\left|\frac{a}{b}\right| \Bigg\}; \qquad 0 \le z \le N, \end{aligned} \tag{A.3.14}$$

where

$$\begin{aligned} a &= \sqrt{N-z} + \sqrt{\tilde{B}}\,; \\ b &= \sqrt{N-z} - \sqrt{\tilde{B}}\,; \\ c &= \sqrt{N-\tilde{B}} + \sqrt{z}\,. \end{aligned}$$

A.4. Derivation of (4.14)

The Hamming bound in equation (4.13) requires the calculation of the quantity

$$D = \log_2\left[\sum_{i=0}^{t}\left|\frac{L}{i}\right|\right] \tag{A.4.1}$$

where $\left|\frac{L}{i}\right| = \frac{L!}{i!(L-i)!}$. Direct calculation of the sum prior to taking the log becomes impractical in many cases because of the large numbers involved. We can, however, approximate D by $\tilde{D} \le D$ with $D-\tilde{D} \cong 1$ or less without directly evaluating any of the binomial coefficients by using the following procedure.

First, we need to find a range of values for t such that

$$D-1 < \log_2 \left(\begin{matrix} L \\ t \end{matrix} \right) \leq D \ . \tag{A.4.2}$$

The right inequality in (A.2) is obvious for all $t \leq L$, with equality when $t = 0$. The left inequality is true if

$$\left(\begin{matrix} L \\ t \end{matrix} \right) > \sum_{i=0}^{t-1} \left(\begin{matrix} L \\ i \end{matrix} \right) . \tag{A.4.3}$$

Since the binomial coefficients increase monotonically for $0 \leq i \leq L/2$, L even, or $0 \leq i \leq (L-1)/2$, L odd, and since the sum in (A.4.3) contains t terms, we can conclude that the largest term in the sum is when $i = t-1$, and thus the sum can be loosely upper bounded by

$$t \left(\begin{matrix} L \\ t-1 \end{matrix} \right) \geq \sum_{i=0}^{t-1} \left(\begin{matrix} L \\ i \end{matrix} \right) , \tag{A.4.4}$$

so if we can find a range of values for t which satisfy

$$\left(\begin{matrix} L \\ t \end{matrix} \right) \geq t \left(\begin{matrix} L \\ t-1 \end{matrix} \right) \tag{A.4.5}$$

we will also satisfy (A.4.3). To do this, we note the recursion relation for binomial coefficients:

$$\left(\begin{matrix} L \\ 0 \end{matrix} \right) = 1; \qquad \left(\begin{matrix} L \\ i \end{matrix} \right) = \left(\begin{matrix} L \\ i-1 \end{matrix} \right) \left(\frac{L-i+1}{i} \right) , \tag{A.4.6}$$

allowing us to simplify (A.4.5) to

$$\frac{L-t+1}{t} \geq t \ , \tag{A.4.7}$$

which means that the left side of (A.4.2) holds when

$$t^2 + t \leq L+1 \ . \tag{A.4.8}$$

Now that we have bounded the log of a sum of a series of binomial coefficients by the log of the largest coefficient in the series, we can compute the logarithm directly by using Stirling's bound on the factorial, which states [18]

$$(2\pi)^{1/2} n^{n+1/2} e^{-n} e^{(12n+1)^{-1}} < n! < (2\pi)^{1/2} n^{n+1/2} e^{-n} e^{(12n)^{-1}} . \quad \text{(A.4.9)}$$

Before evaluating $\left|\begin{matrix} L \\ t \end{matrix}\right| = \frac{L!}{t!(L-t)!}$ by using (A.4.9), note that our goal is to insure that the right inequality in (A.4.2) is satisfied so that we have indeed produced an upper bound on the effective data throughput T given by (4.13). Therefore, the numerator $L!$ should be replaced by the left inequality in (A.4.9), and the right inequality should be used for the denominator terms $t!$ and $(L-t)!$. After taking logarithms, we arrive at the desired result:

$$\begin{aligned} \tilde{D} &= (L+\tfrac{1}{2})\log_2(L) + (12L+1)^{-1} - \tfrac{1}{2}\log_2(2\pi) \\ &\quad - (t+\tfrac{1}{2})\log_2(t) - (L-t+\tfrac{1}{2})\log_2(L-t) \\ &< \log_2 \left|\begin{matrix} L \\ t \end{matrix}\right| \leq D \; ; \qquad t \geq 0, \; t^2 + t \leq L+1 \; . \end{aligned} \quad \text{(A.4.10)}$$

Although the left inequality in (A.4.2) no longer strictly applies, the Stirling bounds are close enough to the actual value for the binomial coefficients that we are still insured of a reasonably tight upper bound on the effective throughput T without having to calculate the sum of a number of (possibly large) binomial coefficients.

VITA

VITA

Robert Kendall Morrow, Jr. was born in Woodbury, New Jersey, on 4 June 1952. He received the B.S. degree in Electrical Engineering from the U.S. Air Force Academy in 1974 and the M.S.E.E. from Stanford University in 1982, and is currently completing his Ph.D. at Purdue University.

Presently a Major in the U.S. Air Force, he has accrued over 2300 hours of military aircraft flying time, and has served for three years on the electrical engineering faculty at the USAF Academy. His interests include digital and analog communication and computer engineering. He is a life member of the Air Force Association and holds an Advanced Class Amateur Radio license.

ABSTRACT

Morrow, Robert Kendall, Jr., Ph.D., Purdue University, May 1988. Bit-to-Bit Error Dependence in Direct-Sequence Spread-Spectrum Multiple-Access Packet Radio Systems. Major Professor: James S. Lehnert.

Slotted direct-sequence spread-spectrum multiple-access (DS/SSMA) packet broadcasting systems with random signature sequences are analyzed within the framework of the lower three layers of the International Standards Organization Reference Model of Open Systems Interconnection. At the physical layer, we show that a widely-used Gaussian approximation (which we call the Standard Gaussian Approximation) for the probability of data bit error in a chip and phase asynchronous system is accurate only when there are a large number of simultaneous users on the channel; otherwise, this approximation can be optimistic by several orders of magnitude. For interfering signals with fixed delays and phases relative to the desired signal, however, the Standard Gaussian Approximation is quite accurate for any number of simultaneous users. To obtain a closer approximation to the probability of data bit error for an asynchronous system, we introduce the Improved Gaussian Approximation, which involves finding the distribution of the multiple-access interference variance over all possible delay and phase values and then taking a Gaussian approximation over the support of the distribution and averaging the results.

To accurately analyze packet performance at the data link layer, we first use the theory of moment spaces to gain insight on the effect of bit-to-bit error dependence caused by the constant relative delays and (possibly) phases of the

interfering signals over the duration of a desired packet. If no error control is used, we find that this error dependence increases the average probability of packet success. When error control is employed and the channel is lightly loaded, then packet performance diminishes when bit error dependencies exist, but performance improves when the channel is heavily loaded and the multiple-access interference is high. Numerical results for the probability of packet success are obtained through the Improved Gaussian Approximation.

At the network layer, provided packet losses occur only from data bit errors due to multiple-access interference, we show that a DS/SSMA packet radio system using the slotted ALOHA protocol possesses a significant throughput advantage over that of an equivalent narrow-band slotted ALOHA system. Furthermore, if error control is used to correct some of the data bit errors in the packet, then the maximum throughput per unit bandwidth of the DS/SSMA system is also higher.

BIT-TO-BIT ERROR DEPENDENCE IN DIRECT-SEQUENCE SPREAD-SPECTRUM MULTIPLE-ACCESS PACKET RADIO SYSTEMS

A Thesis

Submitted to the Faculty

of

Purdue University

by

Robert Kendall Morrow, Jr.

In Partial Fulfillment of the

Requirements for the Degree

of

Doctor of Philosophy

May 1988

To My Wife

ACKNOWLEDGMENTS

I would like to express my gratitude to Prof J. S. Lehnert for his support and advice given throughout the course of this work. My committee members have provided valuable insight in many areas: Prof E. J. Coyle for his networking expertise; Prof J. P. Allebach for his signal processing help; and Prof T. W. Mullikin, who taught me the art of finding integrals in closed form. I am also indebted to Prof J. S. Sadowsky for his help with convergence concepts and for showing me the Ravinia walk.

Thanks are also due to the Department of Electrical Engineering at the United States Air Force Academy and to the Air Force Institute of Technology for their financial support, and to Maj H. F. Bare for his periodic morale-boosting phone calls.

My sincerest thanks go to my wife, Mary, who provided unwavering kindness and caring throughout my academic endeavors.

TABLE OF CONTENTS

Page

Page

LIST OF FIGURES